EPOXY-BASED COMPOSITES AND COATINGS: IMPROVEMENT OF MULTIFUNCTIONAL PROPERTIES

A THESIS SUBMITTED TO
THE GRADUATE SCHOOL OF NATURAL AND APPLIED SCIENCES
OF
MIDDLE EAST TECHNICAL UNIVERSITY

BY

ALMİRA ÇALDIKLIOĞLU

IN PARTIAL FULFILLMENT OF THE REQUIREMENTS
FOR
THE DEGREE OF MASTER OF SCIENCE
IN
CHEMICAL ENGINEERING

JUNE 2019

Approval of the thesis:

EPOXY-BASED COMPOSITES AND COATINGS: IMPROVEMENT OF MULTIFUNCTIONAL PROPERTIES

submitted by **ALMİRA ÇALDIKLIOĞLU** in partial fulfillment of the requirements for the degree of **Master of Science in Chemical Engineering Department, Middle East Technical University** by,

Prof. Dr. Halil Kalıpçılar
Dean, Graduate School of **Natural and Applied Sciences** _____

Prof. Dr. Pınar Çalık
Head of Department, **Chemical Engineering** _____

Prof. Dr. Göknur Bayram
Supervisor, **Chemical Engineering, METU** _____

Prof. Dr. Ülkü Yılmazer
Co-Supervisor, **Chemical Engineering, METU** _____

Examining Committee Members:

Prof. Dr. Naime A. Sezgi
Chemical Engineering, METU _____

Prof. Dr. Göknur Bayram
Chemical Engineering, METU _____

Prof. Dr. Ülkü Yılmazer
Chemical Engineering, METU _____

Assoc. Prof. Dr. Erhan Bat
Chemical Engineering, METU _____

Assoc. Prof. Dr. Özcan Köysüren
Energy Engineering, Ankara University _____

Date: 19.06.2019

I hereby declare that all information in this document has been obtained and presented in accordance with academic rules and ethical conduct. I also declare that, as required by these rules and conduct, I have fully cited and referenced all material and results that are not original to this work.

Name, Surname: Almira Çaldıklıoğlu

Signature:

ABSTRACT

EPOXY-BASED COMPOSITES AND COATINGS: IMPROVEMENT OF MULTIFUNCTIONAL PROPERTIES

Çaldıklıoğlu, Almira
Master of Science, Chemical Engineering
Supervisor: Prof. Dr. Göknur Bayram
Co-Supervisor: Prof. Dr. Ülkü Yılmazer

June 2019, 144 pages

The purposes of this study are to improve mechanical properties, thermal stability, resistance to flammability, electrical conductivity and hydrophobicity of epoxy (E) by incorporation of expanded graphite (EG) and titanium dioxide (T) particles.

In this study, sonication with the use of solvent method was primarily determined for the epoxy-based binary composite and coating preparation. By this method, the epoxy composites and coatings were produced by changing EG concentration as 0.05, 0.1, 0.25, 0.5, 0.75 and 1 wt.% and changing TiO_2 concentration as 0.5, 1, 2 and 5 wt.%. On the other hand, sonication with the use of solvent method was modified for fabrication of the epoxy-based hybrid composites and coatings, and their optimum formulations were determined based on the mechanical properties of the E/EG and E/T binary composites.

The epoxy-based composites were characterized by tensile and impact tests, Shore D hardness test, SEM analysis, thermal analyses, LOI analysis and electrical resistivity test while water contact angle measurement and surface energy analysis were performed on their coatings.

The tensile strength, elastic modulus and impact strength of the neat epoxy were increased by 24%, 25% and 40% over the neat epoxy at 0.1 wt.% EG loading while the electrical resistivity was reduced from 10^{14} to 10^{9} ohm.cm at this concentration. The LOI value of the neat epoxy was increased to 26% by 5 wt.% TiO_2 addition. The E/0.05EG/0.5T hybrid composite provided higher enhancement in tensile and impact properties compared to its binary composites.

Keywords: Epoxy, Expanded Graphite, Titanium Dioxide, Coatings, Mechanical Properties.

ÖZ

EPOKSİ-BAZLI KOMPOZİTLER VE KAPLAMALAR: ÇOKLU FONKSİYONEL ÖZELLİKLERİN GELİŞTİRİLMESİ

Çaldıklıoğlu, Almira
Yüksek Lisans, Kimya Mühendisliği
Tez Danışmanı: Prof. Dr. Göknur Bayram
Ortak Tez Danışmanı: Prof. Dr. Ülkü Yılmazer

Haziran 2019, 144 sayfa

Bu çalışmanın amaçları, genleşmiş grafit (EG) ve titanyum dioksit (T) partikülleri ekleyerek, epoksinin mekanik özelliklerinin, termal stabilitesinin, yanmaya karşı direncinin, elektriksel iletkenliğinin ve hidrofobisitesinin iyileştirilmesidir.

Bu çalışmada, öncelikle çözücü kullanımıyla sonikasyon yöntemi epoksi bazlı kompozitlerin ve kaplamaların hazırlanma yöntemi olarak belirlenmiştir. Bu yöntemle, EG konsantrasyonu ağırlıkça %0,05, 0,1, 0,25, 0,5, 0,75 ve 1 olarak ve TiO_2 konsantrasyonu ağırlıkça %0,5, 1, 2 ve 5 olarak değiştirilerek epoksi kompozitler ve kaplamalar hazırlanmıştır. Diğer bir taraftan, epoksi bazlı hibrid kompozitlerin ve kaplamaların üretimi için çözücü kullanımıyla sonikasyon yöntemi modifiye edilmiştir ve optimum formülasyonları ikili E/EG ve E/T kompozitlerin mekanik özelliklerine göre kararlaştırılmıştır.

Epoksi bazlı kompozitler çekme ve darbe testleri, Shore D sertlik testi, SEM analizi, termal analizler, LOI analizi ve elektriksel direnç testi ile karakterize edilirken, kaplamalara su ile kontak açısı ölçümü ve yüzey enerji analizi uygulanmıştır.

Epoksiye ağırlıkça %0,1 EG eklendiğinde, çekme dayanımı, elastisite modülü ve çarpma dayanımı sırasıyla %24, %25 ve %40 artarken, bu konsantrasyonda

epoksinin 10^{14} ohm.cm olan elektriksel özdirenci 10^{9} ohm.cm'ye düşmüştür. Saf epoksinin LOI değeri ağırlıkça %5 TiO_2 eklenmesiyle %26'ya çıkmıştır. E/0.05EG/0.5T hibrid kompozit, çekme ve darbe özelliklerinde ikili kompozitlerine kıyasla daha çok iyileşme sağlamıştır.

Anahtar Kelimeler: Epoksi, Genleşmiş Grafit, Titanyum Dioksit, Kaplamalar, Mekanik Özellikler.

To my precious family…

ACKNOWLEDGEMENTS

I would like to present my deepest gratitude to my supervisor, Prof. Dr. Göknur Bayram for her guidance, support and encouragement throughout my thesis study. Thanks to her wisdom and patience, I completed my research with love and tried to do my best. I also would like to express my sincere gratitude to my co-supervisor, Prof. Dr. Ülkü Yılmazer for his advice and support. My postgraduate period has become an unprecedented experience for me under favour of their supervision.

I would like to thank Middle East Technical University Scientific Research Fund (BAP) for the financial support throughout the YLT-304-2018-3731 project.

I would like to thank İsa Çağlar from the machine shop for his guidance and advices throughout my research.

I would like to thank my labmates Selin Şahin, Merve Özkutlu and Berrak Erkmen for their help and contribution to my thesis study. I have learned many things from you, thank you!

I would like to thank my dear friends Aslı Karausta, Nisa Erişen, Merve Sarıyer and Fatma Şahin for their friendship and support. You made my last three years unforgettable, thank you!

I would like to thank Bedirhan Kapkiç who had sleepless and tired days with me throughout my research. His advices, continuous support, encouragement and patience during my postgraduate were inestimable. He has always made me feel like very strong and showed me that I can succeed in everything that I want. I am very lucky to have you, thank you!

Lastly, I would like to thank my precious parents, Neslihan and Serdar Çaldıklıoğlu, and my lovely brother Serdar for their endless love, trust and support. They have always stood behind me and supported all my decisions. Without them, I could not become a person who I am now. You are the greatest chance of mine, thank you!

TABLE OF CONTENTS

LIST OF TABLES

TABLES

LIST OF FIGURES

FIGURES

CHAPTER 1

INTRODUCTION

Polymers and polymer composites are favourable substitutes for metallic and ceramic materials and widely utilized for many diverse applications such as sporting goods, musical instruments, automobiles, machine components, construction etc. Polymers and their composites provide many advantages over other materials due to their lightweight, higher resistance to chemicals and corrosion, easier processing and cost-efficient manufacturing. In addition, their properties can be tailored by the addition of organic or inorganic fillers based on the desired properties in the final product [1].

Thermosets constitute one of the main classes of polymeric materials, and they are usually prepared from thermosetting resins which are low viscosity liquids or bulky materials. They are converted to solid plastics by a two-staged chemical reaction which is known as the curing process. During curing, long polymer chains are primarily formed from monomers, and then, these long chains create three dimensional (3D) crosslinked network. The curing reaction is generally induced by a curing agent or heat. Due to the fact that polymer chains are crosslinked by strong covalent bonds after curing, thermosets have enhanced structural integrity, high rigidity, chemical and thermal stability, but cannot be reheated or remoulded. Unsaturated polyesters, polyurethanes, urea formaldehydes, melamines and epoxies are principal examples of thermosetting materials [2].

Epoxy is one of the world-wide known thermosetting materials due to its high compatibility with other materials and high performance in various applications. Epoxies have been extensively used in aerospace and automobile industry, construction, electronic systems, biomedical devices, adhesives, paints and coatings.

They also attract attention in research field since they offer high thermal stability, high chemical resistance and easy processing [3]. However, epoxy-based materials have a few drawbacks that can limit their applications. It is well known that epoxies are brittle since their high crosslink density reduces their fracture toughness. Therefore, they show poor resistance to crack initiation and propagation. In addition to that, their low electrical conductivity and flammability reduce their performance in many applications. These deficiencies can be overcome by the incorporation of micro or nano size reinforcement materials under favour of high adhesion strength of epoxy [4]. The resulting properties of the composites are generally based on characteristics, size and concentration of the reinforcement material, nature of the matrix, preparation method of the composite and interfacial bond strength between the matrix and the fillers [1].

Clay, carbon fiber, graphite, aluminium powder, silica (SiO_2), metal oxides and calcium carbonate ($CaCO_3$) are the most commonly used reinforcements for polymer matrix composites. The suitable reinforcement material is determined according to the desired properties in the final product [5]. In recent years, the utilization of graphite and graphite-based materials in nanocomposites has attracted both academic and industrial interest owing to their large surface area, high aspect ratio, excellent mechanical properties, high electrical and thermal conductivities. Graphite particles involve in stacks of graphene layers which consist of carbon atoms hexagonally bonded to each other on a horizontal plane by strong covalent bonds. On the other hand, graphene layers are held together by weaker Van der Waals forces. If they are completely separated from each other by breaking down Van der Waals forces during the preparation of composites, the maximum enhancements in physical and chemical properties are observed. For this reason, exfoliating graphite particles and dispersing graphene layers homogeneously in the matrix are crucial steps of the composite preparation to achieve highest improvements in various properties [6].

Titanium dioxide (TiO_2) is one of the most interesting metal oxides due to its unique properties such as superior thermal and chemical stability, non-toxicity,

photocatalytic activity, ability to absorb ultraviolet light and high resistance to corrosion. TiO_2 particles have been widely used in the production of antibacterial, anticorrosive and self-cleaning coatings, solar panels, UV-resistant packages and dyes etc. [7]. The physical and chemical properties of the composites reinforced with TiO_2 strongly depend on size, crystalline phase and morphology of the particles. Therefore, it is important to determine the specifications of TiO_2 particles by considering the desired properties in the final product [8].

In this thesis, it was aimed to improve mechanical properties, thermal stability, flammability, electrical conductivity and hydrophobicity of epoxy by the incorporation of expanded graphite (EG) and TiO_2 particles. Although enhancing multifunctional properties of epoxy by EG addition or TiO_2 addition separately have been widely studied in the literature, there is a lack of research in the investigation of their synergistic effects on the properties of the polymer matrices. Therefore, epoxy-based composites and coatings containing EG, TiO_2 and both EG and TiO_2 at different loadings were prepared to observe their contributions to aforementioned properties. Furthermore, the effects of the different preparation methods on mechanical properties, thermal stability and morphology of the binary and the hybrid composites were also investigated.

CHAPTER 2

BACKGROUND

2.1. Polymer Composites

Composites are multifunctional and high-performance materials consisting of two or more than two components which differ from each other in terms of physical and chemical properties. Therefore, the composite made from the mixture of different constituents has a particular appearance and the characteristics of combined properties. Composite materials impart the features of individual identities which are included in their structures and can be designed or tailored to satisfy the requirements of a specific application. In general, composites are prone to have superlative mechanical properties, high resistance to fatigue, creep, corrosion and wear, low density and low thermal expansion coefficient. Thus, they are widely preferred in aerospace and automobile industry, marine structures, trains, tanks, pressure vessels, internal combustion engines, machine components, biological structures and biomedical devices etc. [9].

Composites mainly comprise of two parts called as the matrix material and the reinforcement material. Matrix of the composites can be formed by one type of a material or a blend of different materials whereas one or more than one material can contribute to the structure as reinforcement. Composites are generally classified based on the type of matrix material, and divided into four major categories, namely; polymer matrix composites (PMC), metal matrix composites (MMC), ceramic matrix composites (CMC) and carbon carbon composites (CCC) [10]. Amongst all types of the composites, PMCs have drawn the greatest attention in recent years due to their high performance in advance engineering applications, diverse benefits in processing and cost efficiency. They have high strength to weight ratio, which is

their most outstanding property in industrial applications. Moreover, the production and shaping processes of PMCs do not require high temperature or high pressure and advanced equipments as well as having lower cost with respect to metal or ceramic matrix composites. Despite the various advantages offered by PMCs, polymer matrices are weak in terms of mechanical properties, and they have relatively lower thermal resistance and higher thermal expansion coefficient compared to MMCs and CMCs. Their deficiencies are usually improved by the incorporation of reinforcement materials [11].

In PMCs, the matrix material is responsible for adhering to the reinforcements to improve their dispersion and to protect them against damages while the reinforcement materials provide enhancements in the desired properties by being orderly arrayed in the matrix. In addition, the matrix transfers the load to the reinforcements and determines the critical properties of the composite like thermal stability, resistance to chemicals, moisture and oxidativity as well as substantially affecting strength, toughness, damage tolerance, abrasion resistance and surface properties of the composite [12]. Polymers utilized as the matrix material are mainly divided into two categories which are thermosets (TS) and thermoplastics (TP) [11].

2.1.1. Thermoplastic Matrices in PMCs

Thermoplastics have simple molecular structures and consist of long polymer chains linked by secondary bonds (or intermolecular forces) which provide weak attraction. The weak intermolecular forces between chains can be reversibly ruptured with the application of heat and reformed during cooling, which allows reprocessing and recycling. When TP granules are melted by heat, a viscous liquid is obtained since polymer chains become mobile due to reversible breaking of secondary bonds. The viscous liquid can be easily blended or mixed with other materials to improve desired properties and moulded effectually in various paths. Upon cooling, the polymer is solidified, and its shape is stabilized with the increase in intermolecular interactions. Therefore, TPs restore the bulk properties after processing [13]. The

solid state of TPs can be crystalline, semi-crystalline or amorphous, which is associated to arrangement of polymer chains in their structures. The degree of crystallinity of TPs determines the physical and chemical properties of the matrix. While polystyrene (PS), polymethyl methacrylate (PMMA), polyvinyl chloride (PVC) and acrylonitrile butadiene (ABS) are commonly used commodity plastics in amorphous state, polyethylene terephthalate (PET), polypropylene (PP) and polyethylene (PE) are some of the commodity plastics which have semi-crystalline structure. On the other hand, fully crystalline structure is very rare in TPs [14].

The majority of PMCs with thermoplastic matrices offer such advantages as superior impact strength, damage tolerance, high chemical and shrinkage resistant, easy and short processing owing to lack of crosslink formation, reshaping capabilities and convenience for weight critical applications because of their lower density with respect to most thermosets. However, their manufacturing process needs high energy since high temperature and pressure are required to melt TP granules, to incorporate reinforcement materials into the viscous liquid and to give shape. For this reason, composites with TP matrices are more costly than thermoset matrix composites [15]. Many TPs, like PS, PE or PP, and several TP blends are usually reinforced with glass, carbon or aramid fibers, and they have been widely utilized in automobile, aeronautical and defence industry [14].

2.1.2. Thermoset Matrices in PMCs

Thermosetting resins are usually low viscosity liquids that consist of low molecular weight monomers. During curing, these monomers primarily form long polymer chains, and then, create a three dimensional (3D) crosslinked structure which is highly sophisticated and infusible. Crosslinking means the formation of strong covalent bonds between chains, which is governed by heat supplied from exothermic chemical reactions in the structure or external heat sources. As the crosslink density increases, the mobility of chains decreases, and the resin hardens with the increase in viscosity. At the end of curing process, TS resins are converted to solid structures

which cannot be recycled or remoulded since the curing process is irreversible [16]. TSs cannot be remelted by heat, but they degrade at high temperatures. For this reason, they have high thermal stability, which is one of their most remarkable properties although it causes difficulties in welding processes [17].

In general, PMCs with thermoset matrices offer high strength, high stiffness, high temperature mechanical properties, superior fatigue and creep resistance, anti-corrosion properties and very good dimensional stability due to their strong 3D network. In addition, their infusible structure often improves fire behaviour. During composite manufacturing, highly brittle structure of TSs which resulted in low fracture toughness can be improved by the addition of reinforcement materials that can provide resistance to crack initiation and propagation [18]. In addition, the preparation process of thermoset matrix composites takes longer time and it is more difficult to monitor them compared to the composites with TP matrices since crosslinking is a relatively uncontrollable chemical reaction that requires prolonged period of time [17]. Unsaturated polyesters, vinyl esters, epoxies, phenol formaldehyde and bismaleimide resins are the major TSs available. Among these, epoxies draw great industrial and academic interest, and they have been frequently preferred in composite manufacturing and prepreg carbon fiber or glass fabric preparation [19].

2.1.3. Reinforcements in PMCs

With the existing benefits, desired properties of the matrix can be further improved, or deficiencies related to the matrix can be overcome by inserting an appropriate reinforcement material into the matrix. Due to the fact that reinforcements generally dominate the final properties of the composite despite their lower amount with respect to matrix material, the selection of the reinforcement material is very critical. In the design of a composite material, characteristics, size, orientation and concentration of the reinforcement material are crucial parameters along with the matrix and the interfacial properties [20].

Reinforcement in PMCs is usually provided by continuous or discontinuous fibers, nano or micro size particles, solid or hollow microspheres, flakes and whiskers. Fiber-reinforced composites, particle-reinforced composites and laminar composites are the most common types of strengthened PMCs. These composites combine functionalities of the polymer matrix with the specific properties of the reinforcements, and thus, become convenient products for high performance applications or a particular utilization [10].

Fibers are usually characterized by their filament like structure, where the length is much greater than the cross section, and they have been widely used in PMCs due to their unique properties such as high strength and stiffness, very good tensile properties and lightness in weight [21]. In the fiber structure, molecules are arrayed along the fiber direction and its small size reduces the possibility of defects in the structure. Therefore, fiber form of a material exhibits better mechanical properties than its bulk form. However, the orientation of molecules in the fiber direction results in anisotropic behaviour which means that properties of the fiber differ in different directions. For instance, fibers provide the composites with high tensile strength and elastic modulus along the longitudinal direction of the fiber since most of the load can be carried by the fibers, whereas the composites show poor mechanical properties in the transverse direction owing to load being mostly transported by the matrix. Thus, the suitable arrangement of the fibers in the matrix according to load direction enhances mechanical properties and durability of the composite by enabling the large portion of the load to be carried by the reinforcements [22]. Fibers are generally divided into two categories which are continuous fibers and discontinuous fibers. Continuous fibers have very large aspect ratio, and thus, they have high tendency for bending or buckling. On the other hand, they offer high load carrying capacity and extreme mechanical properties when they are aligned in the matrix. According to the arrangement of fibers, the composites exhibit unidirectional, bidirectional or multidirectional properties. On the contrary, discontinuous fibers or short fibers have low aspect ratio with respect to continuous

fibers, and therefore, it is quite difficult to align them. They are mostly prone to be randomly distributed in the matrix and present isotropic behaviour [23]. Glass fibers, carbon or graphite fibers, ultra-high molecular weight polyethylene (UHMWPE) fibers and basalt fibers are primarily used to reinforce polymer matrices. They have considerable influences on such characteristics of the composites as density, electrical and thermal conductivity, tensile properties, compressive strength, fatigue resistance, failure mechanism and cost [21].

Particle reinforcements constitute another class of composites that have been extensively utilized in the industry and academic researches. The dimensions of particles are approximately equal in all directions while their shapes may be spherical, cubic, platelet or any irregular geometry. SiO_2, TiO_2, $CaCO_3$, aluminium oxide (Al_2O_3), glass spheres, carbon nanotubes, graphite nanoplatelets, graphene layers and layered silicates are the most commonly preferred particle reinforcements for the polymer matrices [24]. Their contributions to the composites are strongly affected by the size, shape and distribution of the particles since particle-matrix interactions are directly related to the available surface area of the reinforcements and the quality of their dispersion in the matrix. Particle reinforcements can be distributed as random or aligned based on demand. Randomly distributed particles exhibit isotropic behaviour whereas aligned ones offer anisotropic properties [25]. In composites, particle reinforcement can be provided by microscopic contribution of large particles or dispersion strengthening mechanism of very small particles which are majorly metallic, non-metallic or metal oxide particles. However, the maximum improvement in desired properties can be achieved by evenly distributed small particles. Particle reinforcement generally enhances stiffness, toughness, hardness, wear resistance and surface properties of polymer matrices although less improvements are achieved in all properties than would be obtained in fiber-reinforced composites [26].

Reinforcement materials which are utilized in PMCs may be in micro or nano size. Materials that have at least one dimension in nanometer are generally known as

nanomaterials and, are highly favourable in the design of the nanocomposites. The smaller particle/filler size results in extremely high surface to volume ratio which promotes strong interactions between the reinforcements and the matrix. Therefore, the insertion of nanoparticles or nanofillers into polymer matrix can bring the final product completely new properties [20].

2.2. Epoxy

Epoxy resin is usually defined as a viscous liquid with low molecular weight that consists of linear molecules involving more than one epoxide group. The epoxide group, also known as the glycidyl group, contains an oxygen atom that form three-membered oxirane ring by bonding to two contiguous carbon atoms.

Epoxy resins are generally produced by the condensation reaction of epichlorohydrin with bisphenol A as seen in Figure 1. Due to the fact one molecule of bisphenol A reacts with two molecules of epichlorohydrin according to stoichiometry, it is possible to vary the molecular weight of epoxy resin by arranging the amounts of both components. Therefore, epoxy resins are usually defined with mean molecular weight. As the mean molecular weight of epoxy resin increases, its reactivity and toxicity decrease. Furthermore, low molecular epoxy resins consisting of short chains exist as fluid at room temperature, whereas high molecular ones are solid. For this reason, low molecular epoxy resins can be handled easily and utilized for casting, coatings or adhesives while solid ones primarily need to be dissolved in organic solvents [27].

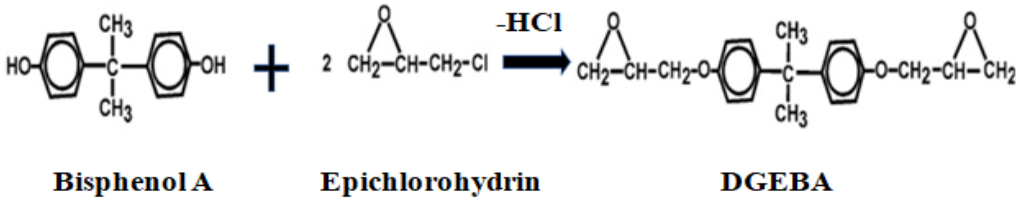

Figure 1. Formation reaction of diglycidyl ether bisphenol A (DGEBA) [27].

Among all epoxies, diglycidyl ether bisphenol A (DGEBA) is the most commonly used one due to its low molecular weight and ability to exist in various viscosities. In addition, DGEBA contains two epoxide groups that increase its reactivity and crosslinking density when it reacts with a hardener. Therefore, they have higher glass transition temperature by the virtue of high crosslinking and better adhering properties owing to the presence of more hydroxyl groups after the reaction with a hardener [28].

To convert epoxy resins into a crosslinked form, application of heat and curing agent is required, which hardens the resin by creating a three dimensional network with epoxy chains. Curing agents which contain amine, amide, acid anhydride, imidazole, phenol or mercaptan organic compounds are majorly used to harden epoxy resins. The structure of amine is closely associated to ammonia (NH_3), and based on the number of alkyl groups substituted instead of hydrogen atoms, primary (NH_2-R), secondary (NH-R_1) and tertiary (N-R_2) amines are defined. On the other hand, the number of amino groups in the structure designates the type of amine molecule, like monoamine, diamine or polyamine. Moreover, amines can be aliphatic which consists of linear carbon chains, cycloaliphatic which contains carbon ring and lastly aromatic where a benzene ring is bonded to the amino group [29].

The crosslinking reaction starts between hydrogen atom of the amine molecule and oxygen atom of the epoxide group. At the first stage, hydrogen atom bonded to one of the amino groups reacts with epoxide group's oxygen atom, which cause the formation of hydroxyl group and the primary amine to be reduced to a secondary amine. Then, the secondary amine reacts with another epoxy group's oxygen atom and the reaction is completed. In addition, the use of amine adducts hardeners, which are produced by being partially reacted with an epoxy resin, is very common owing to their higher reactivity [29].

Epoxy resins are the most adaptable and versatile thermosetting polymers that have been widely used as matrix material in advance applications including aerospace,

automotive, marine, construction, sporting goods, musical instruments, electronic systems, adhesives, paints and coatings. Due to their high performance and ability of being tailored according to the demanded properties, epoxies are one of the most favourable materials in the composite manufacturing. In epoxy-based composites, epoxy matrix provides high dimensional stability owing to low shrinkage during curing, excellent resistance to thermal treatments, corrosion and chemicals because of its infusible crosslinked structure, high strength to weight ratio and superior adhesion properties [16].

2.3. Graphite

Graphite is the one of the crystal forms of carbons, which exists in nature or can be synthesized from petroleum, coal and natural or synthetic organic chemicals. As shown in Figure 2, it consists of graphene layers that are separated from each other by approximately 0.335 nm. Each graphene layer is formed by the association of planar hexagonal rings where carbon atoms are bonded to each other with sp^2 hybridization [30].

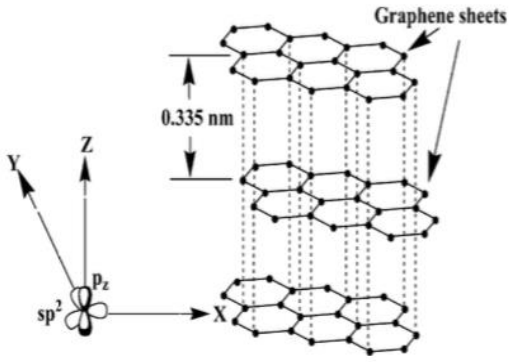

Figure 2. The structure of natural graphite particle [30].

In horizontal plane, carbon atoms are linked by strong covalent sigma type bonds whereas graphene layers are held together by weak Van Der Waals attractions due to the formation of pi type bonds between carbon atoms that belong to the adjacent

graphene layers. The difference in the strength of bonding forces parallel and perpendicular to the planes results in extreme anisotropic behaviour. Therefore, graphite exhibits extraordinary properties along the horizontal plane, such as high thermal conductivity (5000W/mK), electrical conductivity (6000 S/cm), mechanical stiffness (ultimate tensile strength) (130 GPa) and Young's modulus (1TPa) etc., whereas it shows poor properties in the vertical direction. For this reason, orientation and the distribution of graphene layers in polymer matrix have great influence on the final properties of the composite [31].

Although graphene is the fundamental structural element of different carbon allotropes such as graphite, fullerene and carbon nanotube, it has more potential to enhance polymer matrices with respect to others owing to its higher surface to volume ratio. Through the large surface area of graphene layers (2676 m^2/g), matrix-reinforcement interactions increase, which provides significant improvements in the matrix properties. In addition, load transfer becomes more efficient, which results in higher mechanical properties of the composite [32].

Expanded graphite (EG), which is frequently used in polymer composites, is usually produced by the thermal expansion of alkali metal or acid intercalated graphite. At high temperatures, intercalation compounds which are trapped between graphene layers of graphite particles, expand and cause the layers to be separated randomly. This treatment results in the formation of EG particles which still maintain the layered structure of graphite while providing higher aspect ratio and larger contact surface for matrix materials. The schematic representation of EG production from natural graphite is given in Figure 3.

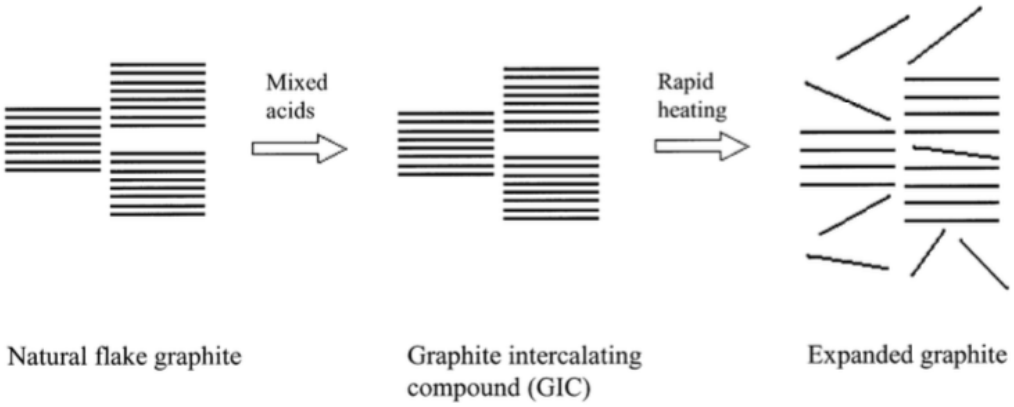

Figure 3. The production of expanded graphite from natural graphite [33].

The thickness of EG particles which comprise of stacks of graphene layers are commonly in micrometer range (<10μm). To obtain EG particles in a thinner form, fluorinated or oxidized graphite particles are exposed to higher temperature treatment after the intercalation process [33].

Due to superior properties of EG along with its lower cost, it is mostly utilized to improve mechanical properties and electrical conductivities of polymer matrices. In addition to that, effects of the EG incorporation to epoxy matrix on thermal stability, flammability and surface properties have been extensively researched in the literature [34-36].

2.4. Titanium Dioxide (TiO_2)

Titanium dioxide, which is also known as titania, is the naturally occurring oxide of titanium and exists in three different crystal structures which are rutile, anatase and brookite. These three structures differ from each other according to the orientation of octahedrons formed by one titanium atom and six oxygen atoms [37]. Three different phases of TiO_2 are shown in Figure 4.

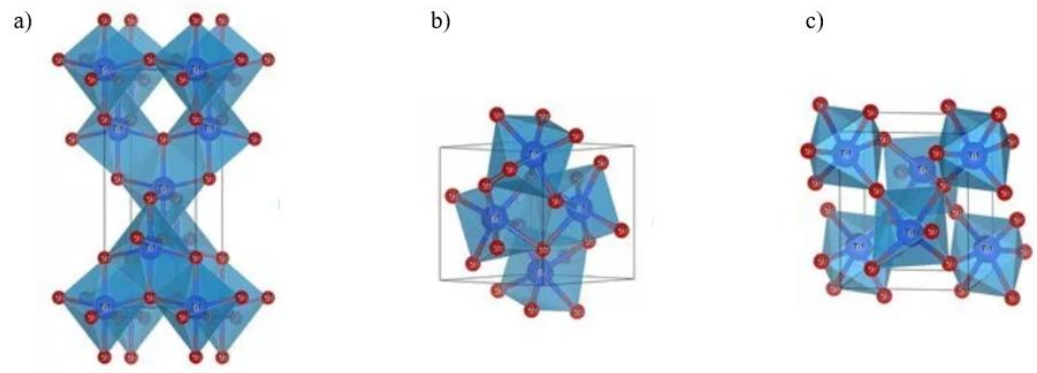

Figure 4. Crystal structures of TiO_2: a) anatase, b) brookite, c) rutile [37].

Phase formation occurs when amorphous titania, which is obtained from aqueous solution of alkoxide precursor, is exposed to hydrothermal treatment at elevated temperatures. The crystal structure of the molecule is determined based on the type and concentration of acidic or basic solution used in the hydrothermal treatment [37]. The brookite phase is the least stable form of TiO_2 due to its distorted structure whereas the rutile phase is the most thermally stable form. The anatase and brookite particles are converted to the rutile form when they are heated to approximately 800°C. On the other hand, the rutile form melts at much higher temperature, close to 1850°C. In addition, all three phases have very high refractive index, and therefore, they reflect most of the light, which results in opaqueness of the product containing TiO_2 particles [38].

TiO_2 is one of the most attracted and the most researched metal oxides due to its unique properties such as non-toxicity, high photocatalytic activity, ability to absorb UV light, good mechanical and thermal properties. Therefore, it has been extensively used in antibacterial, anticorrosive and self-cleaning coatings, paints, food packaging and skin care products [39]. Moreover, TiO_2 particles are generally incorporated into polymer matrices to enhance tensile properties, fracture toughness, thermal stability, flammability and surface properties [40-42]. In the literature, it is pointed out that the final properties of composites reinforced with TiO_2 mostly depend on size,

morphology and crystalline phase of the particles. For instance, elongated nano size TiO_2 particles provide much more efficient load transfer between the matrix and the particles with respect to spherical and larger (micro) size particles due to their higher aspect ratio and larger specific surface area. In addition, type of the crystal structure determines the application area. For example, anatase TiO_2 particles have been widely used to provide photocatalytic activity whereas the ones in rutile form are mostly incorporated into polymer matrices to enhance thermal stability of the final product [38].

2.5. Literature Survey

2.5.1. Dispersion and Concentration of EG Particles in Epoxy Matrix

Polymer composites which are reinforced with EG particles have high potential to exhibit superior mechanical properties, high electrical conductivity, good thermal stability and hydrophobic surface properties owing to sheet-like structure of EG which promotes the matrix-reinforcement interactions. However, these improvements would be achieved if the layers of EG are split down to nanometer thickness. The exfoliation of EG particles cannot be achieved by simple mixing methods since EG particles have high tendency to form agglomerations because of van der Waals forces between layers. In the study carried out by Yasmin et al. [43], four different techniques which are direct mixing, sonication, shear mixing, combined sonication and shear mixing were used to prepare epoxy reinforced with EG particles. To determine the most efficient method that provides higher exfoliation degree and more homogeneous dispersion of EG particles in epoxy matrix, wide angle X-Ray (WAXD) analysis and mechanical tests were performed on the composites containing 1 and 2 wt.% EG. In WAXD analysis, it was observed that sonication of EG particles in acetone before being mixed with epoxy resin resulted in higher decrease in the intensity of characteristic peak of graphite (at 2θ of 26.38 which corresponds to a d-spacing of 3.37Å) which shows higher reduction in the number of multilayered graphite structures. It should be noted that if the matrix

contains only individual graphene nanosheets, the characteristic peak of graphite could not be observed. In addition, tensile test results of the composites revealed that combined sonication and shear mixing method resulted in the highest tensile strength and elastic modulus for both EG concentrations.

Due to the fact that the addition of excess amount of EG into the matrix may result in the formation of voids and agglomerates, which adversely affects the final properties, it is very vital to optimize concentration of EG in polymer composites. Yasmin and Daniel [44], investigated the influences of graphite content on mechanical properties of the epoxy-based composites. They reinforced epoxy matrix with graphite platelets (GP) of sizes ranging from 4 to 76 μm and carried out tensile test on the composites containing 2.5 and 5 wt.% GPs. Test results showed that elastic modulus of epoxy matrix consistently increased with the increase in GP content whereas lower tensile strength was observed at 5 wt.% loading with respect to 2.5 wt.%. The increase in elastic modulus was related to increment in stiffness provided by rigid GPs, while the decrease in tensile strength after a certain concentration of GP was attributed to agglomerations occurring owing to increase in viscosity. It was stated that GPs started to interact mostly with each other instead of epoxy chains at high concentrations, and thus, matrix-reinforcement interactions became weaker, which resulted in poor dispersion of the particles in the epoxy matrix.

2.5.2. Improvement of Mechanical Properties

Epoxies are brittle and show poor resistance to crack initiation and propagation due to their high crosslink density after curing. The deficiency in their toughness properties limiting their various applications can be overcome by the incorporation of micro/nano size fillers or particles which impart additional toughening mechanism. The use of rubber particles to increase impact resistance of epoxy matrices has been a concern of several researchers. However, it was observed that the addition of rubber particles improves toughness and ductility of the final product

while decreasing the thermal and other mechanical properties such as stiffness and strength [45]. On the other hand, in many studies, the effects of such promising nanomaterials as carbon nanotube, graphene, nano clay and nano silica on toughness, which may trigger the fracture mechanism, were also investigated. After a suitable material is determined by considering desired properties and its compatibility with the matrix, obtaining a homogeneous dispersion and good adhesion between the reinforcement and the matrix provide sufficient enhancement in fracture toughness without sacrificing any other properties [18].

The two dimensional structure and large specific surface area of graphene-based materials make them potentially more promising for increasing toughness of epoxy matrices. Kang et al. [46] evaluated the effects of EG and graphite oxide (GO) addition into epoxy matrix on toughness by measuring impact strength. They observed that an EG:GO mass ratio of 1:1 in the prepared composites resulted in better synergistic effect for enhancing toughness while the incorporation of 1 wt.% EG increased the impact strength of epoxy matrix by 21 %. The significant enhancement in toughness was associated to additional failure mechanism provided by graphene-based particles due to the fact that the presence of EG and GO in the epoxy matrix caused crack deflections by tilting of the crack fronts through their 2D structure with large aspect ratio. This study also revealed that the insertion of such particles as EG and GO effectively hindered the crack propagation by providing large amount of plastic deformation. In addition, it was emphasized that the improvements in toughness considerably depend on the weight fraction and the size of the particles which are the parameters that determine the dispersion quality.

The investigation of the effects of TiO_2 addition into epoxy matrix on mechanical properties is one of the important issues, which has been extensively studied by researchers. Srivastava and Tiwari [40], also analyzed how the addition of 3-Glycidoxypropyl-trimethoxsilane (GPTMS) functionalized TiO_2 particles into the epoxy matrix affected tensile properties, toughness and charpy impact strength. They measured the toughness of unfilled epoxy and the composites containing 0.5, 1, 5

and 10 wt. % TiO_2 by calculating the area under load (kN) versus elongation (mm) curve for each one. According to the results, it was stated that 9.1 %, 20 % and 12.16 % increase in tensile strength, charpy impact strength and toughness, respectively were observed at 5 wt. % TiO_2 loading. However, other concentrations (higher or lower) showed lower mechanical properties with respect to unfilled epoxy. The reduction in mechanical properties was related to the fact that insufficient amount of TiO_2 addition disrupted the integrity of epoxy's crosslinked network and caused the formation of weak regions in the matrix whereas agglomerates formed at higher concentrations resulted in easy debonding owing to poor matrix-reinforcement interactions. For this reason, it is very crucial to optimize reinforcement concentration and to obtain homogeneous dispersion during the preparation of the composites in order to achieve desired enhancement in any properties.

On the other hand, Abdelkarim et al. [47] measured the hardness of epoxy composites containing micro size (<20 μm) and/or nano size (<100μm) TiO_2 particles according to ASTMD 2240 standards using a digital hardness tester. Epoxy-based microcomposites and nanocomposites with 0.1, 0.25, 0.5, 0.75, 1, 3.5 and 7 wt. % TiO_2 were separately prepared while the composites which contain both micro and nano size TiO_2 particles were fabricated at 0.1 and 0.75 wt.% loading. The hardness test was carried out on four samples for each formulation to ensure the results by minimizing the standard deviation. The results showed that the initial hardness of unfilled epoxy which is 73.5 was enhanced with the addition of TiO_2 particles while microcomposites generally had higher hardness value compared to nanocomposites. Among the all microcomposites, the highest hardness value of 85.3 was achieved at 0.5 wt. % loading whereas the nanocomposite with 3 wt. % TiO_2 presented the highest hardness value of 84 with respect to other nanocomposites. This situation revealed that the addition of low amount of micro size TiO_2 particles into epoxy matrix provided significant enhancement in hardness, but higher amount of nano size particles were required to obtain same hardness value. Beside this, it was observed that the composites containing the mixture of micro and nano size

TiO_2 particles also exhibited high hardness value of 82.6 at 0.75 wt. % loading. Due to the fact that the hardness of the composites was associated with the depth of the indentation, insertion of larger particles or compact structure which was provided by the broad range of particle size increased the probability of the indenter to coincide with a rigid and stiff reinforcement material rather than the polymer matrix, thus, enhanced the hardness of the final product.

2.5.3. Improvement of Thermal Stability

Thermal stability of polymer matrix composites plays a crucial role in their processing and applications since it directly determines the processing and the usage temperature. In addition to that, thermal stability of a composite also affects its environmental durability and long-term properties since thermal degradation causes reduction in mechanical properties [48].

In the literature, it was stated that improvement in thermal stability of polymer matrix composites was obtained by the introduction of thermally stable particles or the particles that prevented diffusion of oxygen and dissipation of heat within the matrix [49]. Srivastava and Tiwari [40], reinforced epoxy matrix with nanosized TiO_2 particle, which was functionalized with 3-Glycidoxypropyl-trimethoxsilane (GPTMS) to improve dispersion, by using a homogenizer that provided shear mixing in order to examine the influences of TiO_2 addition on thermal stability of the matrix. They evaluated the thermal properties of unfilled epoxy and epoxy-based composites containing 0.5, 1.5 and 10 wt.% TiO_2 by determining their initial decomposition temperature (IDT) which is usually defined as the temperature where the weight loss is 5%, integral procedural decomposition temperature (IPDT) which is calculated based on area under the residual weight (%) versus temperature (°C) curve and char formation at 500°C in TGA analysis. They found that IDT and IPDT values consistently increased up to 5 wt.% TiO_2 addition since the increase in TiO_2 amount resulted in higher crosslink density which enhance the thermal stability of the epoxy matrix. The improvements in thermal properties were also related to the

development of a barrier to heat and oxygen due to the dispersion of TiO_2 particles uniformly in the matrix at low concentrations. In addition, it was stated that the barrier effect provided by TiO_2 particles may reduce the flammability of the matrix. However, a reduction in both values was observed at 10 wt. % loading although they were still higher than those of unfilled epoxy. This situation was associated to the formation of agglomerations at high TiO_2 concentrations which resulted in poor dispersion and less barrier effect. On the other hand, it was realized that char formation at 500°C increased with the rise in TiO_2 amount, which may be an additional mechanism for flame retardancy.

2.5.4. Improvement of Flame Retardancy

Polymer composites are capable of replacing metallic structures due to their unique properties and advantages in processing. However, their flammability is one the challenges in many applications like aerospace, automotive, paints and coatings because of the great potential of fire risk that may cause serious losses and economic damages. Epoxy resins are also sensitive to combustion due to their organic nature which is highly flammable. In addition to this, the incorporation of some organic additives, especially carbon-based materials that have high thermal conductivity, into the matrix may facilitate the ignition of the composites, which is known as the candlewick effect [50]. To cope with this problem, the addition of flame retardants into polymer matrices has been extensively studied in different composite systems. Halogen flame retardants which are bromine and chlorine-based compounds have been often used to increase flame resistance of polymer matrix composites for many years. However, it was revealed that burning of halogenated additives releases toxic gases endangering human life. Therefore, the influences of environmentally friendly materials containing such elements as nitrogen, phosphorus, boron and silicon on flammability of polymer composites were investigated [51]. On the other hand, with the improvements in nanotechnology and nanocomposites, different types of nano materials have been used to enhance flame resistance of polymer matrices in several researches. In many studies, it was realized that such nanoparticles as nano clays,

carbon nanotubes and nano size TiO_2 particles could reduce the flammability by bringing down the combustion of the polymer matrices [41, 52].

The mechanisms for flame retardance in plastics can be divided into two main categories which are hindering the combustion physically and supressing the burning of flammable materials through chemical reactions. While the physical retardance refers to cooling by endothermic reactions, forming a protective barrier against heat and oxygen and dilution of radicals by releasing water vapor or CO_2, chemical retardance occurs in four different ways. The first one is known as vapor phase inhibition resulting from the reaction between flame retardants and burning polymer which causes reduction in the concentration of free radicals and thus blows out the flame. This mechanism is usually executed by halogenated retardants. In solid phase inhibition which is the second way, flame retardants destroy the polymer structure and lead to melting instead of burning. The third chemical retardance mechanism is the char formation. Solid phase retardants form carbonaceous layer which insulates the polymer and prevents the release of gases that may contribute to the combustion. This type of mechanism is mostly deployed by non-halogen retardants. The last one which is called as intumescence is obtained by the insertion of blowing agents into the polymer that create a protective layer [53].

Flammability behaviour of epoxy composites containing TiO_2 has never been studied in the literature up to today. However, the TiO_2 incorporation into such thermoplastic matrices as PMMA and HDPE was frequently performed to provide flame retardancy in the final product [41, 54]. In the study conducted by Laachachi et al. [41], PMMA matrix was reinforced with TiO_2 particles to observe the influences of TiO_2 addition on flammability of the matrix. They prepared PMMA composites with 5, 10, 15 and 20 wt.% nano size TiO_2, respectively. Various parameters including time to ignition (TTI), heat release rate (HRR) and peak of heat release rate (pHRR) were measured by using a cone calorimeter device. When the results were analyzed, it was observed that pHRR was consistently decreased as the mass fraction of TiO_2 increased. In addition to that, all composites presented higher

TTI with respect to unfilled PMMA, while the one containing 5 wt. % TiO_2 had the highest value of TTI due to better dispersion at lower content. They emphasized that poor dispersion of flame retardants resulted in nonuniform flammability behaviour.

2.5.5. Improvement of Electrical Conductivity

Low electrical conductivity is one of the other drawbacks of polymer matrices, which limits their applications especially in aeronautical field and electronic systems since they are vulnerable to lightning strikes and electrostatic accumulation. Epoxy shows poor performance in aerospace structures and wind turbines to provide protection against electrical interference due to its low conductivity. In addition, this deficiency causes safety risks when they are used in high voltage devices as an insulator or coated on floors as an antistatic covering. Therefore, the incorporation of electrically conductive materials into the epoxy matrix enhances its performance in various applications [55]. Due to the fact that carbon and graphite-based fibers are characterized by their high electrical conductivity, the preparation of multilayered composites containing carbon fiber mats is frequently encountered in the literature. Although fiber orientation was changed from layer to layer in laminated structures, increase in electrical conductivity in the thickness direction could not be observed due to the arrangement of fibers in the horizontal plane [56]. After that, such graphite-based particles as carbon black, carbon nanotubes and graphene were inserted into epoxy matrix to reduce volume resistivity of the final product. By obtaining homogeneous dispersion of the particles, the percolation threshold of transition in electrical conductivity from an insulator to semiconductor was achieved [57].

Gantayat et al. [58], measured the electrical conductivity of epoxy composites reinforced with 3, 6 and 9 wt.% EG by using a four point probe resistivity measurement device. When the graph of electrical conductivity versus EG content was plotted, the percolation threshold of transition in electrical conductivity, which is usually described as the lowest amount of filler needed to create a three

dimensional conductive network within the polymer matrix, was obtained between 3 and 6 wt.% EG addition. Moreover, it was stated that the initial conductivity of epoxy matrix which was about $2.3x10^{-15}$ S/cm was increased to $2.11x10^{-5}$ S/cm at 9 wt.% EG, indicating the transition from an insulator to semiconductor. While a continuous increase in electrical conductivity was observed between 3 and 9 wt. % EG in this study, Zheng and Wong [59] obtained a sharp increase in electrical conductivity, which refers to percolation transition, between 1 and 2 wt.% EG addition in PMMA composites. The initial conductivity of PMMA was increased from 10^{-16} S/cm to 10^{-4} S/cm. They also investigated the difference in electrical conductivity enhancement between EG and natural graphite (NG) reinforced PMMA composites. It was found that PMMA/NG composites reached percolation threshold at higher filler content which was between 2 and 5 wt.%, and the conductivity of PMMA was increased to a slightly lower value of 10^{-5} S/cm at 5 wt.% NG addition. However, the conductivity level remained constant after the filler content achieved a critical value in both cases since agglomerations resulting from the increase in viscosity at high concentrations led to poor dispersion, which caused disconnections in conductive pathways. Finally, the difference in conductive behaviour between PMMA/EG and PMMA/NG composites was attributed to the number of available conductive paths in the matrix.

2.5.6. Surface Properties of Epoxy-based Coatings

Coatings are frequently applied onto glass, aluminium alloy and steel surfaces to compensate defects, to strengthen the surface towards the probability of crack formation, to provide protection against corrosion and to increase environmental durability. Among all benefits provided by the coatings, the self-cleaning property has gained significant attention in recent years since it provides reduction in maintenance cost, labour force and time spent for cleaning works. The self-cleaning technology originated from nature, especially from lotus leaves that have self-cleaning property resulting from its hydrophobic structure and have been widely

utilized as coatings in diverse applications such as window glasses, solar panels, wind turbines and exterior paints [60].

Self-cleaning coatings are generally divided into two major categories which are hydrophilic and hydrophobic coatings. Both coating types clean themselves by the motion of water droplets on their surfaces. In hydrophilic case, water droplets spread over the surface, and thus, remove all dirt, dust and other impurities. On the other hand, water droplets on the hydrophobic coatings clean the surface by rolling away. Due to the fact that absorption of water on hydrophilic surfaces may cause degradation of the coating material and loss of properties in time, hydrophilic coatings fail to provide long-term usage. On the contrary, hydrophobic coatings minimize the contact with water, and therefore, increase environmental durability. In addition to that, they also provide anti-icing property since their hydrophobicity prevents the accumulation of snow and reduce the formation of ice on the surface [61].

Hydrophobicity of the coating which is usually defined as water repelling property is evaluated by the contact angle formed between the surface and water droplet. The shape of water droplet on the solid surface is determined by the solid-liquid (γ_{SL}), liquid-vapor (γ_{LV}) and solid-vapor (γ_{SV}) interfacial tensions. The general schematic representation of the balance among three phases is given in Figure 5.

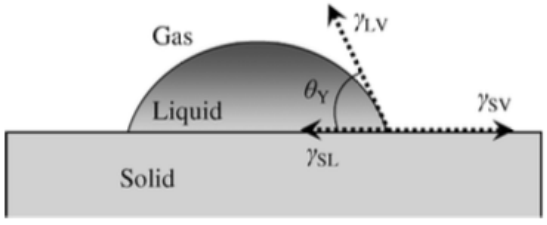

Figure 5. The balance among solid, liquid and gas phases [62].

After the water droplet is stabilized on the surface under these forces, the angle between γ_{LV} and γ_{SL} vectors is defined as water contact angle (WCA). In general, coatings having WCA higher than 90° are characterized as hydrophobic while the ones forming contact angle higher than 150° are usually specified as super or ultra-hydrophobic. Also, it should be noted that increase in hydrophobicity results in higher WCA ad lower sliding angle [62].

In the literature, it is emphasized that hydrophobic properties can be developed by increasing surface roughness which is the height to area aspect ratio of surface topographic features. Due to the fact that roughness prevents the spreading of liquid droplets over the surface and provides the droplets to keep their spherical shapes, it causes increase in WCA, and thus, enhances hydrophobic properties. Increase in surface roughness is simply provided by the application of such physical and chemical techniques as machining, laser abrasion, plasma or chemical etching which may create a variety of micro and nano scale structures [60]. In addition, surface roughness can be obtained by the intended topographic structure of the coating material which results from the arrangement of micro or nano size particles together or separately. The use of the particles in different sizes and even the agglomerations may contribute to the surface roughness since they cause microscopic variations in the elevation of the surface. For instance, the orientation of nanorods and TiO_2 particles in a thin polymer film resulted in a particular topographic structure that increased surface roughness [63].

On the other hand, hydrophobicity can also be improved by chemical modifications with materials that reduce the surface energy of the coatings. Alkyl silane or fluorinated silane, zinc oxide (ZnO) and TiO_2 are the commonly used materials to prepare low surface energy coatings [60]. Low surface energy materials have tendency to exhibit hydrophobicity since their low reactivity to hydrogen bonding prevents the spreading of water droplets over the surface. For this reason, the

coatings made from low surface energy materials or the ones involving additives that can reduce the surface energy may show hydrophobicity [64].

Epoxy resins have been widely utilized as a coating material owing to their high thermal stability, excellent resistance to chemicals, environmental durability and easy processability. The infusible molecular structure of epoxy, which minimizes water absorption, makes it a good candidate for hydrophobic coatings. In the literature, intrinsically hydrophobic materials such as polyhedral oligomeric silsesquioxanes (POSS), polytetrafluoroethylene (PTFE), silicon dioxide (SiO_2), ZnO and TiO_2 particles were often incorporated into polymer matrices to enhance hydrophobicity of the final products [60]. Yu et al. [65], reinforced an epoxy matrix with nano size TiO_2 particles by applying ultrasonication and mechanical stirring, and then, they sprayed the mixture on a steel surface to prepare a hydrophobic coating. The hydrophobicity of the coating containing 2 wt.% nano size TiO_2 was evaluated by performing WCA measurement. According to the results, it was found that WCA of unfilled epoxy coating was increased from 87.5 to 95.5 at 2 wt.% loading. This means that the low amount of TiO_2 addition into the epoxy matrix can convert a hydrophilic coating surface to a hydrophobic one.

On the other hand, it was realized that graphene nanosheets can be used to even convert hydrophilic surfaces to hydrophobic since their 2D structures increase surface roughness significantly [66]. In the study conducted by Monetta et al. [67], aluminium alloy surface was coated with epoxy reinforced with 1 wt.% graphene nanoflakes (GN), which are 2µm in diameter and a few nanometer in thickness, having an average surface area of 500 m^2/g. They carried out WCA measurement on the coated surface, which was 28 µm in thickness, by dropping 8 µl of distilled water onto at least 5 different locations. After the water droplets were stabilized on the surface, which was approximately 60 second after dropping, their shapes were recorded, and the contact angle was measured by using a goniometer. Finally, it was found that 1 wt.% graphene nanoflakes addition increased the water contact angle of the unfilled epoxy from 60° to 75°. Due to the fact that WCA of the epoxy/GN

coating was not in the hydrophobic range, it was suggested to improve dispersion of GNs in the matrix since uneven distribution may have resulted in misleading observations which change depending on the measurement location. They also emphasized that increasing the amount of GNs may provide hydrophobicity if a suitable preparation method is determined.

2.5.6.1. Calculation of Surface Energy of Epoxy-based Coatings

In many studies, surface free energies of various materials are calculated based on Young equation (Equation 2.1) which expresses the balance on the three-phase interface [62].

$$\gamma_{SL} + \gamma_{LV}\cos\theta = \gamma_{SV} \tag{2.1}$$

In the Young equation, γ_{SV} represents the surface free energy of a solid material and γ_{LV} is the surface tension of liquid, whereas γ_{SL} and θ symbolize the interfacial tension and the contact angle, respectively between the solid material and liquid.

For polymer-liquid systems, Young equation is developed to reduce the number of unknowns, and surface free energy (γ^{TOT}) is characterized by dispersion component (γ^{d}), which represents van der Waals forces and dipole-dipole interactions, and polar component (γ^{p}), that symbolizes acid-base interactions [62]. The derived equation for surface free energy and its polar component can be expressed as [68]:

$$\gamma_i^{TOT} = \gamma_i^d + \gamma_i^p \tag{2.2}$$

$$\gamma_i^p = 2\sqrt{\gamma_i^A * \gamma_i^B} \tag{2.3}$$

where γ^{A} and γ^{B} represent the acid and base component of the surface tension, respectively.

Equation 2.4 is derived for the interactions of a solid with a polar liquid.

$$(1 + cos\theta)\gamma_j^{TOT}) = 2\left\{\sqrt{\gamma_i^d\gamma_j^d} + \sqrt{\gamma_i^A\gamma_j^B} + \sqrt{\gamma_j^A\gamma_i^B}\right\} \quad (2.4)$$

Equation 2.4 is reduced to Equation 2.5 for nonpolar liquids due to the absence of acid-base interactions.

$$(1 + cos\theta) * \gamma_j^{TOT}) = 2 * \left\{\sqrt{\gamma_i^d * \gamma_j^d}\right\} \quad (2.5)$$

In the study conducted by Köysüren [69], three different probe liquids which are diiodomethane (DIM), ethylene glycol (EGL) and formamide (FA) were utilized to calculate surface free energies of PP-based and PET-based composites. The dispersive, acid and base components of these probe liquids are given in Table 1.

Table 1. *Total surface energy values and surface energy components of probe liquids [69].*

Probe Liquids	γ^{TOT}	γ^d	γ^p	γ^A	γ^B
DIM	50.8	50.8	-	-	-
EGL	48.0	29.0	19.0	3.0	30.1
FA	58.0	39.0	19.0	2.3	39.6

The contact angle between the composite surface and diiodomethane which is a nonpolar liquid was measured, and with the help of Equation 2.5, dispersive component was easily calculated. After that, the contact angles of the composite surface with ethylene glycol and formamide which are polar liquids were also measured. For each polar liquid, Equation 2.4 was arranged by placing the contact angle value and other known values (surface energy components of probe liquids). Eventually, obtained two equations were solved simultaneously and polar component was found. Finally, by using Equation 2.2 and Equation 2.3, total surface free energy of that composite was calculated.

2.6. The Scope of the Thesis

Epoxy is one of the most popular thermoset matrices in the industry due to diverse benefits provided by its infusible crosslinked network. Along with its many advantages in composite manufacturing, it has several drawbacks such as low toughness resulting from its highly brittle structure, high flammability and low electrical conductivity, which restrict its processing and applications [70].

In the literature, there are many studies related to enhancing mechanical, thermal, and conductivity properties of epoxy by the incorporation of micro/nano size fibers and particles [18, 52, 57]. However, it was realized that limited number of studies focused on the improvement of multifunctional properties of epoxy by EG or TiO_2 particles [30, 34, 40]. Although carbon-based fibers or particles were frequently introduced to epoxy matrix by researchers to develop mechanical properties, electrical and thermal conductivities, a few of them considered their influences on thermal stability and surface properties (hydrophobicity) [35, 36]. On the other hand, the TiO_2 addition into epoxy matrix was generally evaluated in terms of mechanical, thermal and surface properties [40, 41]. However, a study concerning the effects of TiO_2 particles on the flammability of epoxy has not been found in the literature yet.

In addition, epoxy-based hybrid composites were generally prepared by the incorporation of similar type of reinforcement materials. For instance, graphite nanoplatelets and carbon nanotubes were used together [71] or TiO_2 and SiO_2 particles were simultaneously added to epoxy matrix [72]. With the limited availability of studies on the synergistic effects of organic and inorganic particles, physical and chemical properties of epoxy-based hybrid composites containing both EG and TiO_2 particles were investigated in the literature very rarely.

In this thesis, a comprehensive study related to multifunctional properties of the E/EG/T hybrid composites and coatings along with the E/EG and E/T binary composites and coatings was carried out. Primarily, the influences of the individual

addition of EG and TiO_2 particles at different concentrations on mechanical properties, thermal stability and surface properties were investigated. Moreover, flammability analysis was performed for the E/T composites whereas electrical resistivity was measured for the E/EG composites. Later on, the E/EG/T hybrid composites and coatings were prepared with three different formulations and the synergistic effect of EG and TiO_2 particles on mechanical properties, thermal stability, flammability, electrical conductivity and surface properties were analyzed.

CHAPTER 3

EXPERIMENTAL

3.1. Materials

3.1.1. Epoxy Resin

The reactive diluted epoxy resin, Polires 114, was purchased from Polikem Kimyevi Maddeler San. Tic. Ltd. Şti. This glycidyl-ether type epoxy resin is a very low viscosity liquid, which is provided by the addition of a reactive diluent, and it is synthesized by the reaction of bisphenol A [$(CH_3)_2C(C_6H_4OH)_2$] with epichlorohydrin [C_3H_5ClO] in the presence of a basic catalyst. It is mostly cured by polyamine or polyamide hardeners. The general properties of Polires 114 epoxy resin which was taken from the technical data sheet provided by Polikem are given in Table 2.

Table 2. *The properties of Polires 114 [73].*

Properties	Value
Weight per epoxy equivalent, g/eq	195-206
Viscosity at 25°C, cps	600-800
Specific Gravity	1.12-1.15
Color number (gardner)	1

3.1.2. Curing Agent

The curing agent, Epilox®-Hardener M 1164, is a modified polyamine adduct hardener for epoxy resins, and was purchased from Polikem Kimyevi Maddeler San.

Tic. Ltd. Şti. Table 3 indicates the general properties of this curing agent which was obtained from the technical data sheet.

Table 3. *The properties of Epilox®-Hardener M 1164 [74].*

Property	**Value**
NH-equivalent weight, g	93
Amine number, mg KOH/g	300-350
Viscosity at 25°C, cps	170-270
Density at 20°C, g/cm^3	1.04
Color number (gardner)	< 2

3.1.3. Expanded Graphite (EG)

The expanded graphite (EG), Timrex® C-Therm 001, which is a chemically inert carbon-based material, was supplied by TIMCAL. It is usually obtained by the expansion of intercalated graphite particles at high temperature. The general properties provided by the supplier are shown in Table 4.

Table 4. *The properties of Timrex® C-Therm 001 [75].*

Property	**Value**
Ash content, wt. %	0.3
Bulk density, g/cm^3	0.15

3.1.4. Titanium Dioxide (TiO_2)

The titanium dioxide (TiO_2), which is generally called as titania, was provided by Onay Boya Kimya İmalat İhracat San. Tic. A.Ş. with the trade name of TiOx-280.

The particles are in rutile phase and were exposed to surface treatment with zirconium, aluminum and organic compounds. The general properties of titania provided by the supplier are given in Table 5.

Table 5. *The properties of TiOx-280* [76].

Property	**Value**
Mass fraction of TiO_2, wt. %	92
Moisture when packed, wt. %	0.5
Residue on sieve 45μm (325 mesh), wt. %	0.010
pH of water suspension	6.5-8.0
Tint reducing power, arb. units	2000-2300
Specific density, g/cm^3	3.9
Opacity, g/cm^2	23-25
Dispersibility, μm	11-13
Oil absorption, g/100g of pigment	18-20
Whiteness, arb. units	96.5-97.0

3.1.5. Acetone

Acetone which was purchased from Sigma Aldrich was utilized as a solvent in the preparation of the neat epoxy and the composites. Its general properties obtained from the technical data sheet are shown in Table 6.

Table 6. *The properties of Acetone [77].*

Property	Value
Molecular Formula	$(CH_3)_2CO$
Purity, % (GC)	≥ 99
Density at 20°C, g/mL	0.790-0.792
Melting point at 1 atm, °C	-94
Boiling point at 1 atm, °C	56
Vapor pressure at 20°C, mmHg	184

3.2. Experimental Procedure

3.2.1. Preparation of Neat Epoxy

The preparation process of neat epoxy is presented as a flow chart in Figure 6. Primarily, epoxy resin (ER) and curing agent (CA) were separately degassed in an oven at 40°C under vacuum for 2 hours to remove air bubbles and lower their viscosities for better mixing. In the meantime, acetone was exposed to ultrasonication in a cold water bath for 5 hours. Next, sonicated acetone and degassed epoxy resin were mixed by magnetic stirrer at 60°C until all of the acetone was evaporated. After acetone was completely removed, epoxy resin was again kept in the oven at 40°C under vacuum for 30 minutes to remove air bubbles formed during magnetic mixing, and then, cooled to room temperature. Subsequently, epoxy resin and curing agent at room temperature were mechanically mixed at 40 rpm for 25 minutes with a mixing ratio (epoxy/curing agent) of 100:50 by weight. Later on, the mixture of epoxy resin and curing agent was poured into the silicone molds which have many advantages over other mold types such as high flexibility, non-stick property, heat and solvent resistance, weatherability, water repellency and

long-lasting durability [78]. The preparation of silicone molds is given in Appendix A. After that, the molded samples were kept at room temperature for 30 minutes to initiate pre-curing process. Finally, the molds were put into the oven for further curing at 90°C for 16 hours and post-curing at 130°C for 3 hours.

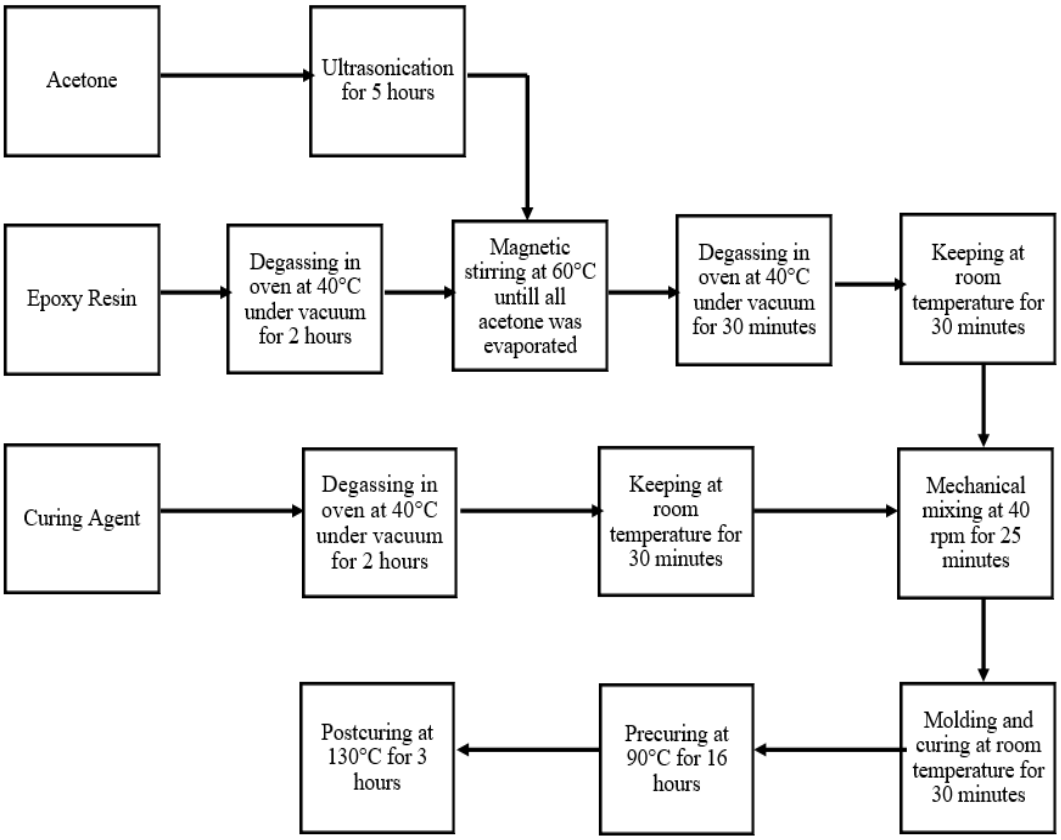

Figure 6. Flowchart of the preparation of the neat epoxy.

3.2.2. Preparation of Epoxy-based Composites Containing EG or TiO_2

In this study, epoxy composites reinforced with 0.5 wt. % EG were primarily prepared by 3 different processing techniques which are direct mixing method, solvent-free sonication method and sonication with the use of solvent method. Mechanical test results of the epoxy with 0.5 wt. % EG composites fabricated by these methods were evaluated in order to determine the most efficient method for

further epoxy-based composite preparation providing the most homogeneous dispersion of EG particles in the matrix. Afterwards, epoxy/EG and epoxy/TiO_2 composites were fabricated with the application of the chosen processing method.

3.2.2.1. Direct Mixing Method

The block diagram of the direct mixing method is given in Figure 7. Firstly, epoxy resin and curing agent were separately degassed in the oven at 40°C under vacuum for 2 hours to eliminate air bubbles and reduce their viscosities. Next, EG was directly added into the curing agent and mixed by magnetic stirrer at room temperature for 24 hours. Following the magnetic stirring, the mixture was again degassed in the oven at 40°C under vacuum for 30 minutes to get rid of air bubbles formed during mixing. Then, epoxy resin was added into the mixture at room temperature, and it was mechanically stirred at 40 rpm for 25 minutes. Finally, the composite mixture was poured into the silicone molds and cured as carried out in the neat epoxy preparation.

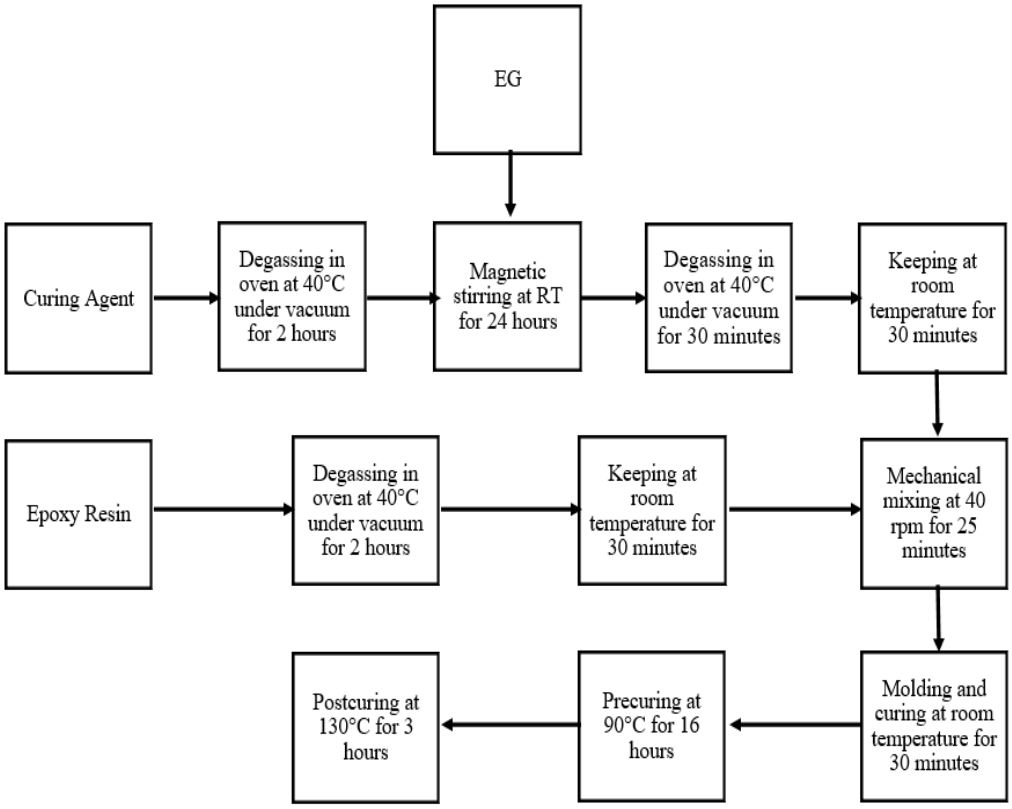

Figure 7. Block diagram of the epoxy-based composite preparation by direct mixing method.

3.2.2.2. Solvent-free Sonication Method

Figure 8 presents the solvent-free sonication method as a block diagram. Primarily, epoxy resin and curing agent were degassed in the oven at 40°C under vacuum for 2 hours as in the case of direct mixing method. At the same time, EG was added into acetone and the solution was sonicated in a cold bath for 5 hours. Next, the solution was mixed on a hot plate (approx. 60°C) until all acetone was evaporated. After that, degassed epoxy resin was added onto dried EG powder and mixed by magnetic stirrer at room temperature for 3 hours. In pursuit of the mixing, it was kept in the oven at 40°C under vacuum for 30 minutes for degassing. Lastly, the curing agent was added at room temperature, and the mixture was mechanically stirred at 40 rpm for 25 minutes. At the end of the final mixing process, the composite mixture was molded and cured in the same way as in the direct mixing method.

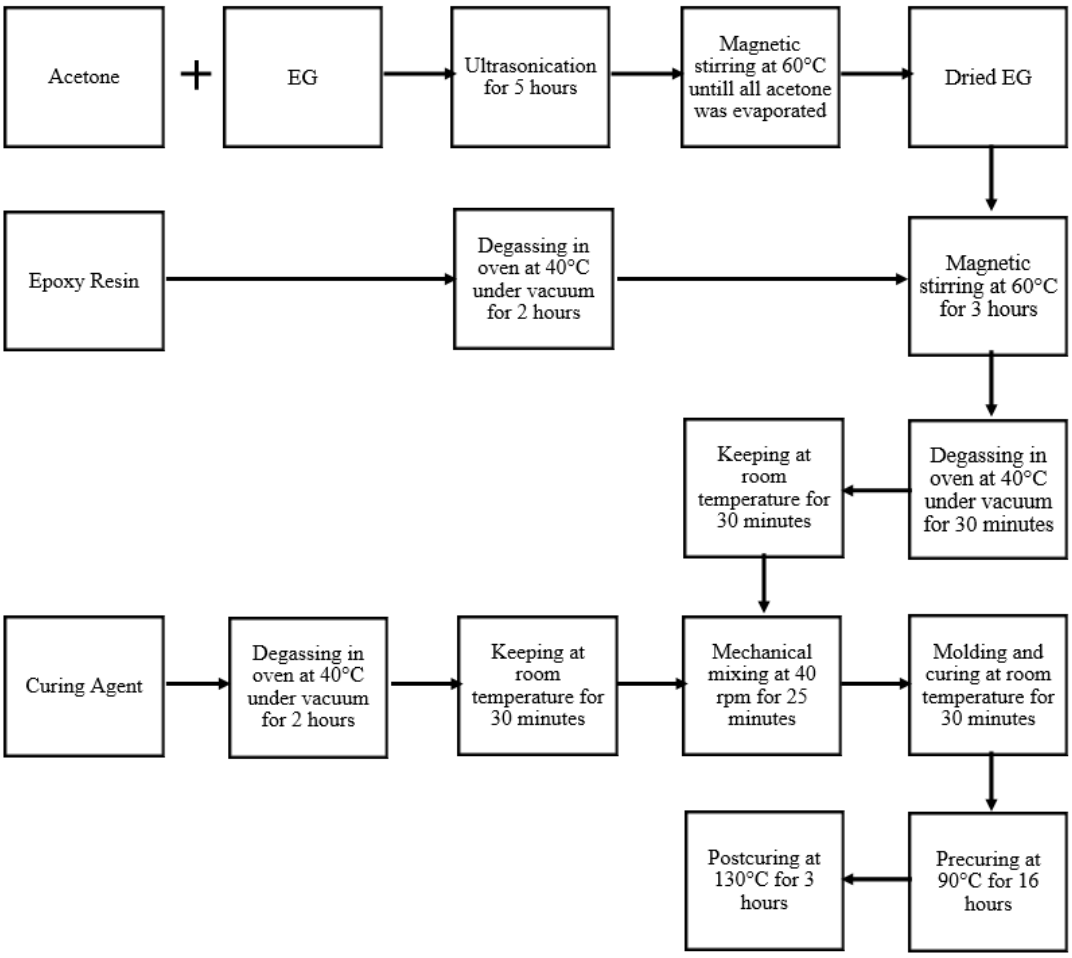

Figure 8. Block diagram of the epoxy-based composite preparation by solvent-free sonication method.

3.2.2.3. Sonication with the Use of Solvent Method

The steps of the sonication with the use of solvent method are shown in the block diagram given in Figure 9. The main difference from the solvent-free sonication method is the addition of epoxy resin before the evaporation of acetone. In this technique, the steps of degassing of the matrix materials and ultrasonication of the solution containing acetone and EG were initially performed as in the solvent-free sonication method. After the solution was sonicated for 5 hours, degassed epoxy resin was instantly added to the solution and mixed by magnetic stirrer on a hot plate until all acetone was removed. Later on, the mixture of epoxy resin and EG was put

into the oven and held at 40°C under vacuum for 30 minutes. Finally, degassed and cooled curing agent was mechanically blended with the mixture, which was also cooled to room temperature, at 40 rpm for 25 minutes, and then, the composite mixture was molded and exposed to the same curing process which was performed in the other methods.

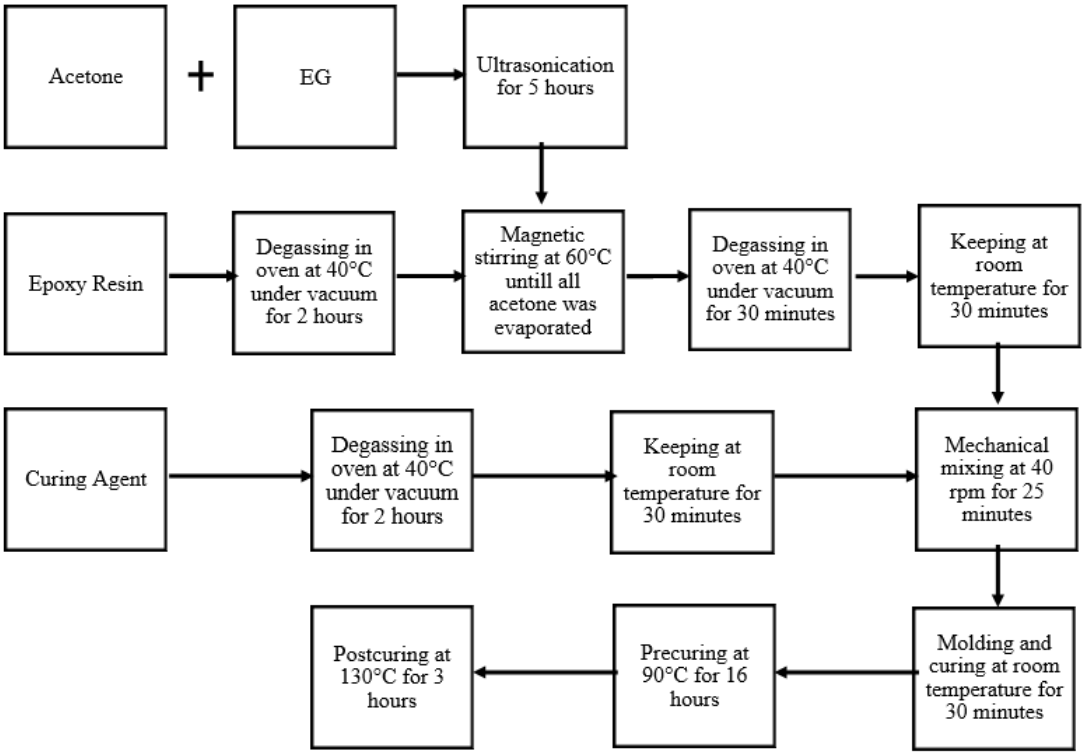

Figure 9. Block diagram of the epoxy-based composite preparation by sonication with the use of solvent method.

3.2.3. Preparation of Epoxy-based Hybrid Composites Containing Both EG and TiO_2

Epoxy-based hybrid composites which contain 0.1 wt. % EG and 0.5 wt. % TiO_2 particles were initially fabricated by the same processing method, preparation process I (PP1), used in the preparation of epoxy/EG and epoxy/TiO_2 composites. The flowchart of PP1 is given in Figure 10. As performed in the earlier composite

preparations, epoxy resin and curing agent were initially degassed whereas the solution of acetone and blended particles was exposed to ultrasonication for 5 hours. Later, degassed epoxy resin was added to the solution and mixed by a magnetic stirrer on a hot plate till acetone was completely evaporated. Next, the mixture of epoxy resin and particles was again degassed in the oven for another 30 minutes and cooled to room temperature. Then, it was mechanically stirred with the curing agent, which was also cooled to room temperature after degassing, at 40 rpm for 25 minutes. Finally, the hybrid composite mixture was molded and cured same as before. However, simultaneous incorporation of both reinforcement materials caused poor mixing owing to sudden increase in viscosity of the mixture and also resulted in formation of many air bubbles. For this reason, the old processing method was modified in 3 different ways.

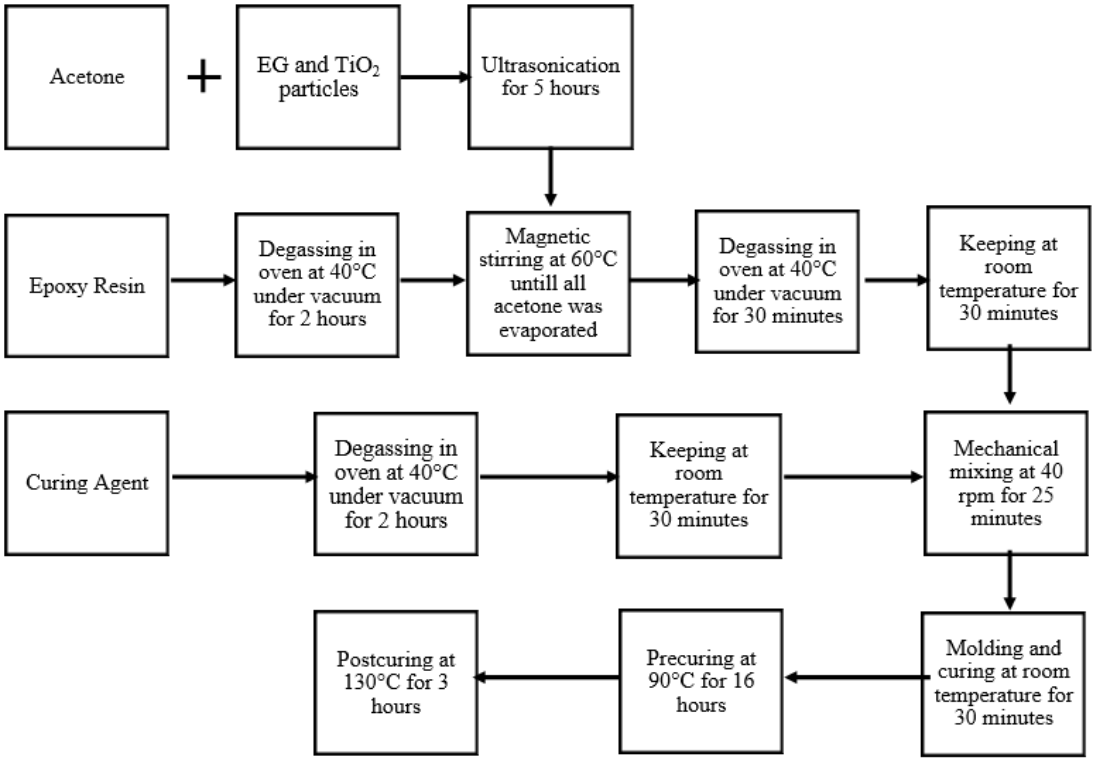

Figure 10. Flowchart of the preparation of the epoxy-based hybrid composites by PP1.

In the preparation process II (PP2), the mixture of epoxy resin and particles was also mechanically mixed at 400 rpm for 2 hours after magnetic stirring since more powerful and intense mixing was required to handle the increased viscosity and to obtain better dispersion. With the addition of this step, PP2 provided easier and much more homogeneous dispersion of the particles in the matrix, but also caused increase in the number of air bubbles due to high mixing rate. In preparation process III (PP3), to overcome the air bubble problem, the mixture was kept in oven at 40°C under vacuum after mechanical mixing for a longer time which is 24 hours. At the end of the process, it was observed that air bubbles were decreased but not totally eliminated. Therefore, the degassing temperature after mechanical mixing was increased from 40°C to 80°C in preparation process IV (PP4). With all these modifications which are addition of mechanical mixing, prolonging degassing period and increasing degassing temperature after mechanical mixing, PP4 resulted in better outcomes in terms of dispersion of the particles and physical structure of the composites although air bubbles were not completely eliminated. Consequently, other hybrid composites which have different formulations were produced by the application of PP4. The flowchart of PP4 is presented in Figure 11.

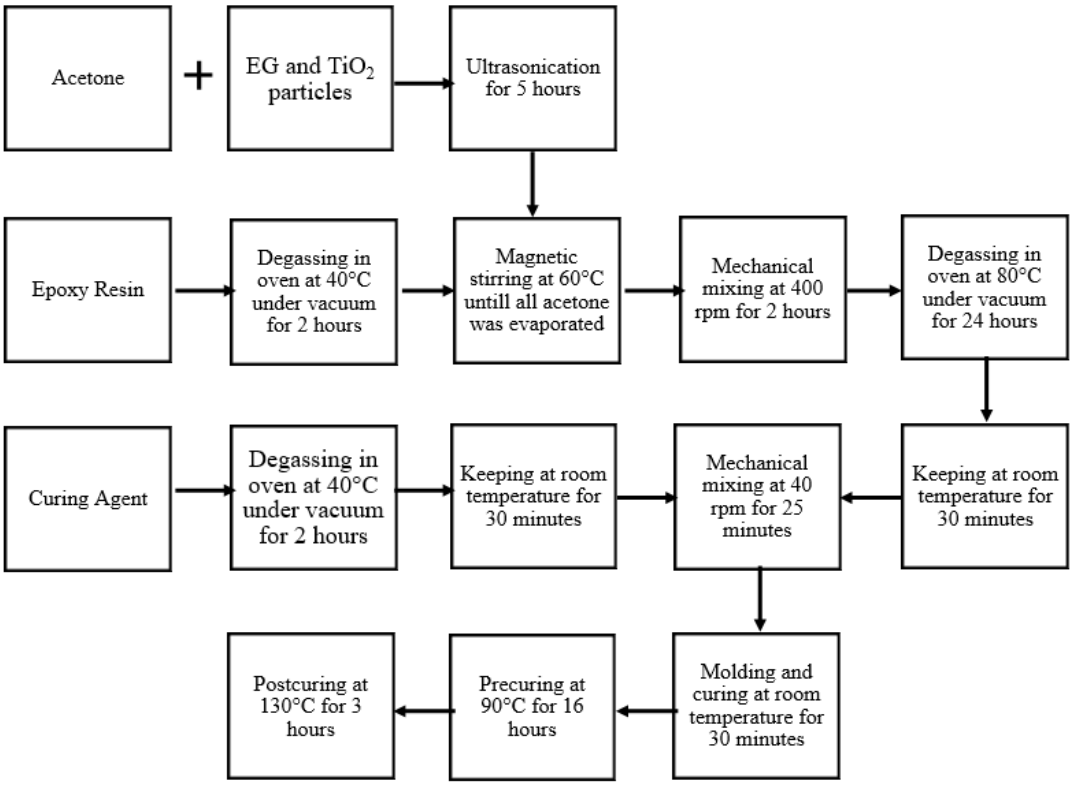

Figure 11. Flowchart of the preparation of the epoxy-based hybrid composites by PP4.

3.2.4. Preparation of Epoxy-based Coatings

After the composite mixture was prepared by the chosen method, small amount of it was spread over an 8x8 cm glass surface by a plastic film applicator while the rest of it was poured into the silicone molds. The thickness of the coatings was approximately 0.5 mm and the coated glass surfaces were cured in the oven as mentioned in the preparation of epoxy-based composites.

Table 7 shows the composition of the neat epoxy and all of the epoxy-based composites. It should be noted that formulations of hybrid composites were decided based on mechanical properties of epoxy/EG and epoxy/TiO_2 composites.

Table 7. *Compositions of the neat epoxy and the epoxy-based composites.*

Sample Code	Composition (%)		
	E (ER:CA=2:1)	**EG**	**TiO_2**
E	100	-	-
E/0.05EG	99.95	0.05	-
E/0.1EG	99.90	0.1	-
E/0.25EG	99.75	0.25	-
E/0.5EG	99.50	0.5	-
E/0.75EG	99.25	0.75	-
E/1EG	99.00	1	-
E/0.5T	99.50	-	0.5
E/1T	99.00	-	1
E/2T	98.00	-	2
E/5T	95.00	-	5
E/0.05EG/0.5T	99.45	0.05	0.5
E/0.1EG/0.5T	99.40	0.1	0.5
E/0.1EG/5T	94.90	0.1	5

3.3. Characterization Methods

3.3.1. Mechanical Characterization of Epoxy-based Composites

3.3.1.1. Tensile Test

The tensile test was performed at room temperature with a Shimadzu Autograph AG-IS 100 kN universal tensile testing instrument, which is photographed in Figure 12, on the dog bone shape specimens produced according to ASTM D638-10. The dimensions of the specimen are given in Table 8. For the tensile test, the load cell was selected as 100 kN whereas the crosshead speed was specified as 4 mm/min. In virtue of the data provided by this test, tensile strength, elastic modulus and elongation at break values of the composites were easily calculated. To determine the exact values, five specimens for each formulation were tested, and their average tensile properties with standard deviations were calculated.

Figure 12. Shimadzu Autograph AG-IS 100kN universal tensile test instrument.

Table 8. *The dimensions of the tensile test specimen.*

Property	Value
Length, mm	115
Gauge Length, mm	65
Width, mm	6
Thickness, mm	4

3.3.1.2. Impact Test

The impact test was carried out at room temperature with a Ceast Resil Impactor 6967 instrument, which is given in Figure 13, on the bar shape specimens prepared with respect to ISO 179 standard. Table 9 shows the dimensions of the specimen. During the impact test, a 7.5 J pendulum was used, and the impact energy values of the specimens based on their cross-sectional area were measured. After the test was applied to five specimens for each formulation, the average of their impact strength and their standard deviation were calculated.

Figure 13. Ceast Resil Impactor 6967 impact test instrument.

Table 9. *The dimensions of the impact test specimen.*

Property	Value
Length, mm	80
Width, mm	10
Thickness, mm	4

3.3.1.3. Shore D Hardness Test

Shore D hardness test was applied to bar shape specimens at room temperature according to ASTM D 2240 standard with an instrument which is photographed in Figure 14. Two measurements were taken from one specimen while five specimens were tested in total for each formulation. Therefore, Shore D hardness value of each formulation was calculated by taking average of ten data. In addition to this, standard deviation of ten data for each formulation was also determined.

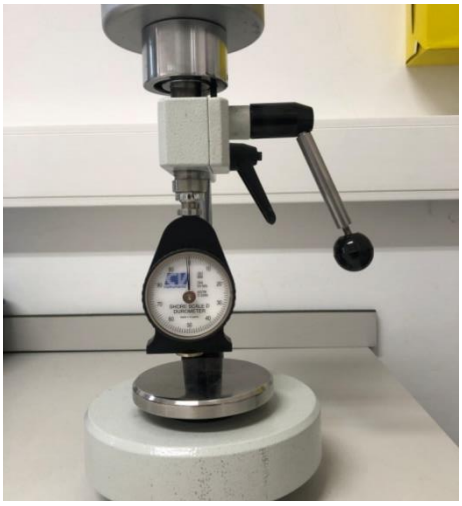

Figure 14. Shore D hardness test instrument.

3.3.2. Thermal Analyses

3.3.2.1. Differential Scanning Calorimeter (DSC) Analysis

Differential scanning calorimetry analysis was carried out on cured and uncured neat epoxy and cured epoxy-based composites using a Shimadzu DSC-60 differential scanning calorimeter. During the analysis, samples were heated from room temperature to 200°C with a rate of 10°C/min under nitrogen atmosphere to observe the curing degree of neat epoxy and the glass transition temperatures (T_g) of cured samples. The calculation of curing degree for epoxy is given in Appendix B. Besides, T_g values of the neat epoxy and all composites were validated after the analysis was repeated for three samples which have same formulation.

3.3.2.2. Thermal Gravimetric Analysis (TGA)

Thermogravimetric analysis was performed using a Shimadzu DTG-60/60H instrument in order to observe the influences of EG or/and TiO_2 addition on the thermal stability, thermal degradation temperature and char yield of the epoxy as well as determining the thermal stability of the neat epoxy, EG and TiO_2 particles. In TGA analysis, samples were heated from room temperature to 800°C with a rate of 10°C/min under nitrogen atmosphere.

3.3.3. Morphological Analysis

3.3.3.1. Scanning Electron Microscopy (SEM) Analysis

In SEM analysis, QUANTA 400F field emission scanning electron microscope was utilized to analyze the morphology of pure EG and TiO_2 particles, and to obtain information about the dispersion of the particles in the epoxy matrix and failure mechanism by examining the fractured surfaces of the tensile test samples. Before the analysis, fractured surfaces of the composites were coated with a thin layer of gold-palladium alloy in order to provide conductivity for the analysis.

3.3.3.2. X-Ray Diffraction (XRD) Analysis

XRD analysis was executed for pure EG and TiO_2 particles using a Rigaku Ultima IV X-Ray diffractometer to evaluate the crystalline structure and phase based on their characteristic peaks. The EG and TiO_2 particles were scanned from 2° to 50° and 10° to 70° respectively with a rate of 1°/min by the diffractometer with a CuK_α radiation source operating at 40 kV and 30 mA. The test results are shown in Appendix C.

3.3.4. Flame Retardancy Characterization of Epoxy-based Composites

3.3.4.1. Limiting Oxygen Index (LOI) Test

LOI test was performed on bar shape specimens of neat epoxy and epoxy-based composites with the use of a Dynisco polymer LOI test instrument, which is shown in Figure 15, according to ASTM D2863 standard to observe the effects of additives and their concentrations on the flammability of epoxy. Schematic representation of the test is given in Figure 16. During the test, the bar shape specimen which was placed vertically between holders was ignited from the top, and the oxygen concentration in the mixture of O_2 and N_2 which was required for burning of 50 mm distance or burning in 180 seconds was determined.

Figure 15. Dynisco polymer LOI test instrument.

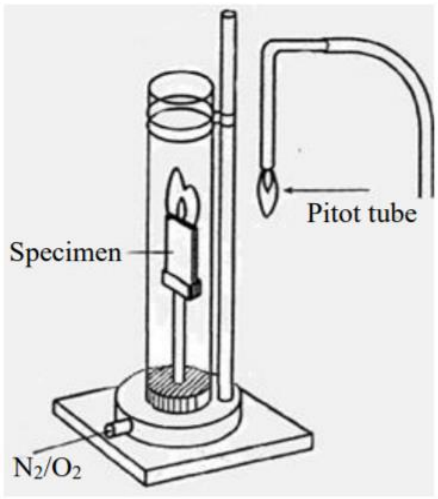

Figure 16. Schematic representation of the LOI test [79].

LOI values were calculated by Equation 3.1 after at least two samples of each set of composites showed the same behavior at that particular O_2 concentration.

$$\text{LOI } (O_2\%) = \frac{[O_2]}{[O_2] + [N_2]} \text{x} 100 \tag{3.1}$$

3.3.5. Electrical Characterization of Epoxy-based Composites

Electrical or volume resistivity of neat epoxy and epoxy-based composites which is usually defined as resistance to current flow was measured by Keithley 2400 two-point probe resistivity determiner that is photographed in Figure 17. Schematic representation of the test is given in Figure 18.

Figure 17. Two-point probe electrical resistivity determiner, Keithley 2400.

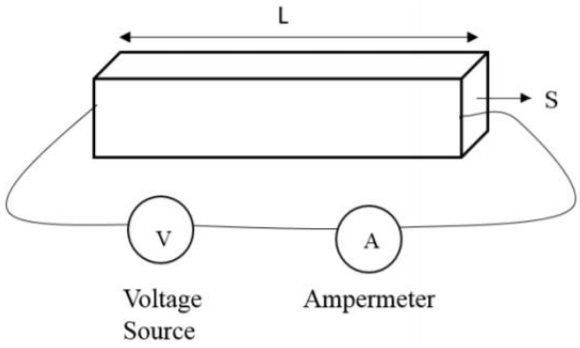

Figure 18. Schematic representation of the electrical resistivity measurement [79].

In the test, the probes were separately attached to two ends of the rectangular prism shape specimen and the resistance value (R) related to its dimensions was measured. After that, the volume resistivity (ρ) which is inherent in the material was calculated by using Equation 3.2.

$$\rho = \frac{R \times S}{L} \tag{3.2}$$

In the equation, S represents the cross-sectional area of the specimen whereas L is the distance between the probes. The constant voltage was specified as 20 V during

the tests, and it was repeated on five samples of each set of composites to achieve high accuracy.

3.3.6. Surface Characterization of Epoxy-based Coatings

3.3.6.1. Water Contact Angle (WCA) Measurement

The contact angle between coatings and water droplets were measured in order to evaluate water repellency property of the coatings and to observe the influences of additives on the hydrophobicity level of epoxy. During the measurement, 10μL of distilled water was dropped onto the coating surface and this period was recorded as a video. Then, the moment that the water droplet was stabilized on the surface was photographed and the contact angle was measured by FIJI-Image J program. On each coating surface, three measurements were carried out and the average of three contact angles together with standard deviation was determined.

3.3.6.2. Surface Energy Calculation

The surface energy calculation was required to interpret the hydrophobicity of the coatings in addition to water contact angle. Primarily, 10 μL of probe liquids which are diiodomethane (DIM), ethylene glycol (EGL) and formamide (FA) were separately dropped onto the coating surfaces. As carried out in the water contact angle measurement, it was recorded as a video, and then, the pictures of stabilized droplets were taken to measure the contact angles by FIJI-Image J program. This measurement was repeated for three times for each probe liquid on one coating. After the average contact angles between the coatings and probe liquids were determined, those values were utilized in the Young equation to calculate the surface energy values of the coatings.

CHAPTER 4

RESULTS AND DISCUSSION

4.1 Determination of Mixing Method for E/EG and E/T Composites

Dispersion quality of organic or inorganic particles in polymer matrix strongly affects physical and chemical properties of the composite since the matrix-reinforcement interactions can be enhanced by exfoliation and homogeneous distribution of the particles [20]. For this reason, determining the processing technique for the preparation of epoxy-based composites became the preliminary purpose in this study. In accordance with this purpose, epoxy with 0.5 wt.% EG composites were fabricated by three different mixing methods. Mechanical properties and morphologies of the E/0.5EG composites prepared by these methods were comparatively evaluated to decide on the most sufficient one which provided the best dispersion of the particles in the epoxy matrix. In the subsequent experiments, epoxy-based composites that contained EG or TiO_2 particles at different loadings were produced by the application of the chosen method.

4.1.1. Mechanical Properties of E/0.5EG Composites Fabricated by Different Mixing Methods

Tensile and impact tests were carried out on epoxy-based composites for 0.5 wt.% EG loading fabricated by direct mixing method, solvent-free sonication method and sonication with the use of solvent method to observe the influences of processing technique on mechanical properties. Figures 19-22 show tensile strength, elastic modulus, elongation at break and impact strength values of the E/0.5EG composites prepared by these three methods whereas their values are given in Appendix D.

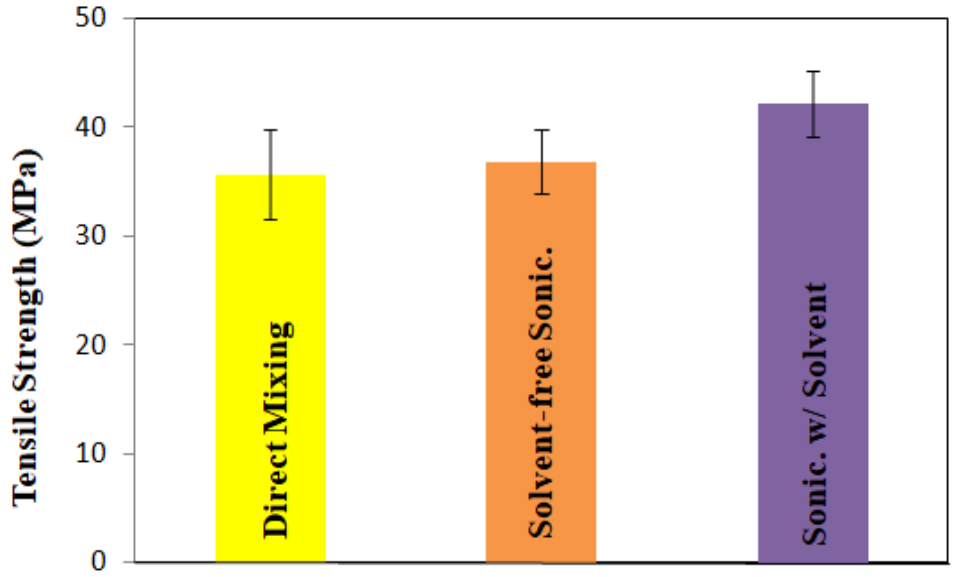

Figure 19. Tensile strengths of E/0.5EG composites prepared by different mixing methods.

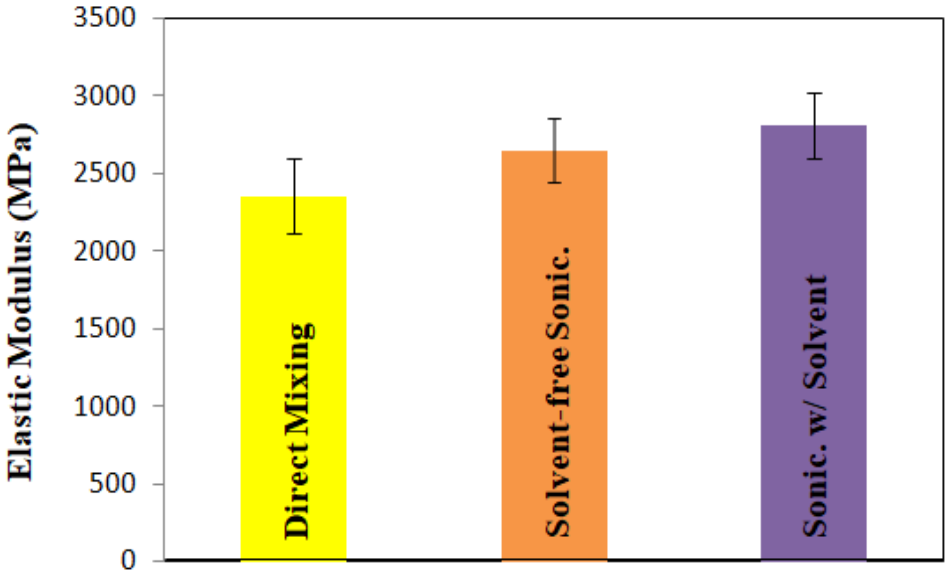

Figure 20. Elastic moduli of E/0.5EG composites prepared by different mixing methods.

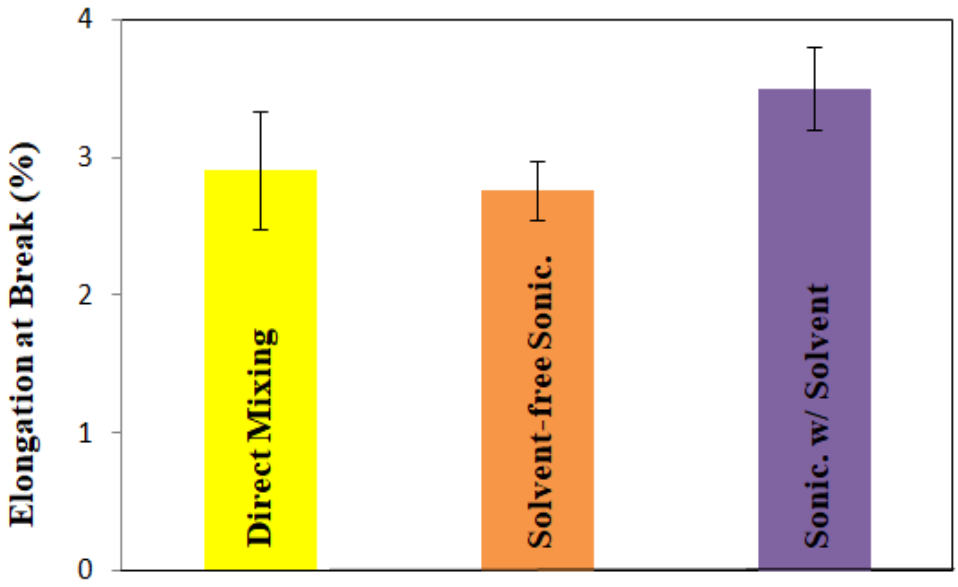

Figure 21. Elongation at break of E/0.5EG composites prepared by different mixing methods.

Due to the fact that tensile properties of the composites mostly depend on the interface properties along with the individual characteristics of the matrix and the reinforcement materials, the enhancement in mechanical properties can be attributed to improved matrix-reinforcement interactions which provide better dispersion [43]. When the tensile test results of the composites were analyzed, it was observed that sonication with the use of solvent method provided higher tensile strength, elastic modulus and elongation at break value with respect to others whereas direct mixing method resulted in the lowest tensile strength and elastic modulus. This showed that sonication of the particles in a solvent before being mixed with the epoxy resin or the curing agent improved their dispersion in the matrix, and thus, mechanical properties. The EG particles that were separated during the sonication process exhibited higher surface area of contact with the matrix molecules, and therefore, provided enhanced matrix-reinforcement interactions. For this reason, separated particles could be dispersed much more homogeneously in the matrix, which resulted in higher tensile properties. Moreover, the composites produced by the sonication with the use of solvent method had higher tensile properties compared to

the ones prepared by the solvent-free sonication method although the particles were exposed to sonication in both techniques. The difference between these two methods was associated to evaporation of the solvent (acetone) before epoxy resin addition in solvent-free sonication method since EG particles may be stuck together again with the removal of acetone, forming agglomerates in the matrix. In the sonication with the use of solvent method, the presence of acetone during mixing of epoxy resin and EG particles further enhanced the dispersion by lowering the viscosity and making the insertion of epoxy molecules between EG layers easier.

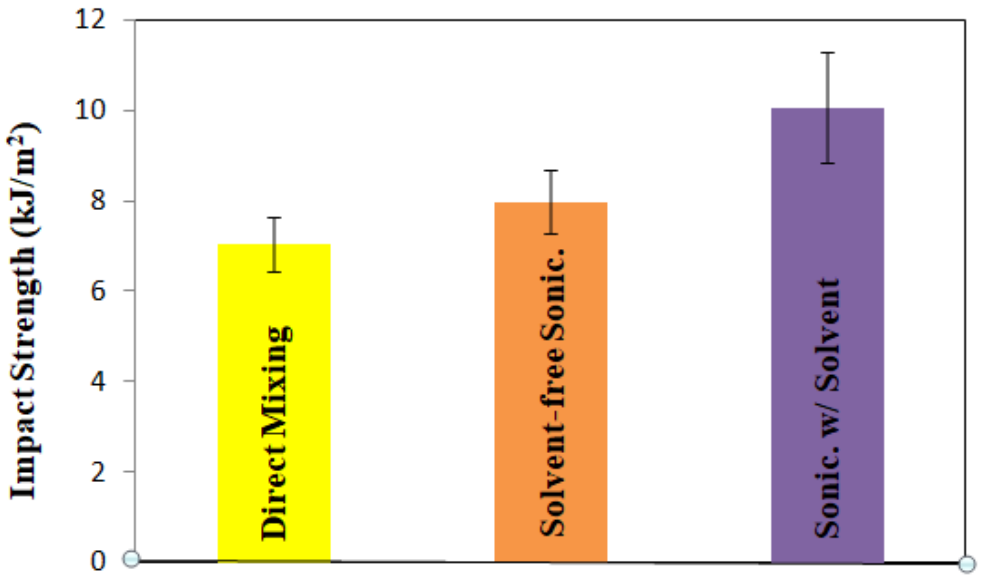

Figure 22. Impact strengths of E/0.5EG composites prepared by different mixing methods.

Dispersion of the particles in epoxy matrix also plays a crucial role in impact strength of the composites due to the fact that homogeneous distribution of EG particles delays the crack formation and increases the possibility of cracks to be deflected by the particles [80]. According to the impact test results, the composites prepared by direct mixing method had the lowest impact strength, which probably resulted from the formation of agglomerates owing to poor interactions between the epoxy matrix and the EG particles. As observed in the tensile test, sonication of the

particles in the beginning increased the impact strength by improving their dispersion. In addition, mixing epoxy resin with the solution of acetone and EG instead of dried EG particles during the sonication with the use of solvent method also provided further increase in the impact strength because of more homogeneous distribution of less agglomerated EG particles in epoxy matrix.

Consequently, sonication with the use of solvent method provided better enhancement in all mechanical properties while the E/0.5EG composites fabricated by direct mixing method generally had the lowest tensile and impact properties compared to the others. In the study conducted by Yasmin et al., the effects of sonication on the mechanical properties of epoxy-based composites containing EG particles were investigated, and similar results were obtained [43].

4.1.2. SEM Analyses of E/0.5EG Composites Fabricated by Different Mixing Methods

Morphologies of the E/0.5EG composites which were separately prepared by direct mixing method, solvent-free sonication method and sonication with the use of solvent method were examined by SEM to observe the EG dispersion in the epoxy matrix. SEM images of the tensile fractured surfaces of the E/0.5EG composites fabricated by these three methods are given in Figure 23.

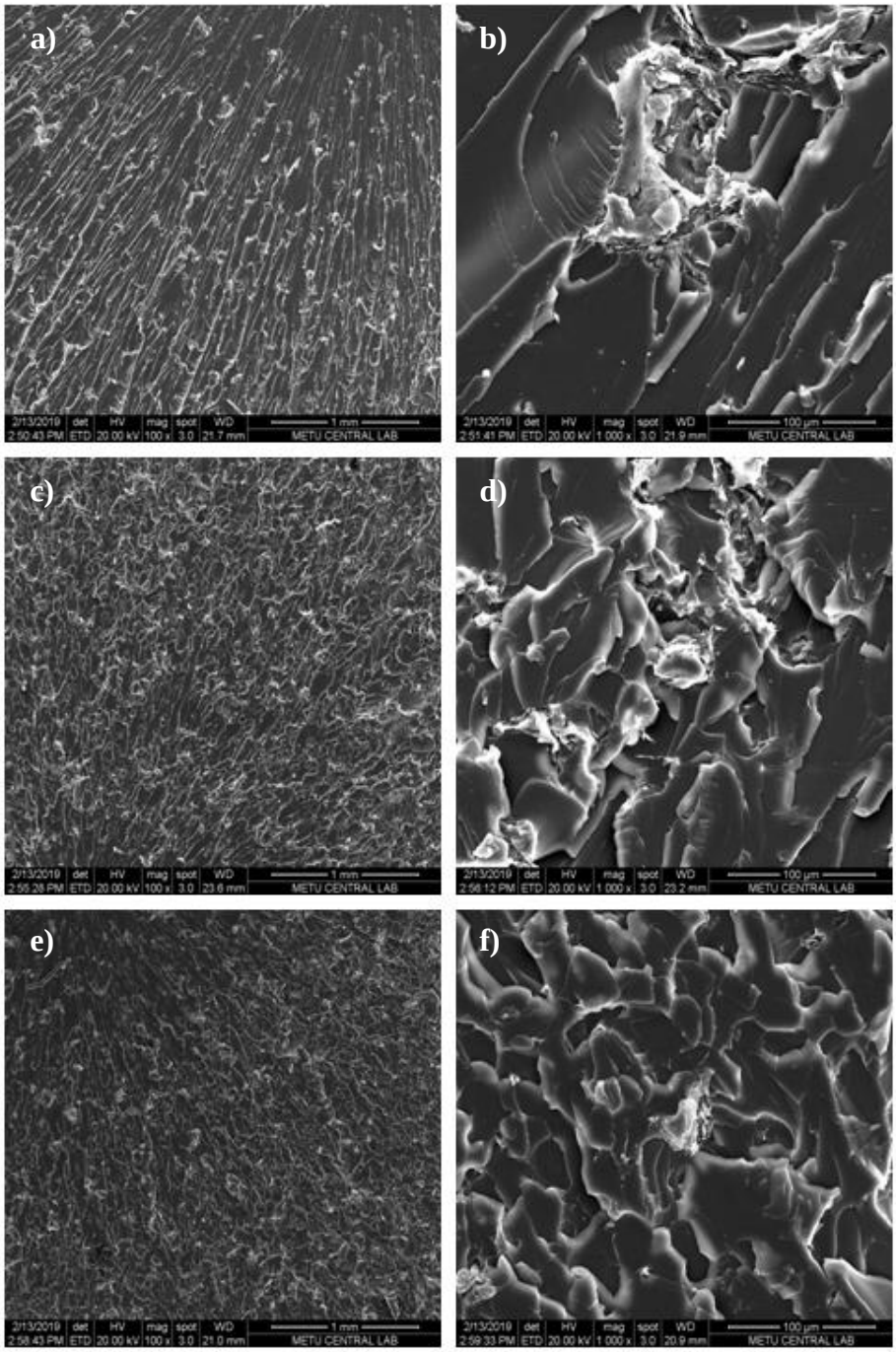

Figure 23. SEM images of a) the E/0.5EG by direct mixing at 100x magnification, b) the E/0.5EG by direct mixing at 1000x magnification, c) the E/0.5EG by solvent-free sonication at 100x magnification, d) the E/0.5EG by solvent-free sonication at 1000x magnification, e) the E/0.5EG by sonication with the use of solvent at 100x magnification and f) the E/0.5EG by sonication with the use of solvent at 1000x magnification.

As seen in Figures 23a and 23b, the composite produced by direct mixing method had smoother fracture surface, and it was realized that more straight cracks occurred during its failure. On the other hand, the composites prepared by solvent-free sonication method and sonication with the use of solvent method presented rougher fracture surfaces, and crack deflections were observed on their surfaces. In the literature, it is stated that smooth fracture surfaces and straight cracks indicates brittle structure and poor matrix-reinforcement interactions which result in easy debonding [80]. This explains why the composites fabricated by direct mixing method showed the lowest tensile and impact properties. In addition, it is also emphasized that rough fracture surfaces result from good interfacial properties, and deflecting cracks prevents failure upon an impact by providing energy absorption [80]. For this reason, the composites prepared by solvent-free sonication method and sonication with the use of solvent method showed higher tensile and impact properties compared to the one produced by direct mixing method. In addition, less agglomerations and higher uniformity were observed in the SEM images of the composite fabricated by sonication with the use of solvent method owing to mixing before solvent evaporation. Therefore, this method provided better enhancement in all the mechanical properties among the three different mixing methods.

4.2. Effects of EG or TiO_2 Addition to the Epoxy Matrix

After the most sufficient mixing method for epoxy-based composites was determined as the sonication with the use of solvent method, EG and TiO_2 particles were separately incorporated to the epoxy matrix with the application of this method. In this section, E/EG composites with 0.05, 0.1, 0.25, 0.5, 0.75 and 1 wt.% filler content and E/T composites with 0.5, 1, 2 and 5 wt.% filler content were characterized in terms of their mechanical and thermal properties, morphology, electrical conductivity and flammability. On the other hand, the surface properties of their coatings were analyzed by water contact angle (WCA) measurement and surface energy calculation.

4.2.1. Mechanical Properties of E/EG and E/T Composites

4.2.1.1. Tensile Test Results

The tensile properties of the neat epoxy, the E/EG composites and the E/T composites at different loadings are presented in Figures 24-26 whereas average results and standard deviation values are given in Appendix D.

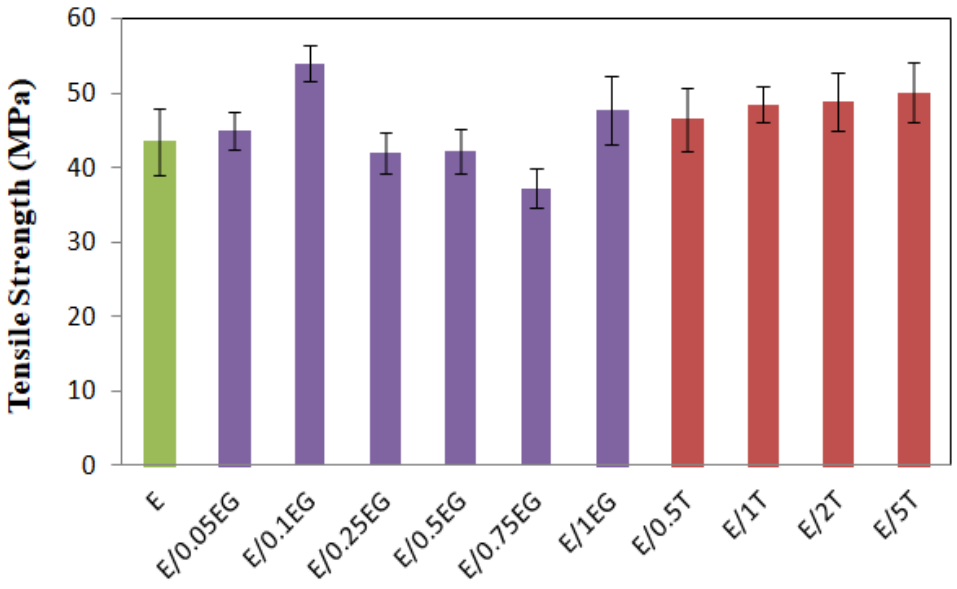

Figure 24. Tensile strengths of the neat epoxy, the E/EG and the E/T composites at different loadings.

When the tensile strength values of the E/EG composites that are shown in Figure 24 are considered, it is observed that 0.1 wt.% EG addition resulted in the highest tensile strength while the tensile strength of the composites significantly decreased as the EG amount was increased. In the literature, it is stated that EG particles enhance mechanical properties of the epoxy matrix when they could be separated and well-dispersed in the matrix. However, their high tendency to agglomerate due to van der Waals forces between graphene layers makes the insertion of epoxy molecules between the particles more difficult at high EG concentrations, causing formation of agglomerations. Therefore, stress concentrated regions occur in the

matrix at high EG loadings, which ends up in lower tensile strength [44]. In the light of this information, it can be said that the EG particles could be sufficiently separated and homogeneously dispersed at 0.1 wt.%, and the reduction in tensile strength beyond 0.1 wt.% EG addition resulted from agglomerations of EG particles. However, a slight increase in tensile strength was obtained when the EG amount reached 1 wt.%. This can be explained by the fact that EG agglomerations might behave like large graphite particles and reinforced the epoxy owing to their relatively homogeneous distribution in the matrix [81].

On the other hand, tensile test results of the E/T composites that are exhibited in Figure 24 revealed that tensile strength was continuously enhanced with the increase in TiO_2 amount in the composite and the highest tensile strength was obtained at 5 wt.% loading. This indicated that TiO_2 particles were less prone to form agglomerates compared to EG particles owing to their surface modification with organic compounds, and thus, they could be uniformly dispersed in the matrix even at high concentrations. For all E/T composites, increase in tensile strength can be associated to dispersion strengthening mechanism offered by small TiO_2 particles which was improved by the increase in the TiO_2 content [82].

Maximum enhancement in tensile strength was obtained for the E/0.1EG composites among all E/EG and E/T composites, and it was increased by 24% over the neat epoxy with 0.1 wt.% EG addition. The E/T composites generally had tensile strength values close to E/1EG composites, and 5 wt.% TiO_2 addition resulted in 15% increase in comparison to the tensile strength of the neat epoxy.

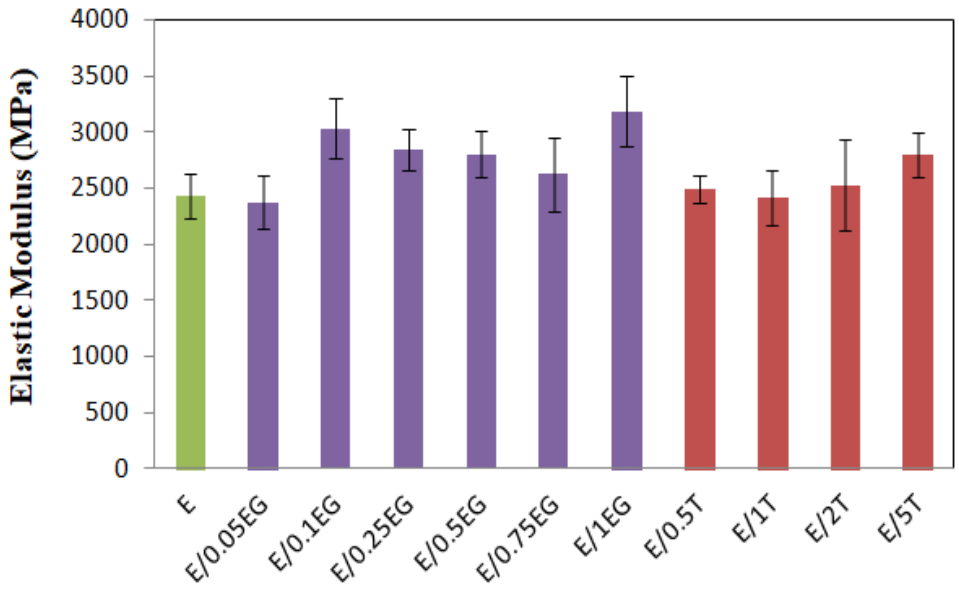

Figure 25. Elastic moduli of the neat epoxy, the E/EG and the E/T composites at different loadings.

According to elastic modulus values of E/EG composites which are presented in Figure 25, it can be stated that EG addition to epoxy matrix generally resulted in higher elastic modulus values with respect to the neat epoxy. At 0.1 wt.% EG loading, it was significantly enhanced due to well-dispersed stiff EG particles. However, a gradual reduction in elastic modulus was observed with the increase in EG content although those composites had still higher elastic modulus values than the neat epoxy. This reduction was attributed to formation of agglomerations at higher concentrations. In the study carried out by Young et al., it was observed that the increase in EG amount resulted in sudden increase of the viscosity that led to poor dispersion of the particles in the matrix. Therefore, the EG particles were aggregated, and the introduction of epoxy molecules between them was mostly inhibited. This situation caused the load transfer from the matrix to the particles to become insufficient, resulting in lower elastic modulus at higher particle concentrations [83]. Moreover, less force is required to achieve a certain strain in the composites having agglomerates due to the fact that the matrix constitute easily deformable regions in the structure. Thus, those composites present low elastic

modulus [84]. On the other hand, 1 wt.% EG addition exhibited unexpected increase in elastic modulus, which probably resulted from the reinforcing effect of large particles as occurred in the tensile strength [81].

Among all E/T composites, 5 wt.% TiO_2 addition provided a slight enhancement in the elastic modulus of epoxy while the other composites had similar values with the neat epoxy as seen in Figure 25. This showed that the high TiO_2 content provided the applied load to be carried mostly by the particles instead of epoxy matrix, and therefore, increased the elastic modulus. Moreover, the improvement in the elastic modulus by the TiO_2 incorporation into the crosslinked network of epoxy matrix was associated to increased stiffness in the study conducted by Al-Turaif [85].

When the elastic modulus values of all E/EG and E/T composites were compared to the elastic modulus of the neat epoxy, it can be stated that the highest improvement in elastic modulus was observed in E/1EG composites in which the modulus was increased by 25% over that of the neat epoxy. On the other hand, E/5T composites provided an increase of 15% over the elastic modulus of epoxy.

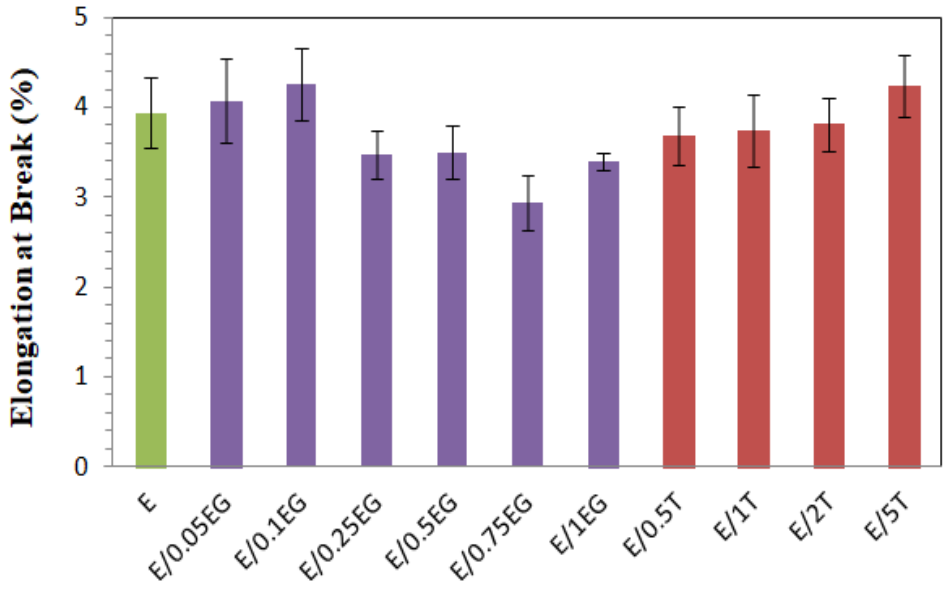

Figure 26. Elongation at break of the neat epoxy, the E/EG and the E/T composites at different loadings.

Elongation at break values of the E/EG composites which are given in Figure 26 showed that the EG addition up to 0.1 wt.% gradually increased the elongation amount of epoxy before failure whereas further increase in EG content decreased the elongation at break value below that of the neat epoxy. This can be explained by the fact that homogeneously dispersed EG particles increased the plastic deformation, and thus offered higher elongation before failure [80]. However, poor matrix-reinforcement interactions at high concentrations and the domination of the composites by highly brittle EG particles with the increase in EG amount led to decrease in elongation at break [86].

On the contrary, introduction of 0.5 wt.% TiO_2 to epoxy matrix decreased the elongation at break value below that of the neat epoxy, but the increase in TiO_2 content gradually enhanced the elongation and increased it over that of the neat epoxy at 5 wt.% loading. This showed that the addition of TiO_2 particles improved the extensibility of the epoxy matrix after a certain content [87].

When the elongation at break values of all E/EG and E/T composites are considered, the maximum enhancement is observed in the composites which contained 0.1 wt.% EG and 5 wt.% TiO_2 particles separately. Both formulations increased the elongation at break value of the neat epoxy by 8%.

4.2.1.2. Impact Test Results

The impact strength values of the neat epoxy, the E/EG composites and the E/T composites at different loadings are shown in Figure 27. Their average results and standard deviation values are given in Appendix D.

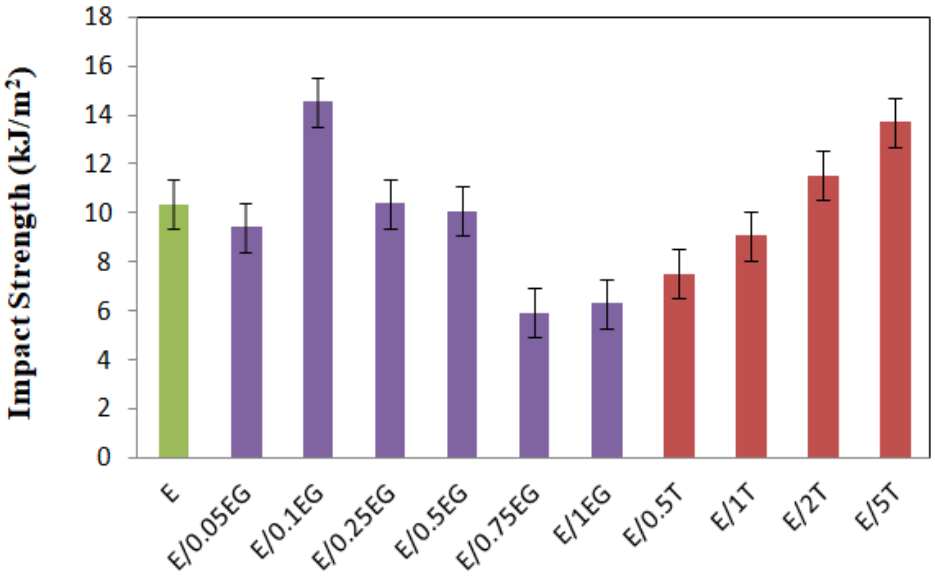

Figure 27. Impact strengths of the neat epoxy, the E/EG and the E/T composites at different loadings.

According to impact test results of E/EG composites, only 0.1 wt.% EG addition provided an enhancement in impact strength whereas the other concentrations exhibited similar or lower values in comparison to the impact strength of the neat epoxy. This probably originated from the fact that homogeneously dispersed EG particles at low concentrations considerably prevented crack formation and crack propagation whereas agglomerates formed at higher concentrations facilitated the

failure upon an impact. In the literature, it was expressed that EG particles have the ability to deflect cracks by tilting the crack fronts owing to their two dimensional structure. However, poor matrix-reinforcement interactions at high concentrations enabled crack propagation due to easy interfacial debonding while the increase in the viscosity resulting from high amount of EG addition caused void formations, which decrease the ability of the material to absorb energy [45, 80].

When the results of E/T composites were compared to the neat epoxy, it was observed that the incorporation of TiO_2 particles into epoxy matrix improved the impact strength beyond a certain concentration (after 2 wt.%). Addition of TiO_2 particles at low concentrations (0.5 and 1 wt.%) initially decreased the impact strength below the impact strength of the neat epoxy. However, further increase in TiO_2 content resulted in higher impact strengths than that of the neat epoxy. In the study conducted by Srivastava and Tiwari, it was stated that the introduction of TiO_2 particles to epoxy matrix increased the crosslink density [40]. This increase in crosslink density caused higher brittleness which explained the reduction in impact strength for 0.5 and 1 wt.% TiO_2 loading. However, increase in brittleness was probably compensated by crack deflections which was observed in SEM analysis of the E/2T and the E/5T composites, and thus, higher impact strength values were obtained for these composites.

In general, addition of 0.1 wt.% EG increased the impact strength by 40% while it was increased by 32% for 5 wt.% TiO_2 incorporation.

4.2.1.3. Shore D Hardness Test Results

The average of Shore D hardness values and their standard deviations of the neat epoxy, the E/EG and the E/T composites at different loadings are shown in Table 10.

Table 10. *Shore D hardness values of the neat epoxy, the E/EG and the E/T composites at different loadings.*

Sample Code	Shore D Hardness Value	Standard Deviation
E	80.5	1.3
E/0.05EG	81.4	0.6
E/0.1EG	82.2	0.4
E/0.25EG	82.5	0.7
E/0.5EG	81.2	0.7
E/0.75EG	81.1	0.7
E/1EG	81.0	0.6
E/0.5T	80.4	1.4
E/1T	80.9	1.5
E/2T	81.4	0.8
E/5T	82.5	0.7

According to test results, the incorporation of EG or TiO_2 particles into the epoxy matrix did not change the hardness significantly, when the standard deviations are considered, due to very low amount of the particles. However, it was realized that slight hardness alterations are usually discussed in the literature [47]. Therefore, it can be stated that the incorporation of EG or TiO_2 particles into epoxy matrix generally resulted in slightly higher hardness with respect to the hardness of the neat epoxy due to increase in stiffness [85, 88]. Among all E/EG composites, 0.25 wt.% EG containing ones had relatively higher hardness value with respect to others.

However, further increase in EG content reduced the hardness progressively while it gradually increased up to 0.25 wt.% loading. This can be explained by the dispersion of the particles in the composites since homogeneous distribution of the particles increased the chance of the indenter to come across with stiff EG particles instead of epoxy regions [88]. Therefore, the reason of the reduction in hardness with the increase in EG amount beyond a particular content might be the poor dispersion at higher concentrations. Also, increase in the viscosity at high EG concentrations caused formation of voids in the matrix which constitute soft regions. On the contrary, in E/T composites, it was observed that the hardness was increased slightly with the TiO_2 amount and the relatively higher value was obtained for the E/5T composites. The hardness value obtained by the introduction of 0.25 wt.% EG could be barely achieved at 5 wt.% TiO_2 loading. This showed that higher amount of TiO_2 was required to offer the same improvement in hardness which was provided by the low EG content since TiO_2 particles were smaller in size compared to EG particles.

4.2.2. SEM Analyses of E/EG and E/T Composites

SEM analyses were carried out on pure EG and pure TiO_2 particles, the neat epoxy, the epoxy-based composites with 0.1, 0.25, 0.5, 0.75 and 1 wt.% EG and the epoxy-based composites at 0.5, 1, 2 and 5 wt.% TiO_2 loading to understand the dispersion of the particles in epoxy matrix. SEM images of pure EG and pure TiO_2 particles were utilized to identify them in the composites, and they are given in Appendix C. On the other hand, SEM images of the tensile fractured surfaces of the composites were compared to those of the neat epoxy to observe the difference in their fracture mechanisms. Moreover, morphologies of the E/EG composites and the E/T composites were comparatively examined to evaluate the dispersion of the particles in the epoxy matrix. SEM images of the neat epoxy and the E/EG composites at x500 and x1000 magnification are given in Figures 28-30.

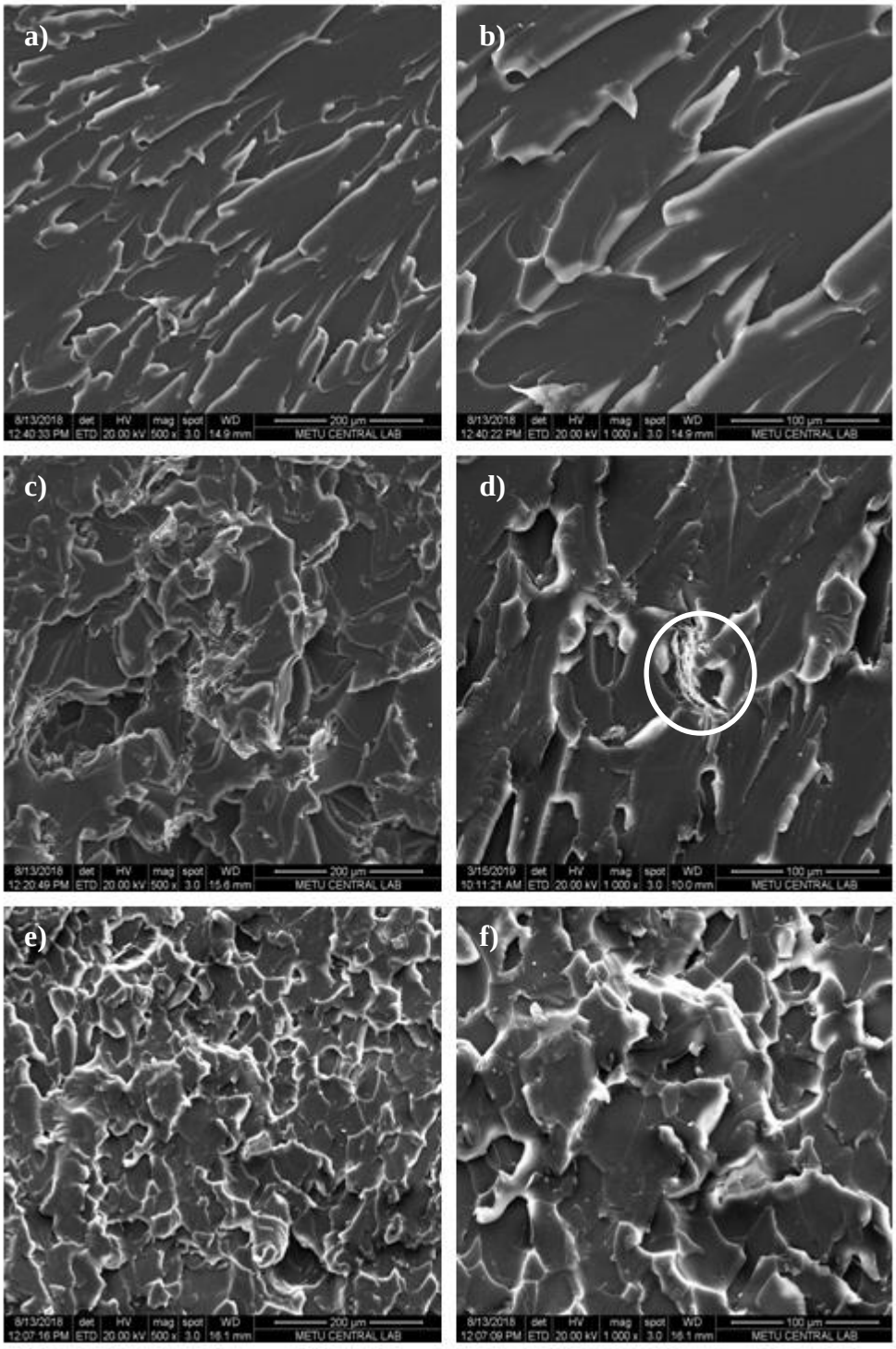

Figure 28. SEM images of a) the neat epoxy at 500x magnification, b) the neat epoxy at 1000x magnification, c) the E/0.05EG at 500x magnification, d) the E/0.05EG at 1000x magnification, e) the E/0.1EG at 500x magnification and f) the E/0.1EG at 1000x magnification.

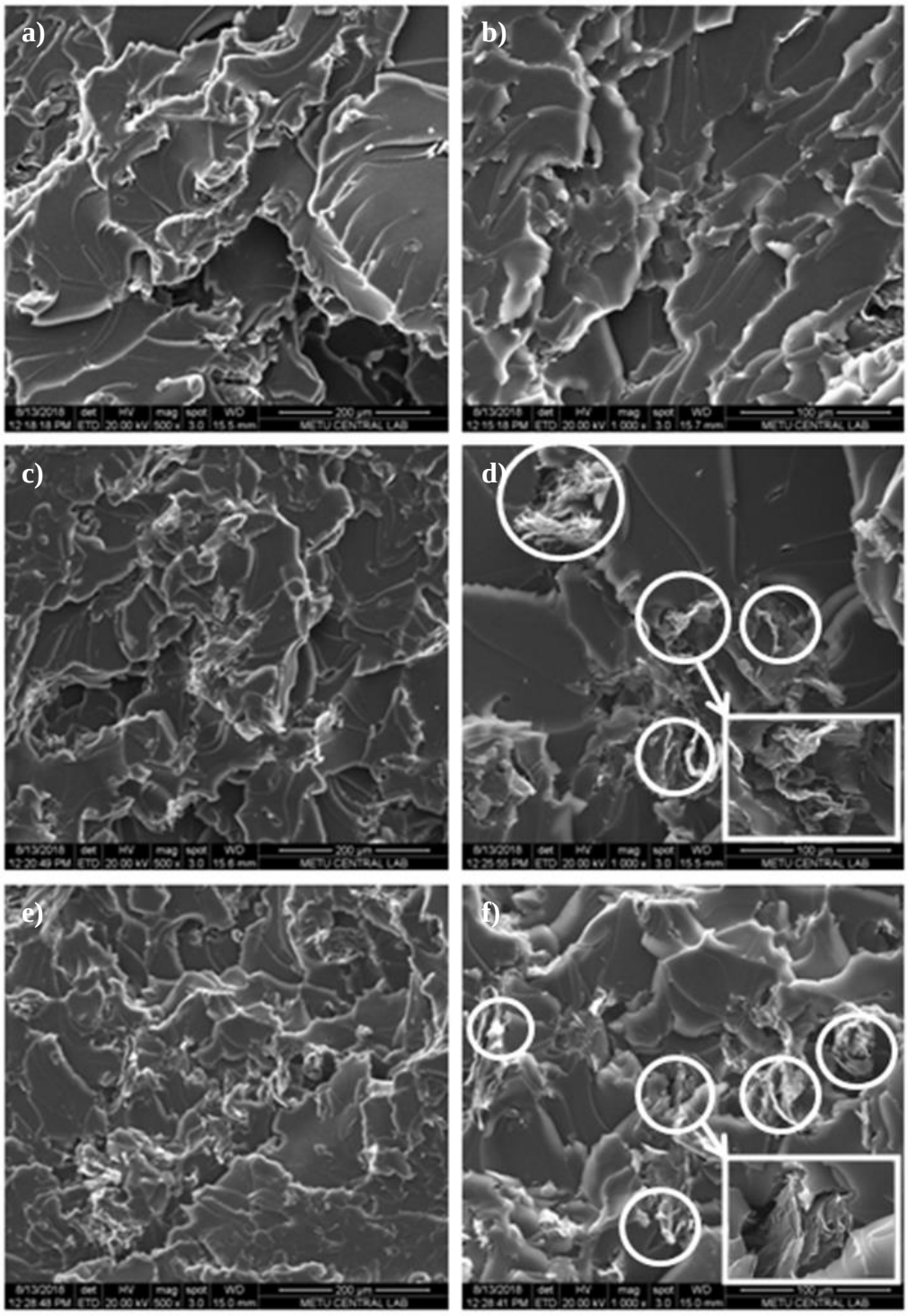

Figure 29. SEM images of a) the E/0.25EG at 500x magnification, b) the E/0.25EG at 1000x magnification c) the E/0.5EG at 500x magnification, d) the E/0.5EG at 1000x magnification, e) the E/0.75EG at 500x magnification and f) the E/0.75EG at 1000x magnification.

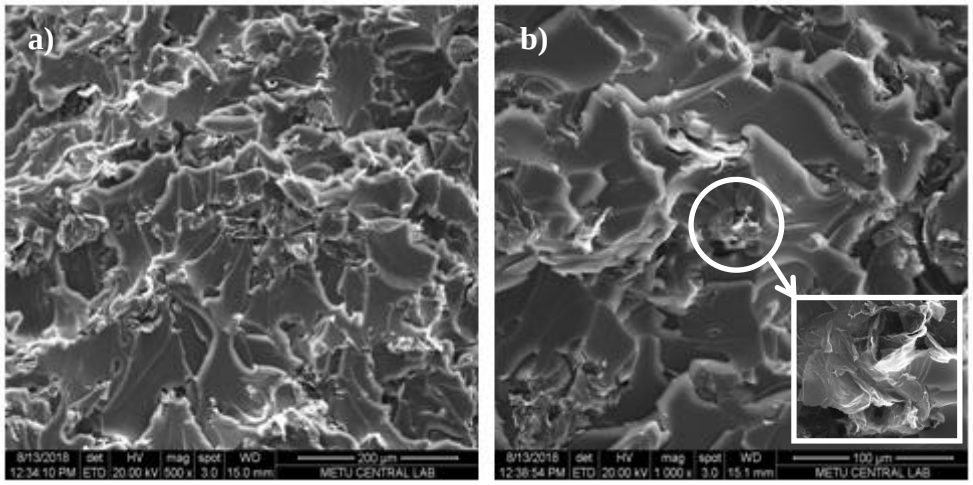

Figure 30. SEM images of a) the E/1EG at 500x magnification and b) the E/1EG at 1000x magnification.

As seen in Appendix C, two dimensional EG particles exhibit wrinkle-like texture and high aspect ratio which increase the interactions with epoxy matrix. It is obvious that smooth regions observed in the structure of neat epoxy were mostly replaced by rippled regions in E/EG composites. The increase in the surface roughness indicated the enhanced matrix-reinforcement interactions resulting in more difficult interfacial debonding [80]. Among all E/EG composites, the composite of E/0.1EG presented the highest homogeneity with respect to others, and thus, showed the highest mechanical properties. In addition, agglomerates were observed in the composites containing higher amount of EG, and they became more significant with the increase in EG content. That's why, a gradual reduction in mechanical properties was observed as the EG amount in the composites was increased. However, it was realized that agglomerates were also uniformly dispersed in the matrix at 1wt.% EG loading. This might be the reason of the slight increase in mechanical properties when the EG content reached 1 wt.%. Moreover, the massive cracks seen in the fracture surface of the neat epoxy were replaced by smaller cracks especially in the composite containing 0.1 wt.% EG due to the fact that uniformly dispersed EG layers could deflect most of the cracks by tilting the crack front [80]. Therefore, they

provided an additional fracture mechanism and enhanced toughness and impact strength of epoxy at 0.1 wt.% EG loading.

SEM images of the neat epoxy and the E/T composites at x1000 and x5000 magnification are presented in Figures 31 and 32.

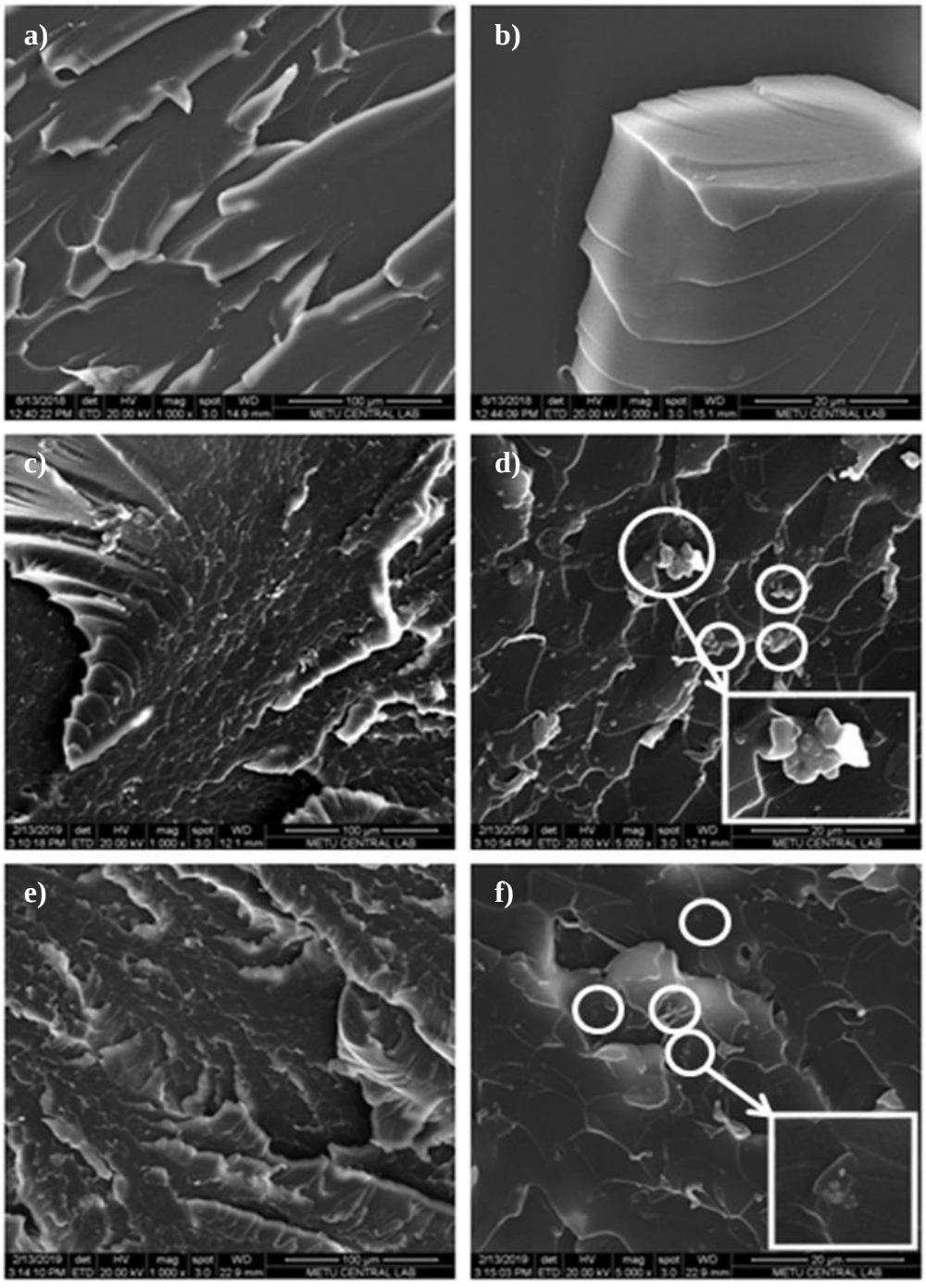

Figure 31. SEM images of a) the neat epoxy at 1000x magnification, b) the neat epoxy at 5000x magnification, c) the E/0.5T at 1000x magnification, d) the E/0.5T at 5000x magnification, e) the E/1T composites at 1000x magnification and f) the E/1T composites at 5000x magnification.

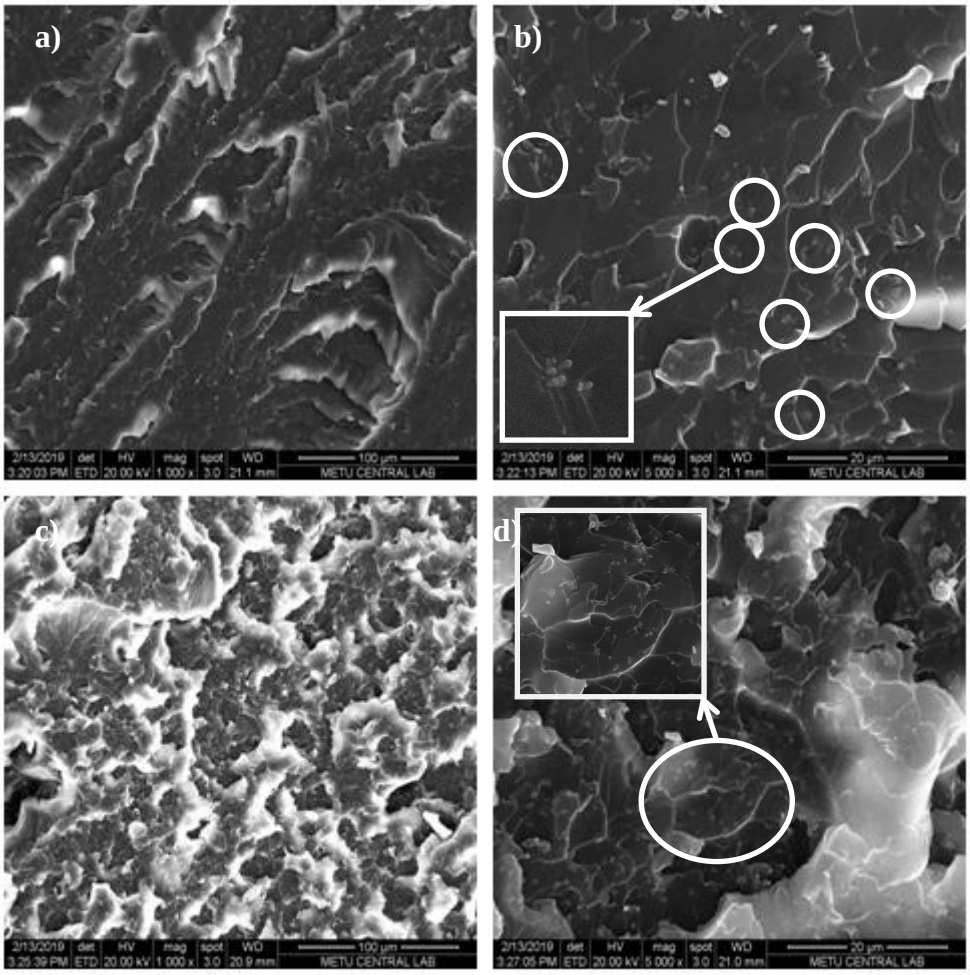

Figure 32. SEM images of a) E/2T at 1000x magnification, b) E/2T at 5000x magnification, c) E/5T composites at 1000x magnification and d) E/5T composites at 5000x magnification.

As seen in the SEM image of pure TiO_2 particles which are given in Appendix C, they have a spherical shape and small diameter. When the morphologies of the E/T composites were examined, it was observed that TiO_2 particles mostly seemed to be embedded in the matrix, which caused difficulties in their observation, especially at low concentrations. Due to the fact that much higher amount of TiO_2 was required compared to EG to obtain a significant change in the morphology and fracture mechanism of the neat epoxy, E/T composites generally showed lower mechanical properties with respect to the E/EG composites. The addition of TiO_2 particles into epoxy matrix increased the surface roughness, but it was not as much as the

improvement provided by EG particles owing to the one dimensional structure of TiO_2 particles [89]. Furthermore, It was realized that surface roughness was progressively increased with the TiO_2 amount, which indicated that interfacial debonding became more difficult as the TiO_2 concentration was increased. For this reason, a gradual increase in tensile properties with the increase in TiO_2 content is comprehensible. Among all E/T composites, the composite of E/5T exhibited the highest amount of crack deflections which was observed from its highly tortuous and rough fracture surface [80]. This explained the significant increase in impact strength at 5 wt.% TiO_2 content.

4.2.3. Thermal Analyses of E/EG and E/T Composites

4.2.3.1. DSC Analysis Results

The glass transition temperature (T_g) of the neat epoxy, the E/EG and the E/T composites with different loadings of EG and TiO_2 are shown in Figure 33 whereas their values are given in Appendix E.

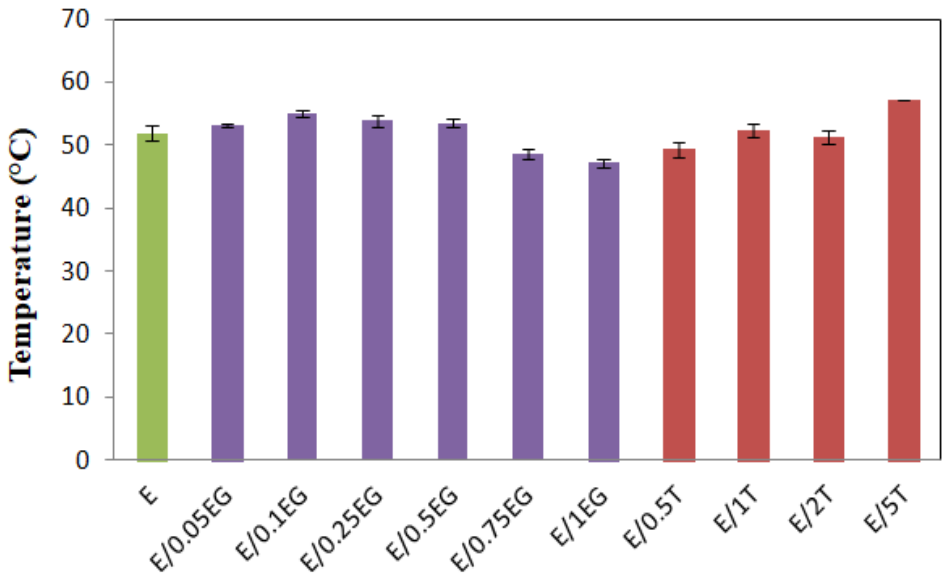

Figure 33. Glass transition temperatures of the neat epoxy, the E/EG and the E/T composites at different loadings.

When the analysis results of E/EG composites are considered, it is observed that the glass transition temperature of the epoxy was increased up to 0.5 wt.% EG loading while it reached its maximum value at 0.1 wt.% loading which increased T_g by 3°C over that of the neat epoxy. However, further increase in EG content after 0.5 wt.% decreased T_g to far below the glass transition temperature of the neat epoxy. In the literature, it is stated that properly dispersed graphite particles in epoxy matrix limit chain mobility by causing molecular confinement owing to their high stiffness, and thus, provide increase in the glass transition temperature [90]. That's why, the increase in T_g value was attributed to relatively homogeneous dispersion of the particles at low EG concentrations, which provides sufficient chain confinement. On the other hand, the reduction in T_g at higher concentrations resulted from the increase in chain mobility owing to the formation of agglomerates. Furthermore, EG incorporation into the crosslinked network of epoxy causes formation of physical crosslink points in the matrix instead of stronger chemical crosslinks. Due to the fact that physical crosslinks are more flexible with respect to chemical crosslinks, the excessive number of physical crosslinks inside the epoxy matrix decreases the strength of the structure, which results in lower T_g values [90]. Therefore, the reduction in T_g at higher EG concentrations might have originated from the presence of excess number of physical crosslinks in the matrix. In addition to this, the increase in the viscosity at high particle concentrations causes void formation during mixing, which lowers the T_g [91]. Moreover, the intercalated compounds which remain between EG layers might decrease the curing degree by reacting with epoxy resin or curing agent resulting in the reduction of T_g [70].

In E/T composites, a slight increase in the glass transition temperature was observed with the increase in TiO_2 content although the incorporation 0.5 wt.% TiO_2 into epoxy matrix resulted in the reduction of T_g value. It is thought that the decrease in the glass transition temperature at low TiO_2 content might have resulted from weak adhesion between the particles and the matrix which caused increase in chain mobility [90]. The composite at 5 wt.% TiO_2 loading provided the highest

enhancement among all E/EG and E/T composites by increasing the T_g of the epoxy by 5°C. The increase of the glass transition temperature at higher TiO_2 concentrations was associated to the increase in chain confinement and crosslink density [40].

4.2.3.2. TGA Results

The influences of addition of EG or TiO_2 particles on the thermal stability of epoxy were examined by performing TGA analysis on the neat epoxy, the E/EG and the E/T composites at various contents. In the analysis, the first and second decomposition temperatures of the neat epoxy and the epoxy-based composites were calculated by taking the first derivative of the weight loss versus temperature curve. In addition to that, the temperatures where the weight loss was 5%, 10%, 50% and 90% and the char formation at 800°C were determined respectively for each formulation.

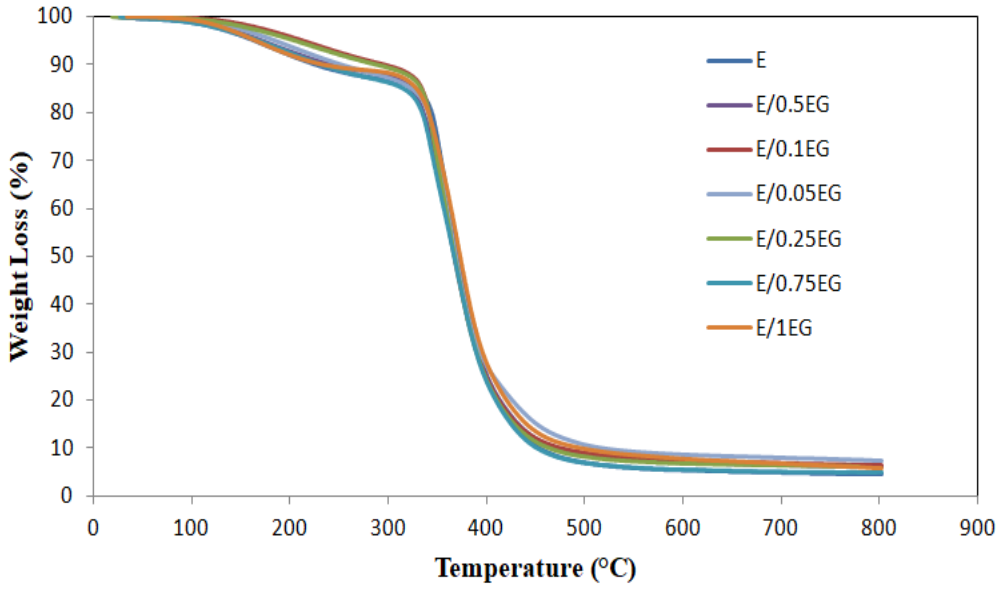

Figure 34. TGA results of the neat epoxy and the E/EG composites at different loadings.

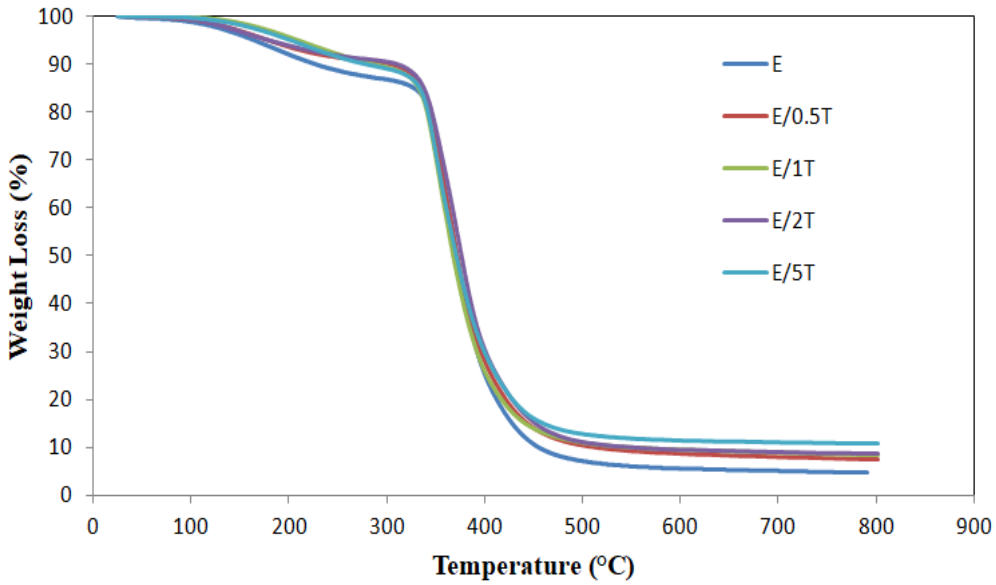

Figure 35. TGA results of the neat epoxy and E/ET composites at different loadings.

The TGA curves of the E/EG composites are given in Figure 34 along with the TGA curve of the neat epoxy whereas those belonging to E/T composites are shown in Figure 35. As seen in Figures 34 and 35, epoxy matrix showed two-stage thermal degradation. The first step probably originated from the decomposition of low molecular weight materials like diluents or the pendant chains of the matrix whereas the second step indicated the degradation of main chains of the neat epoxy. Detailed information related to the degradation of the neat epoxy and the epoxy-based composites are given in Table 11.

Table 11. *TGA data for the neat epoxy, the E/EG and the E/T composites at different loadings.*

Sample Code	T_d (°C)		$T_{d,5\%}$ (°C)	$T_{d,10\%}$ (°C)	$T_{d,50\%}$ (°C)	$T_{d,90\%}$ (°C)	Char formation at 800°C (% wt.)
	First (T_{d1})	Second (T_{d2})					
E	184	361	152	214	370	447	4.7
E/0.05EG	223	354	184	252	369	513	5.3
E/0.1EG	225	348	194	258	368	461	5.5
E/0.25EG	217	355	182	256	367	458	5.6
E/0.5EG	216	354	171	242	367	458	6.1
E/0.75EG	188	360	168	232	365	469	5.1
E/1EG	185	360	166	215	372	492	5.7
E/0.5T	194	358	179	265	372	484	7.3
E/1T	192	362	180	268	373	496	8.2
E/2T	200	372	188	280	376	506	8.8
E/5T	202	375	192	278	378	718	10.8

When the first decomposition temperatures (T_{d1}) of the E/EG composites where the weight losses were approximately 8% are compared to that of the neat epoxy, it is observed that the EG addition into epoxy matrix at any concentration increased T_{d1} value of the neat epoxy. This can be explained by the barrier effect of EG particles which retarded the volatilization of the primary materials in the matrix. The

efficiency of this barrier effect could be enhanced when sufficient amount of particles were homogeneously dispersed in the matrix [44]. For this reason, the highest increase in T_{d1} value was observed at 0.1 wt.% EG loading which exhibited much more homogeneous structure with respect to other E/EG composites. On the other hand, the composites containing higher amount of EG provided less increase in the first decomposition temperature due to poor dispersion of the particles and formation of agglomerates. When the temperature values of the composites which indicated 5% and 10% weight losses respectively are analyzed, the same trend is obtained for both $T_{d,5\%}$ and $T_{d,10\%}$ as observed in the comparison of T_{d1} values. According to the second decomposition temperatures (T_{d2}) of the composites that were obtained approximately at 80% weight loss for each formulation, it can be stated that addition of EG particles reduced the T_{d2} value of the neat epoxy, which probably resulted from high thermal conductivity of the particles. The presence of EG particles in the epoxy matrix enhanced the heat transfer in the matrix, and thus, expedited the decomposition process [92]. Furthermore, it was realized that lower EG concentrations caused higher decrease in T_{d2} while the increase in EG content resulted in T_{d2} values that are closer to that of the neat epoxy. This was attributed to the emergence of the thermally conductive pathway in the matrix that provided by the homogeneous dispersion of EG layers [92]. Due to the fact that higher EG concentrations caused poor dispersion and agglomerates, a proper pathway for heat transfer could not be established. Therefore, the composites at higher EG loadings showed T_{d2} values similar to that of the neat epoxy. On the contrary, a gradual increase was observed in the temperature values of the 90% weight loss with the rise in EG content, which indicated that the degradation became slower as the EG amount was increased. This probably resulted from the fact that EG particles decomposed in the last stages in the composites, and it took longer time compared to epoxy as seen in Appendix C. Finally, it was observed that the 50% weight loss occurred at similar temperature values for all the E/EG composites and the neat epoxy.

According to TGA results of E/T composites, it can be stated that the introduction of TiO_2 particles into epoxy matrix increased both T_{d1} and T_{d2} values of the neat epoxy. The increase in T_{d1} with the TiO_2 content resulted from the increase in the solid content which prevented the heat and oxygen diffusion as well as the volatilization of the primary materials [40]. Unlike E/EG composites, this barrier effect was improved with the increase in TiO_2 amount due to homogeneous dispersion of TiO_2 particles even at high concentrations and the continuously increasing solid content. The highest increase in T_{d1} was obtained at 5 wt.% loading, but it was lower than the enhancement provided by the 0.1 wt.% EG addition. This showed that the two-dimensional structures offered more sufficient barrier effect with respect to one-dimensional ones. The same trend observed in the T_{d1} values of the composites was also obtained in the evaluation of the temperatures respectively associated to 5% and 10% weight loss. In addition, the increase in TiO_2 content was gradually increased T_{d2} value of the neat epoxy due to the fact that TiO_2 particles increased the crosslink density [40]. Among all E/EG and E/T composites, the most significant enhancement in T_{d2} was observed at 5 wt.% TiO_2 loading. Lastly, a slight increase in the temperature at 50% weight loss and a significant rise in the temperature at 90% weight loss were observed as the TiO_2 amount in the composite was increased, which indicated slower thermal degradation, and thus, higher thermal stability at higher TiO_2 concentrations. The improvements in thermal stability via TiO_2 addition was also attributed to the high thermal stability of TiO_2 particles in the rutile phase. Among the three different crystal structures of TiO_2, which are anatase, rutile and brookite, the rutile phase has the highest thermal stability and melts between 1830-1850°C [93]. That's why, it was thought that the enhancement of thermal stability in the composites might have originated from the superior thermal properties of the rutile TiO_2 particles. The TGA curve of TiO_2 particles used in this study is given in Appendix C.

When the char formation of the neat epoxy and all E/EG and E/T composites are evaluated, an incremental increase in the char formation was observed with the rise

in particle content. According to TGA results of pure EG and TiO_2 which are given in Appendix C, both types of the particles did not decompose completely at 800°C, which resulted in higher char formation. Therefore, the increase in their concentration yielded to more char formation. In addition to this, it was noticed that the neat epoxy had a residue which was 4.7% of its initial weight at 800°C owing to the presence of additives that reduced its viscosity.

4.3. Determination of Preparation Process for Epoxy-based Hybrid Composites

According to mechanical properties of the binary E/EG and E/T composites, formulations for epoxy-based hybrid composites were determined as E/0.05EG/0.5T, E/0.1EG/0.5T and E/0.1EG/5T. The hybrid composite of E/0.1EG/0.5T was primarily prepared by the sonication with the use of solvent method, which was carried out in the fabrication of the binary E/EG and E/T composites in the earlier experiments. However, this method which was defined as preparation process I (PP1) caused mixing problems and formation of air bubbles due to sudden increase in the viscosity resulting from the simultaneous addition of both EG and TiO_2 particles during the preparation of epoxy-based hybrid composites. Therefore, PP1 was modified in three different ways by adding mechanical stirring step, increasing degassing time and changing degassing temperature step by step, and the E/0.1EG/0.5EG composites were prepared by PP2, PP3 and PP4 methods, respectively. To determine the most efficient preparation process, mechanical and thermal properties of the composites that fabricated by four different methods were evaluated. After that, other hybrid formulations were produced by the application of the chosen method.

4.3.1. Mechanical Properties of E/0.1EG/0.5T Hybrid Composites Fabricated by Different Methods

Tensile test, impact test and Shore D hardness test were performed on the E/0.1EG/0.5T composites which were fabricated respectively by PP1, PP2, PP3 and PP4 methods. Due to the fact that epoxy-based hybrid composites suffered from

poor mixing and the presence of air bubbles originating from inadequacy of the preparation method, mechanical properties of the composites were compared to each other to select the best preparation process that resulted in homogeneous distribution of the particles and less air bubbles.

Figures 36-39 show the tensile properties and impact strengths of the E/0.1EG/0.5T composites. Their average tensile strength, elastic modulus, elongation at break and impact strength values along with their standard deviations are given in Appendix D.

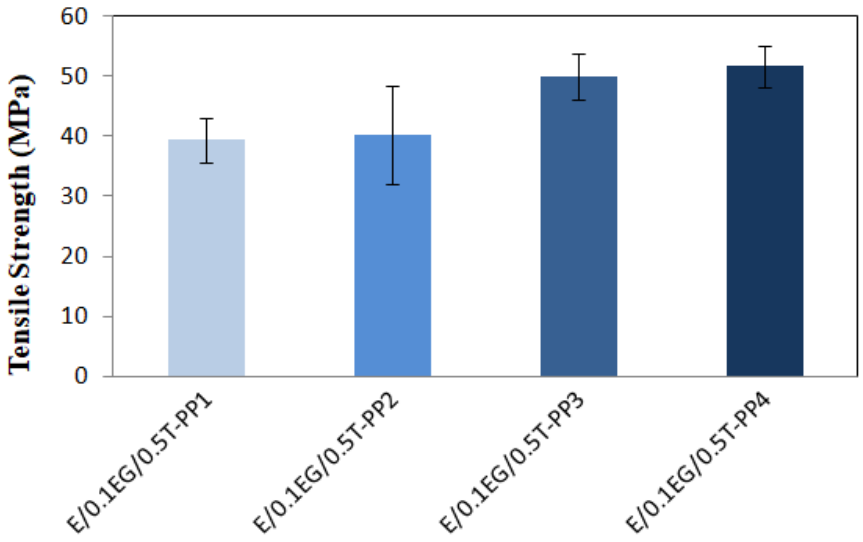

Figure 36. Tensile strengths of the E/0.1EG/0.5T hybrid composites prepared by different methods.

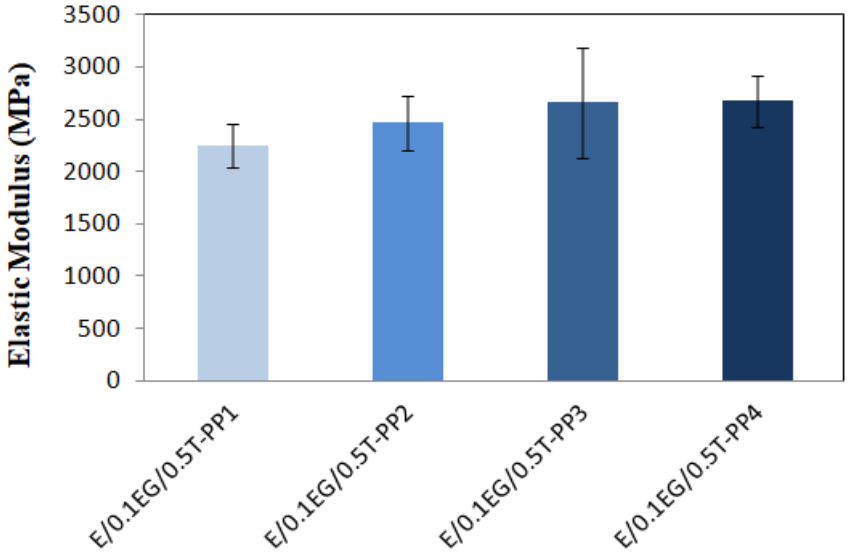

Figure 37. Elastic moduli of the E/0.1EG/0.5T hybrid composites prepared by different methods.

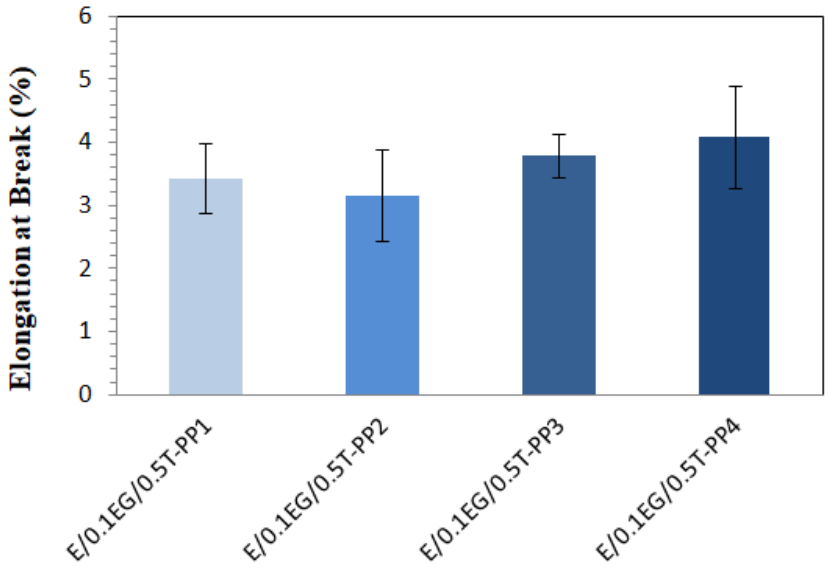

Figure 38. Elongation at break of the E/0.1EG/0.5T hybrid composites prepared by different methods.

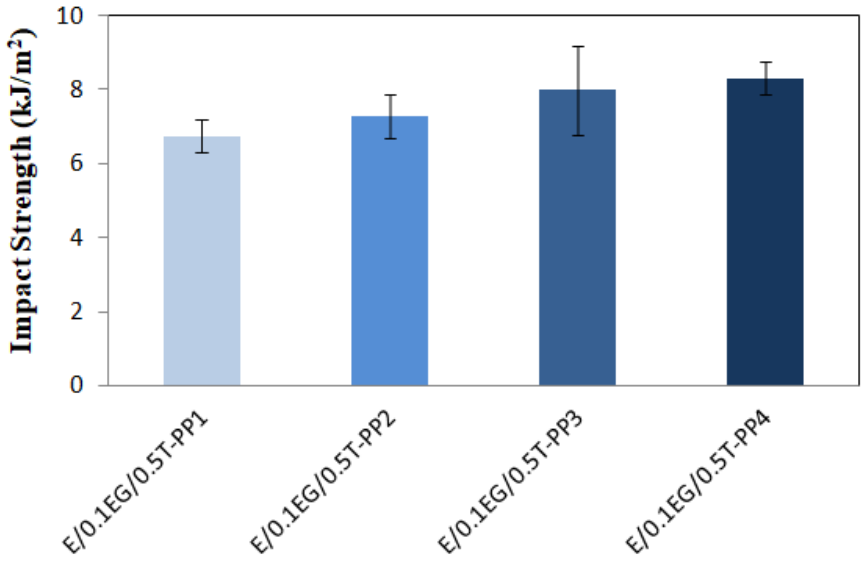

Figure 39. Impact strengths of the E/0.1EG/0.5T hybrid composites prepared by different methods.

As seen in the graphs, the composites prepared by PP4 exhibited relatively higher tensile strength, elastic modulus, elongation at break and impact strength with respect to the ones produced by other methods. This revealed that the combination of three modifications which are the addition of mechanical stirring step, increasing degassing period and degassing temperature provided better hybrid composite structure. The mechanical stirring enhanced the interfacial properties, and thus, provided much more homogeneous dispersion while increasing degassing period and degassing temperature simultaneously resulted in higher reduction in the number of air bubbles.

On the other hand, Shore D hardness test results of the E/0.1EG/0.5T composites fabricated by different preparation processes are given in Table 12.

Table 12. *Shore D hardness values of the E/0.1EG/0.5T hybrid composites prepared by different methods.*

Sample Code	Shore D Hardness Value	Standard Deviation
E/0.1EG/0.5T-PP1	81.3	0.6
E/0.1EG/0.5T-PP2	81.4	0.6
E/0.1EG/0.5T-PP3	81.7	0.8
E/0.1EG/0.5T-PP4	82.0	0.8

When the hardness values of the composites are compared to each other, it is observed that all composites presented almost similar hardness values. However, a slightly higher hardness value of the composite prepared by PP4 might indicate that PP4 provided better distribution of the stiff EG and TiO_2 particles in the matrix with respect to other methods. In addition to this, it should be noted that the reduction in the number of air bubbles also enhanced the hardness [88]. For this reason, relatively higher hardness value of the E/0.1EG/5T composites produced by PP4 might also have originated from the presence of less air bubbles in the structure.

4.3.2. Thermal Properties of E/0.1EG/0.5T Hybrid Composites Fabricated by Different Methods

DSC and TGA analyses were carried out on the E/0.1EG/0.5T hybrid composites which were produced by PP1, PP2, PP3 and PP4 respectively to understand the effect of preparation method on thermal properties.

The graph which is given in Figure 40 shows the glass transition temperatures of the composites obtained by DSC analyses while their values are shown in Appendix E.

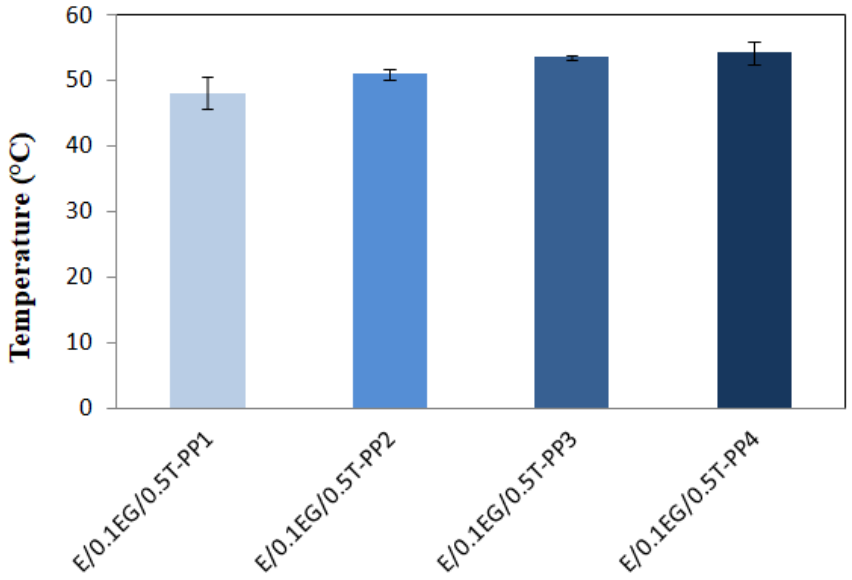

Figure 40. Glass transition temperatures of the E/0.1EG/0.5T hybrid composites prepared by different methods.

According to analyses results, the composites prepared by PP1 and PP2 exhibited lower T_g values than that of the neat epoxy which probably resulted from the presence of air bubbles in their structures [91]. On the other hand, PP3 and PP4 provided composites with relatively higher T_g values compared to the neat epoxy while the highest increase in T_g was obtained in the one fabricated by PP4. This showed that air bubbles were mostly eliminated, and better dispersion of the particles was obtained with the application of PP4.

The weight loss versus temperature curves of the E/0.1EG/0.5T hybrid composites prepared by different methods are shown in Figure 41.

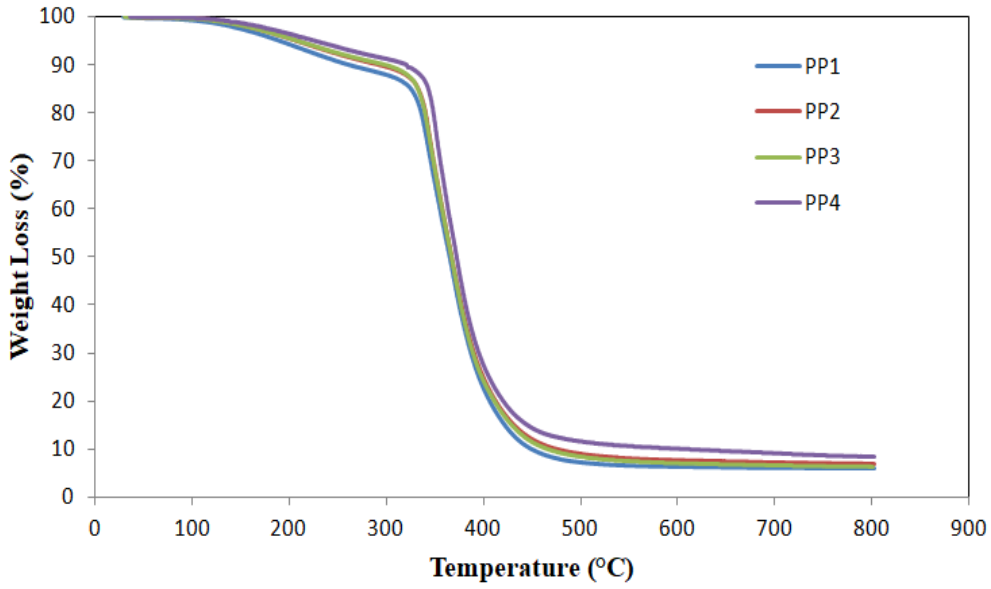

Figure 41. TGA results of the E/0.1EG/0.5T hybrid composites prepared by different methods.

The first and second decomposition temperatures, temperature values at 5%, 10%, 50% and 90% weight losses and char formations at 800°C are given in Table 13.

Table 13. *TGA data of the E/0.1EG/0.5T hybrid composites prepared by different methods.*

Sample Code	T_d (°C)		$T_{d,5\%}$ (°C)	$T_{d,10\%}$ (°C)	$T_{d,50\%}$ (°C)	$T_{d,90\%}$ (°C)	Char formation at 800°C (% wt.)
	First (T_{d1})	Second (T_{d2})					
E/0.1EG/0.5T-PP1	213	357	190	261	364	449	6.0
E/0.1EG/0.5T-PP2	219	357	192	272	366	460	6.9
E/0.1EG/0.5T-PP3	220	360	193	279	366	456	6.4
E/0.1EG/0.5T-PP4	219	368	208	305	371	523	6.3

In comparison to the neat epoxy, it is realized that the first decomposition temperature and temperatures at 5% and 10 wt.% weight losses were higher in all E/0.1EG/0.5T composites since the addition of EG and TiO_2 particles retarded the volatilization of primary materials in the matrix by providing barrier effect [40, 44]. In addition, it is seen that all composites presented almost similar temperature values at 50% weight loss a that of the neat epoxy whereas the temperature at 90% weight loss was higher in the composites owing to the presence of the particles which had higher decomposition temperatures than epoxy. However, only the composite prepared by PP4 increased the second decomposition temperature over that of the

neat epoxy. Therefore, PP4 was found to be more appropriate method for the preparation of epoxy-based hybrid composites with high thermal stability.

4.4. Effects of Simultaneous Addition of EG and TiO_2 to the Epoxy Matrix

4.4.1. Mechanical Properties of E/EG/T Hybrid Composites

4.4.1.1. Tensile Test Results

Tensile properties of the neat epoxy and the epoxy-based hybrid composites are shown in Figures 42-44 while their average tensile strength, elastic modulus and elongation at break values with their standard deviations are given in Appendix D. To evaluate the synergistic effect of EG and TiO_2 particles on the tensile properties, the test results of the hybrid composites were compared to the binary composites which are also given in the following figures.

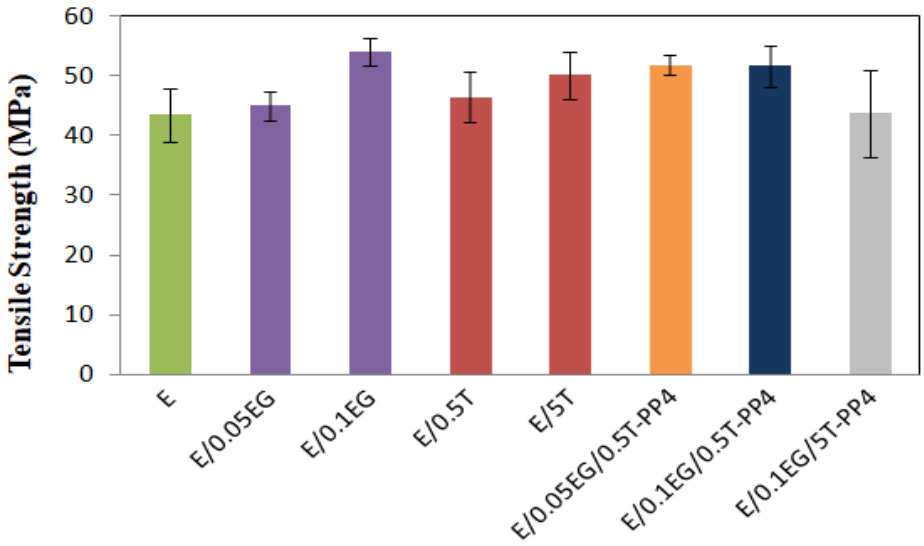

Figure 42. Tensile strengths of the neat epoxy and the epoxy-based hybrid composites with different formulations.

According to the tensile strength values of the hybrid composites shown in Figure 42, it can be stated that the E/0.05EG/0.5T composite which contained the lowest amount of additives showed the highest enhancement in tensile strength by providing 19% increase in the tensile strength over that of the neat epoxy. Moreover, the E/0.05EG/0.5T hybrid composite had higher tensile strength with respect to the binary composites of E/0.05EG and E/0.5T. When the TiO_2 content was kept constant and the EG amount in the hybrid composite was increased to 0.1 wt% (E/0.1EG/0.5T), almost the same tensile strength value as that of E/0.05EG/0.5T composite was obtained. However, the tensile strength of the E/0.1EG/0.5T composite was slightly lower than the E/0.1EG composite, which resulted from the fact that the presence of EG and TiO_2 particles together in the matrix adversely affected the dispersion at high particle contents. Therefore, further increase in the particle content (E/0.1EG/5T) resulted in much lower tensile strength value than those of the E/0.1EG, E/5T and the other hybrid composites.

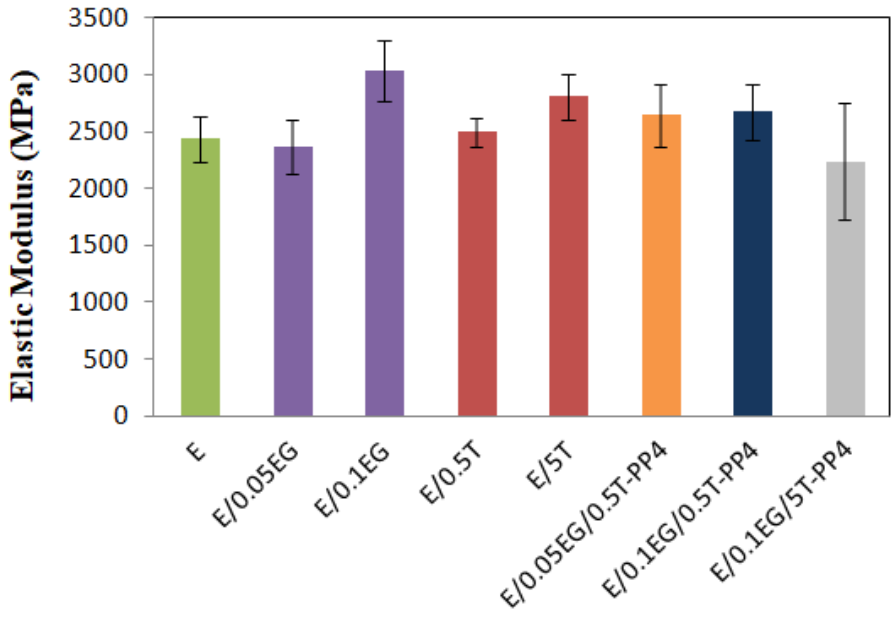

Figure 43. Elastic moduli of the neat epoxy and the epoxy-based hybrid composites with different formulations.

When the elastic modulus values of the hybrid composites and the particular binary composites were compared to each other as seen in Figure 43, similar trend was observed as in the case of the evaluation of their tensile strengths. The E/0.05EG/0.5T hybrid composite increased the elastic modulus by 8% over the neat epoxy, and also presented higher elastic modulus than its binary counterparts of E/0.05EG and E/0.5T. Although the E/0.1EG/0.5T hybrid composite exhibited closer elastic modulus to the E/0.05EG/0.5T, its elastic modulus was much lower than that of binary composite of E/0.1EG, which resulted from formation of agglomerates. On the other hand, the E/0.1EG/5T composite which contained the highest amount of the particles had lower elastic modulus even than the neat epoxy. These observations indicated that the interfacial properties could be enhanced only at low particle contents in the hybrid composites.

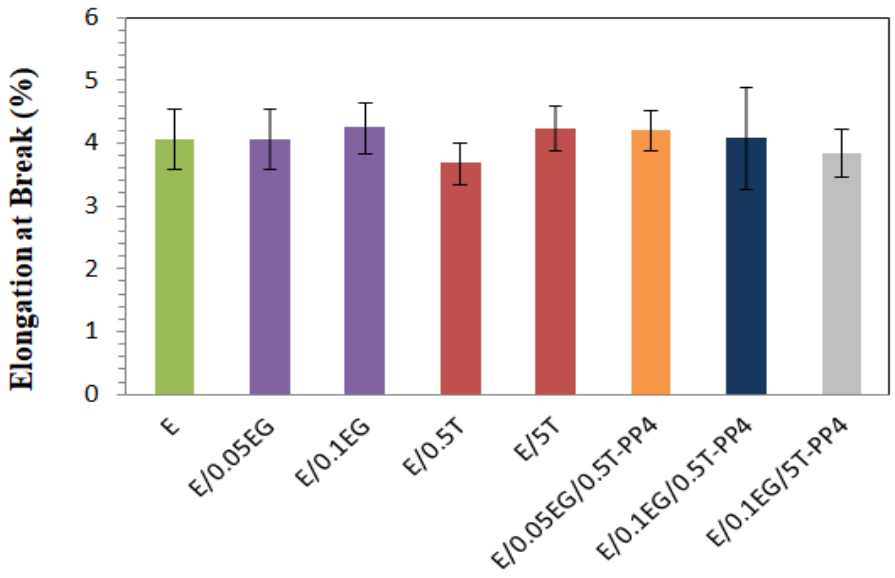

Figure 44. Elongation at break values of the neat epoxy and the epoxy-based hybrid composites with different formulations.

Among all of the epoxy-based hybrid composites shown in Figure 44, the E/0.05EG/0.5T composite which contained the lowest amount of EG and TiO_2

particles exhibited slightly higher elongation at break value. In addition to that, it was the only hybrid formulation that provided higher elongation than its binary counterparts.

All of these results corroborated the fact that simultaneous incorporation of different reinforcement materials at low concentrations resulted in higher tensile strength and elastic modulus with respect to the composites which contained only one type of the reinforcement material at the same loading. However, the increase in the concentration of the reinforcements in hybrid composites caused reduction in both values, and these composites also showed lower tensile strength and elastic modulus than their binary counterparts. This behavior originated from the alteration in the particle distribution based on the contents of the particles. At low EG and TiO_2 loadings, the particles individually interacted with the epoxy matrix, and thus, they could be dispersed uniformly in the matrix. However, with the increase in their concentrations, they began to prefer each other instead of epoxy molecules. Therefore, matrix-reinforcement interactions became poorer, which resulted in the decrease of tensile properties.

4.4.1.2. Impact Test Results

The impact strengths of the neat epoxy and the epoxy-based hybrid composites are shown in Figure 45, and their values are given Appendix D. As in the tensile test results, the hybrid composites were also compared to their binary counterparts to observe the synergistic effect of EG and TiO_2 particles on impact strength.

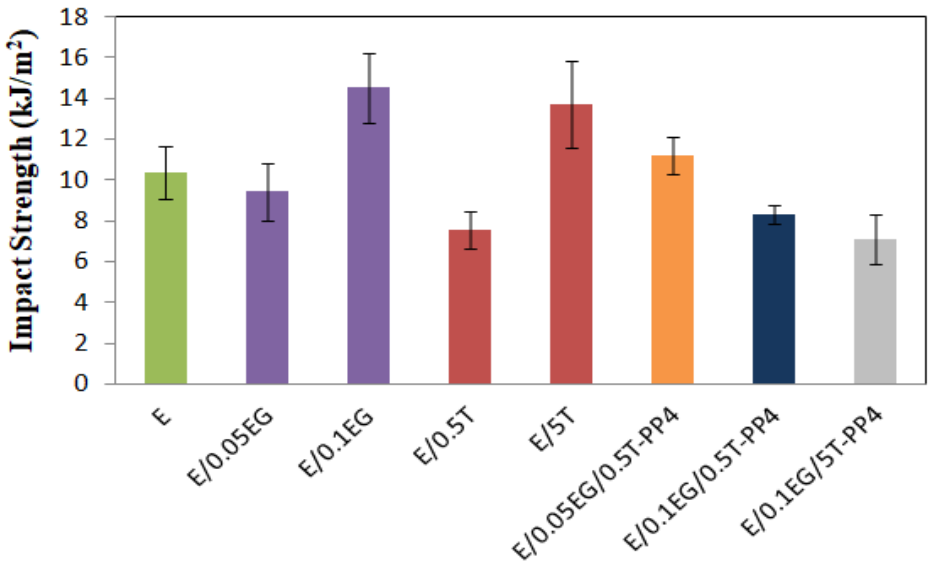

Figure 45. Impact strengths of the neat epoxy and the epoxy-based hybrid composites with different formulations.

Among all of the epoxy-based hybrid composites, only the E/0.05EG/0.5T composite which had lowest particle concentration provided an enhancement in impact strength and increased it by 8% over that of the neat epoxy. On the contrary, other hybrid formulations exhibited lower impact strength values than that of the neat epoxy. In addition, the E/0.05EG/0.5T was the only hybrid formulation that improved the impact strength of the neat epoxy more than its binary counterparts. This showed that hybrid formulations were favorable only at low particle contents. In the hybrid composites, gradual decrease in impact strength with the increase in total particle content was attributed to formation of more air bubbles at high concentrations. The addition of higher amount of EG and TiO_2 particles at the same time caused sudden increase in the viscosity. During mechanical stirring at high rpm, this resulted in high number of air bubbles which could not be totally eliminated in the degassing process. Therefore, the presence of air bubbles in the composite structure decreased the impact strength since it decreased the energy absorption upon an impact [45]. In addition to this, the weak interactions between the particles and

the epoxy matrix at high concentrations might be another reason of the reduction in impact strength. Due to the fact that dispersion of the particles became poorer resulting from the weak matrix-reinforcement interactions at high particle contents, cracks could not be deflected sufficiently [80]. Thus, the hybrid composites at higher EG and TiO_2 loadings exhibited lower impact strength values.

4.4.1.3. Shore D Hardness Test Results

Shore D hardness values and standard deviations of the neat epoxy, the epoxy-based hybrid composites and their binary counterparts are shown in Table 14.

Table 14. *Shore D hardness values of the neat epoxy and the epoxy-based hybrid composites with different formulations.*

Sample Code	Shore D Hardness Value	Standard Deviation
E	80.5	1.3
E/0.05EG	81.4	0.6
E/0.1EG	82.2	0.5
E/0.5T	80.4	1.4
E/5T	82.5	0.7
E/0.05EG/0.5T-PP4	81.2	1.0
E/0.1EG/0.5T-PP4	82.0	0.8
E/0.1EG/5T-PP4	82.9	0.6

When the hardness values of the hybrid composites are considered, it is observed that hardness was gradually increased as the amount of EG and TiO_2 in the composite was increased, unlike tensile and impact properties. All hybrid formulations presented relatively higher hardness values than the neat epoxy, and the maximum improvement was obtained in the E/0.1EG/5T composite which had the highest particle concentration among all hybrid composites. The hardness of the neat epoxy was increased to 82.9 from 80.5 by the simultaneous addition of 0.1 wt.% EG and 5 wt.% TiO_2. Furthermore, the E/0.1EG/5T composite also exhibited slightly higher hardness with respect to its binary composites which are E/0.1EG and E/5T while other hybrid composites presented hardness values close to their binary counterparts (when the standard deviations were considered). In the earlier sections, it was stated that increasing the particle content of the hybrid composites resulted in poor dispersion and formation of agglomerates, therefore, decreased the tensile and

impact properties. However, an opposite trend was observed in the evaluation of hardness values of the hybrid composites. This can be explained by the increase in the locational stiffness with the increase in total particle amount. In SEM analysis, it was observed that EG and TiO_2 particles preferred each other at high loadings, and most of the TiO_2 particles settled inside or near the stacks of EG layers. This situation caused the formation of quite stiff regions in the matrix, and thus, enhanced the hardness value of whole composite structure [94].

4.4.2. SEM Analyses of E/EG/T Hybrid Composites

Tensile fractured surfaces of the E/0.05EG/0.5T, E/0.1EG/0.5T and E/0.1EG/5T composites were examined through SEM analyses. SEM images of the neat epoxy and all epoxy-based hybrid composites at 1000x and 5000x magnifications are given in Figures 46 and 47.

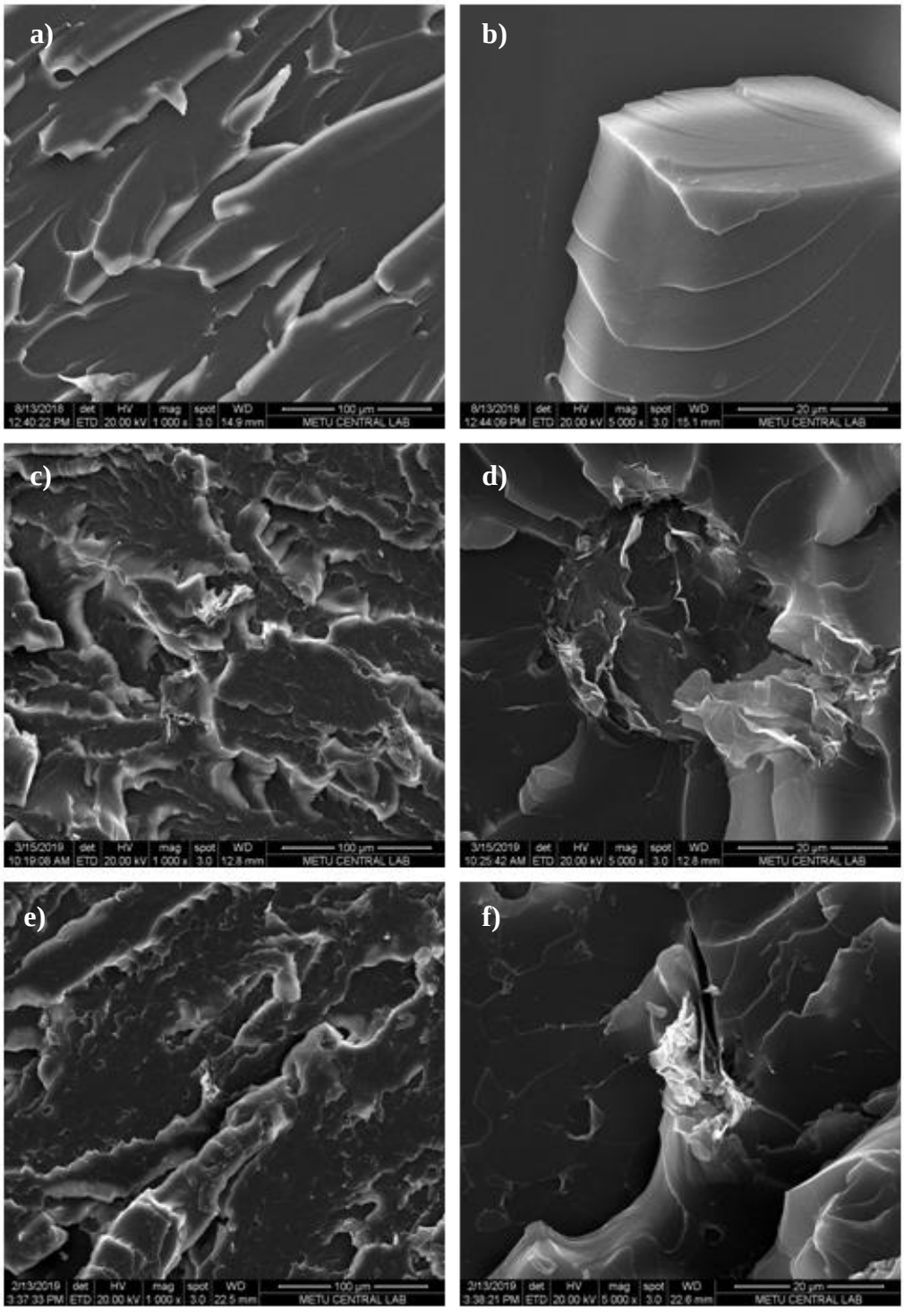

Figure 46. SEM images of a) the neat epoxy at 1000x magnification, b) the neat epoxy at 5000x magnification, c) the E/0.05EG/0.5T at 1000x magnification, d) the E/0.05EG/0.5T at 5000x magnification, e) the E/0.1EG/0.5T at 1000x magnification and f) the E/0.1EG/0.5T at 5000x magnification.

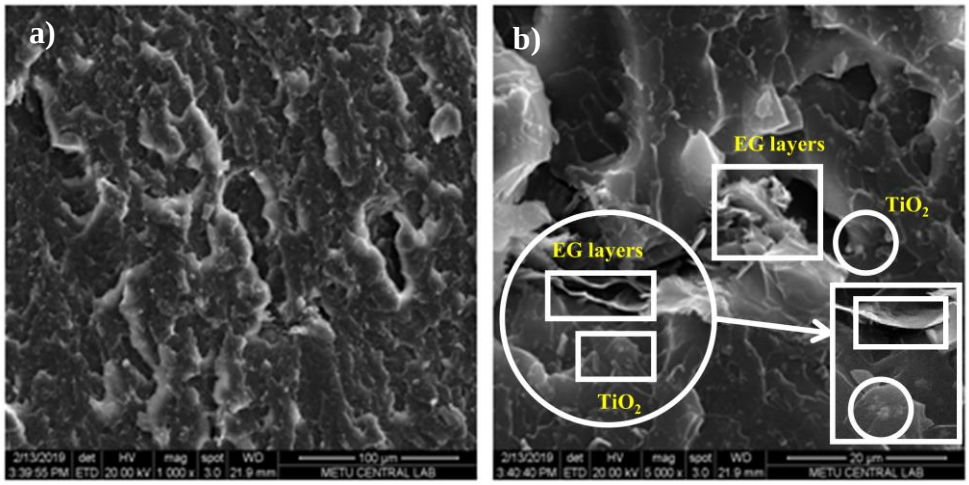

Figure 47. SEM images of a) the E/0.1EG/5T hybrid composite at 1000x magnification and b) the E/0.1EG/5T hybrid composite at 5000x magnification.

According to SEM images given above, it can be stated that the E/0.05EG/0.5T hybrid composite had less agglomerations with respect to the others due to the fact that the particles could be dispersed much more homogeneously at low concentrations. Better matrix-reinforcement interactions in its structure might be the main reason of the enhanced tensile and impact properties [43]. On the other hand, it is realized that EG and TiO_2 particles were present as clusters at higher particle concentrations, which prevent them exhibiting their own characteristics and caused easy debonding under a load. This explained the reduction in mechanical properties as the total particle amount was increased. In addition, large voids were observed around the reinforcements, which resulted from the increase in the viscosity at high particle content. These voids decreased the energy absorption upon an impact as well as affecting the thermal properties adversely [45, 91].

4.4.3. Thermal Analyses of E/EG/T Hybrid Composites

4.4.3.1. DSC Analysis Results

The effects of simultaneous addition of EG and TiO_2 particles into epoxy matrix on the glass transition temperature were investigated by performing DSC analysis.

Figure 48 shows the T_g values of the neat epoxy, the epoxy-based hybrid composites and their binary counterparts, whereas their values are given in Appendix E.

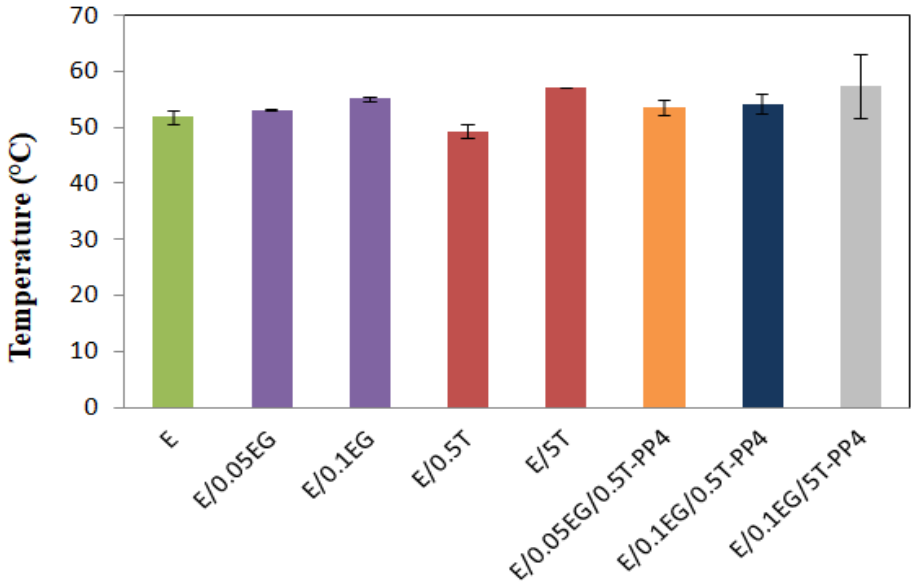

Figure 48. Glass transition temperatures of the neat epoxy, the epoxy-based hybrid composites with different formulations and their binary counterparts.

The epoxy-based hybrid composites presented slightly higher T_g values than the neat epoxy, while the highest T_g was observed in the E/0.1EG/5T composite which is 5°C higher than that of the neat epoxy. The increase in T_g was attributed to decrease in chain mobility and increase in physical crosslink density owing to the presence of stiff particles in the matrix [40, 90]. The E/0.05EG/0.5T hybrid composite exhibited higher T_g value than its binary counterparts while the E/0.1EG/0.5T had lower T_g value than its EG contained binary counterpart (E/0.1EG). This probably resulted from the increase in agglomerate content and formation of voids in the matrix owing to the presence of TiO_2 particles along with 0.1 wt.% EG [91]. On the other hand, E/0.1EG/5T composite exhibited higher T_g value than its both binary counterparts. This indicated that chain confinement was enhanced significantly by simultaneous

addition of the particles at higher content, and this situation surpassed the effects of agglomerates and voids.

4.4.3.2. TGA Results

TGA analysis was applied to epoxy-based hybrid composites at different loadings to understand how the incorporation of EG and TiO_2 particles together into epoxy matrix affected the thermal stability. Figure 49 shows the weight loss versus temperature curves of the neat epoxy, the epoxy-based hybrid composites and their binary counterparts.

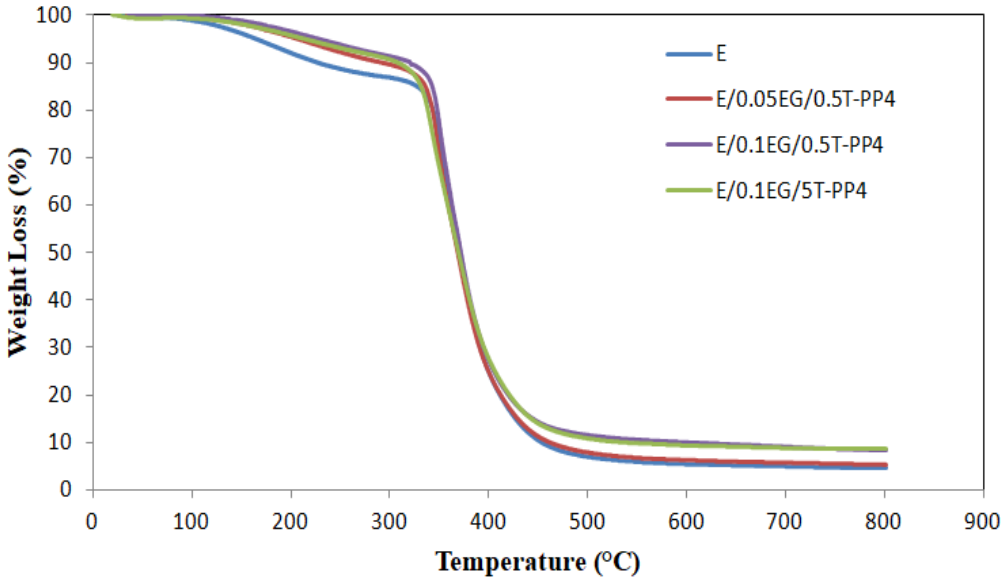

Figure 49. TGA results of the neat epoxy, the epoxy-based hybrid composites with different formulations and their binary counterparts.

In addition, their first and second decomposition temperatures, temperature values at 5%, 10%, 50% and 90% weight loss and char formations at 800°C are given in Table 15.

Table 15. *TGA data of the neat epoxy, the epoxy-based hybrid composites with different formulations and their binary composites.*

Sample Code	T_d (°C)		$T_{d,5\%}$ (°C)	$T_{d,10\%}$ (°C)	$T_{d,50\%}$ (°C)	$T_{d,90\%}$ (°C)	Char formation at 800°C (% wt.)
	First (T_{d1})	Second (T_{d2})					
E	184	361	152	214	370	447	4.7
E/0.05EG	223	354	184	252	369	513	5.3
E/0.1EG	225	348	194	258	368	461	5.5
E/0.5T	194	358	179	265	372	484	7.3
E/5T	202	375	192	278	378	718	10.8
E/0.05EG/0.5T-PP4	220	361	205	289	368	462	5.4
E/0.1EG/0.5T-PP4	219	368	208	305	371	523	6.3
E/0.1EG/5T-PP4	219	370	212	307	370	532	10.6

When the analysis results of hybrid composites are compared to those of the neat epoxy, it is observed that all hybrid composites exhibited higher first and second decomposition temperatures than the neat epoxy, which indicated the improvement

of thermal stability of epoxy by hybrid formulations. Furthermore, temperature values at 5%, 10% and 90% weight loss were also increased by the simultaneous addition of EG and TiO_2 particles at all concentrations whereas any significant change could not be observed in the temperature of 50% weight loss. Higher temperatures at the same weight losses indicated that the degradation of epoxy was retarded when the particles were added. Slower degradation was accepted as a sign of enhanced thermal stability [41].

When the results of hybrid composites were compared to each other, it was observed that the second decomposition temperature was enhanced as well as $T_{d,5\%}$, $T_{d,10\%}$ and $T_{d,90\%}$ values with the increase in total particle content. It showed that the presence of thermally conductive EG particles along with TiO_2 particles or increasing EG amount in hybrid formulations from 0.05 wt.% to 0.1 wt.% did not affect the thermal stability adversely since their barrier effect became more dominant than the ability to dissipate heat.

To understand the synergistic effect of EG and TiO_2 particles, the values of hybrid composites were also compared to those of their binary counterparts. The E/0.05EG/0.5T hybrid composite presented higher second decomposition temperature, $T_{d,5\%}$ and $T_{d,10\%}$ compared to its binary composites of E/0.05EG and E/0.5T whereas the E/0.1EG/0.5T composite generally provided higher enhancement in thermal properties with respect to its binary composites of E/0.1EG and E/0.5T. In earlier sections, it was stated that EG addition at 0.1 wt.% increased the decomposition rate of epoxy since EG particles provided heat dissipation over the matrix via thermally conductive pathways [92]. In the hybrid case, TiO_2 particles which have very low thermal conductivity damaged the conductive network by surrounding the EG layers as seen in SEM analysis. Therefore, EG particles could absorb heat like TiO_2 particles instead of conducting it all over the matrix. Due to the inhibition of heat dissipation and the increase in heat absorption capacity in the hybrid formulation, the E/0.1EG/0.5T hybrid composite provided higher

enhancement in thermal stability compared to the E/0.1EG and E/5T binary composites.

On the other hand, the E/0.1EG/5T hybrid composite had lower second decomposition temperature, $T_{d,50\%}$ and $T_{d,90\%}$ values compared to its binary composite of E/5T while it generally exhibited better thermal decomposition properties than the E/0.1EG binary composite. This might have resulted from the difference in thermal stability of EG and TiO_2 particles. Due to the fact that EG had lower decomposition temperature than TiO_2 in rutile phase, the presence of EG particles brought forward the degradation of the hybrid composite. In addition, EG layers started to agglomerate as the total particle content in hybrid formulation was increased, which accelerated the thermal degradation [44].

4.5. Performance Tests for Epoxy-based Composites

4.5.1. LOI Test Results

LOI test was performed on the neat epoxy, the E/T composites and the epoxy-based hybrid composites to observe the influences of the TiO_2 incorporation into the matrix on the flammability of epoxy. In the literature, it was stated that TiO_2 particles can be utilized as a flame-retardant material since it created a protective barrier against heat and oxygen [40]. In addition to that, char formation is one of the mechanisms for flame retardancy due to the fact that it indicates the generation of carbonaceous layer during burning which hinders the release of combustible gases [53]. In TGA results, it was observed that the E/T composites had higher char formation than the neat epoxy, and the amount of char formation increased with the increase in TiO_2 content. Therefore, how the presence of TiO_2 particles in the matrix and the increase in its concentration affected the flammability behavior of epoxy were investigated. LOI values of the neat epoxy and the epoxy-based composites containing TiO_2 (binary and hybrid composites) are given in Table 16.

Table 16. *LOI values of the neat epoxy, the E/T composites at different loadings and the epoxy-based hybrid composites with different formulations.*

Sample Code	Limiting Oxygen Index (O_2 %)
E	23
E/0.5T	24
E/1T	25
E/2T	26
E/5T	26
E/0.05EG/0.5T-PP4	25
E/0.1EG/0.5T-PP4	25
E/0.1EG/5T-PP4	26

When the LOI values of the neat epoxy and the binary E/T composites are compared to each other, it is realized that limiting oxygen index of epoxy gradually increased up to 2 wt.% TiO_2 loading and remained constant after that concentration. Therefore, the maximum enhancement in flammability was provided by 2 wt.% TiO_2 addition which increased the LOI value of the neat epoxy from 23 to 26. Besides, the E/5T composite presented the same LOI value as E/2T did. This showed that the introduction of TiO_2 particles changed the flammability behavior of epoxy and imparted flame retardancy up to a certain capacity. On the other hand, addition of 0.05 or 0.1 wt.% EG along with 0.5 wt.% TiO_2 to epoxy matrix increased LOI value above the one obtained in the E/0.5T composite. This indicated that the presence of EG and TiO_2 particles together in the matrix improved the barrier effectiveness while the windle-wick effect was not observed. However, any difference in LOI value between the E/0.05EG/0.5T and the E/0.1EG/0.5T composites could not be

observed, which probably resulted from the slight increase in EG content. Moreover, the E/0.1EG/5T composite also exhibited the LOI value of 26 which was same with the E/5T composite. Due to the fact that the amount of TiO_2 particles in that composite was much higher than the EG concentration, the structure of E/0.1EG/5T composite was dominated by TiO_2 particles, and it mainly reflected the flammability characteristics of 5 wt.% TiO_2 addition.

4.5.2. Electrical Resistivity Test Results

Electrical (or volume) resistivity of the neat epoxy and the epoxy-based composites which contained EG (binary and hybrid composites) were measured, and the results are shown in Figure 50 whereas average volume resistivity values are given in Appendix F.

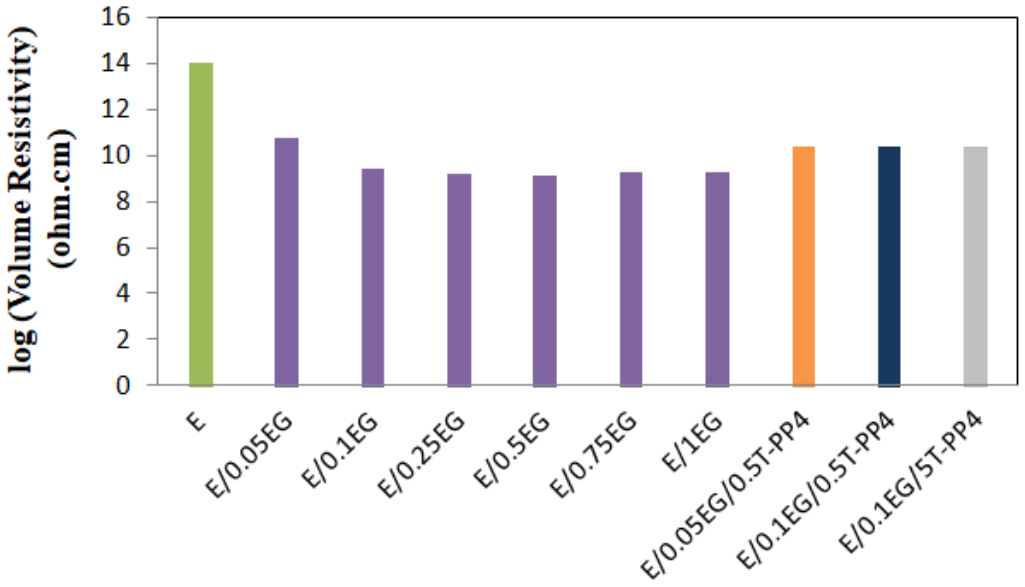

Figure 50. Electrical (volume) resistivity values of the neat epoxy, the E/EG composites at different loadings and the epoxy-based hybrid composites with different formulations.

Carbon-based materials have been widely used in various researches to enhance electrical conductivity of the materials [57]. Graphene exhibits low electrical

resistivity of $4x10^5$ ohm.cm in basal plane [95] while the electrical resistivity of the neat epoxy is generally defined as higher than 10^{10} ohm.cm, which is in the insulator range [96]. Due to the fact that the resistivity measurement device (Keithley 2400) is unable to measure electrical resistivities of the insulating materials, the resistivity of the neat epoxy was taken from the literature as 10^{14} ohm.cm [47]. According to test results of E/EG composites, the resistivity of the neat epoxy was decreased to 10^9 ohm.cm at 0.1 wt.% EG loading, and almost remained constant after that concentration. Therefore, percolation threshold of transition in electrical conductivity from insulator range to nearly semiconductor range was determined as 0.1 wt.% EG addition. However, the expected improvement in electrical conductivity which was obtained in the literature could not be obtained [58, 59]. This probably resulted from the absence of adequate pathways for electrical conduction owing to very low amount of EG particles in the bulk epoxy [59]. On the other hand, epoxy-based hybrid composites exhibited higher resistivity with respect to E/EG composites. Nevertheless, they decreased the resistivity of the neat epoxy to 10^{10} ohm.cm. In the case of hybrid composites, the presence of TiO_2 particles which generally have electrical resistivity between 10^{13} and 10^{18} ohm.cm [47] along with the conductive EG particles in the epoxy matrix may contribute to formation of disconnections on the conductive pathways that were developed by EG particles since most of the TiO_2 particles surrounded EG layers as seen in SEM analysis.

4.6. Surface Properties of Epoxy-based Coatings

The epoxy resin, which was loaded with EG, TiO_2 and both EG and TiO_2 particles, were coated on glass surfaces, and the epoxy-based coatings which were almost 0.5 mm in thickness were obtained after the curing process. In this section, the effects of separate or simultaneous addition of EG and TiO_2 particles into the epoxy matrix on the surface properties were examined. Due to the fact that high hydrophobicity is mostly desired in the coating applications, it was aimed to improve hydrophobicity of epoxy coatings by introducing EG and/or TiO_2 particles into epoxy at different concentrations. Hydrophobicity of the coating is generally determined by measuring

the contact angle between the surface and water droplets or calculating surface energy of the coating. High water contact angle and low surface energy indicated hydrophobicity which is water repelling property [62]. That's why, water contact angle measurement and surface energy calculation were carried out on the surfaces coated by neat epoxy, E/EG, E/T and E/EG/T composite mixtures in order to observe the changes in hydrophobic behavior.

4.6.1. WCA Measurement Results

WCA measurement was performed as explained in the experimental section, and the results are given in Figure 51. As seen in the figure, the neat epoxy coating presented WCA of 75°, which indicated its hydrophilic structure. The hydrophilicity of the neat epoxy was attributed to its high polarity and ability of forming hydrogen bonds with water and polar solvents [96].

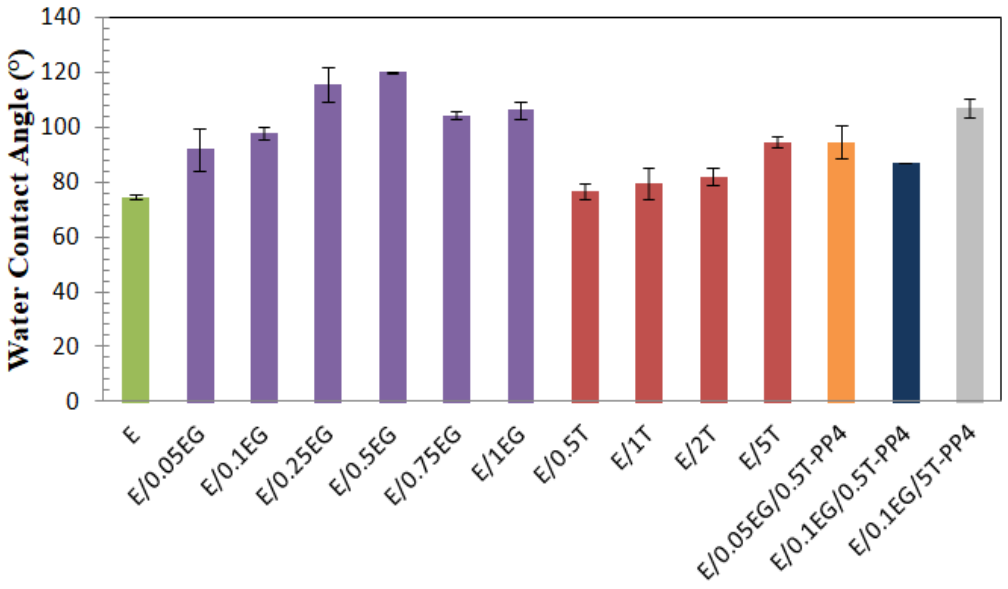

Figure 51. WCA values of the neat epoxy, E/EG, E/T and E/EG/T coated surfaces.

According to WCAs of the E/EG coatings, it can be stated that addition of EG at all concentrations converted the surface to hydrophobic since all E/EG composites exhibited WCA higher than 90°. In the study conducted by Yu et al. [66], it was observed that EG particles exhibited large contact angle with polar solvents which are ethylene glycol and formamide rather than non-polar solvents like diiodomethane. This showed that they cannot be easily wetted by polar solvents. Also, it was found that water contact angle varied from 90-95° on graphite to 120-130° on graphene [97]. Therefore, it is expected that EG particles poorly interact with water droplets, and therefore, enhanced hydrophobicity when they are added to the epoxy matrix. In addition to that, surface roughness is another parameter for hydrophobicity since rough surfaces limit the contact with liquid droplets [60]. In SEM analysis, it was realized that EG particles exhibited two-dimensional wrinkle-like structure which enhance the surface roughness [80]. Although they provided roughness in microscopic scale, this might be the other reason of the improvement in hydrophobicity. The hydrophobicity was gradually enhanced up to 0.5 wt.% EG loading, and the maximum WCA value was obtained on the E/0.5EG coatings. On the other hand, increasing EG amount in the coating above 0.5 wt.% lowered WCA. In the literature, it was found that multilayered graphite structures had higher WCA than single graphene layer [98]. Therefore, obtaining the highest WCA on the E/0.5EG coating was associated to the presence of stacks of graphene layers in its structure whereas thinner EG layers were present at lower concentrations. However, larger agglomerations that formed at higher concentrations caused the E/0.75EG and E/1EG coatings to exhibit lower WCAs due to the fact that agglomerations of stacks of graphene layers that were formed at high concentrations prevented the EG layers externalizing their own surface characteristics [98].

When the test results of the E/T coatings were considered, it was seen that WCA gradually increased with the increase in TiO_2 amount, but the hydrophobic level could be achieved at 5 wt.% loading. This can be primarily explained by the increase in surface roughness provided by the dispersion of TiO_2 particles in the epoxy

matrix. The increase in WCA with the TiO_2 content showed that surface roughness could be enhanced further with the increase in TiO_2 concentration since the presence of higher amount of particles in the matrix resulted in more indented structure [99]. Moreover, intrinsically hydrophobic structure of TiO_2 particles in rutile phase contributed to the hydrophobicity of the coatings. In the literature, it was emphasized that water repellant property of TiO_2 strongly depends on its crystalline phase. Among the three different phases which are anatase, rutile and brookite, rutile phase particles have the highest thermal and chemical stability as well as the lowest ability for water dissociation. Therefore, they are generally known as naturally hydrophobic materials [100]. In addition, it was observed that water contact angle on TiO_2 varied from 72° to 122° depending on its synthesis method [101].

Finally, the epoxy-based hybrid coatings also provided the increase in hydrophobicity since all formulations presented higher WCA with respect to the neat epoxy coated one. In addition, it can be stated that increase in total particle content gradually increased WCA while the maximum enhancement in hydrophobicity was observed in the E/0.1EG/5T coatings among all of the hybrid coatings. Moreover, this formulation exhibited higher WCA than its binary coatings which are E/0.1EG and E/5T. This probably resulted from the diversity of particle size due to the coexistence of EG and TiO_2 particles in the matrix since the presence of particles in various sizes and even agglomerates increased the surface roughness significantly [63].

4.6.2. Surface Energy Calculation Results

Surface energy calculation was carried out on the coatings according to the method used in the thesis of Köysüren [69] in order to observe relation between hydrophobicity and surface energy. The acid (γ^A) and base (γ^B) components, the dispersive (γ^d) and polar (γ^p) components of the surface energy and the total surface energy (γ^{TOT}) for each coating are given in Table 17 whereas contact angles with probe liquids are shown in Appendix G.

Table 17. *Surface energy data of the neat epoxy, E/EG, E/T and E/EG/T coatings.*

Sample Code	γ^A	γ^B	γ^p	γ^d	γ^{TOT}
E	0.00	17.02	0.12	43.82	43.94
E/0.05EG	0.46	9.11	4.09	37.83	41.93
E/0.1EG	0.73	2.06	2.45	37.95	40.41
E/0.25EG	1.63	0.10	0.82	37.37	38.19
E/0.5EG	0.80	0.50	1.27	36.69	37.96
E/0.75EG	0.51	1.35	1.66	40.65	42.31
E/1EG	1.77	0.29	1.43	38.64	40.07
E/0.5T	0.00	1.87	0.11	38.40	38.51
E/1T	0.00	2.88	0.03	37.01	37.04
E/2T	0.02	4.52	0.57	36.43	37.00
E/5T	0.01	4.22	0.41	35.18	35.59
E/0.05EG/0.5T-PP4	0.00	0.00	0.00	40.43	40.43
E/0.1EG/0.5T-PP4	0.02	0.00	0.01	29.76	29.77
E/0.1EG/5T-PP4	0.05	2.05	0.64	27.87	28.51

When the test results are assessed, it is observed that addition of EG and TiO_2 particles separately or simultaneously reduced the total surface energy of the neat epoxy coatings.

The E/EG coatings exhibited lower contact angles with polar and nonpolar probe liquids than the neat epoxy coated surface due to poor wetting properties of EG particles and the increase in surface roughness via the wrinkle-like structure of EG [102]. Therefore, they executed relatively lower surface energy values compared to the neat epoxy coating. Among all E/EG coatings, the highest reduction in surface energy was obtained at 0.5 wt.% loading as in the case of WCA evaluation. Moreover, it was noticed that surface energy values of other E/EG coatings were also consistent with their WCA values.

On the other hand, 5 wt.% TiO_2 loaded coating, which exhibited higher WCA than the other E/T binary coatings, had the lowest surface energy among all E/T coatings. When the surface energies of E/T and E/EG coatings were compared to each other, it was realized that the addition of TiO_2 particles lowered the surface energy more than the EG incorporation even at the lowest concentration. In the literature, TiO_2 particles in rutile phase have been frequently defined as very low surface energy materials [103]. Therefore, difference in surface energy between the E/T and the E/EG coatings probably resulted from the fact that modification of the epoxy with low surface energy TiO_2 particles affected the total surface energies of the coatings more than roughness or wettability properties. However, the E/EG coatings generally presented higher WCA values compared to the E/T coatings although E/T coatings had much lower surface energy values. This showed that WCA measurement was mostly controlled by the surface roughness. EG particles provided higher roughness via their two dimensional structures with respect to one dimensional TiO_2 particles.

In addition, the lowest surface energy was obtained by the simultaneous incorporation of 0.1 wt.% EG and 5 wt.% TiO_2 into epoxy, which resulted from their synergistic effect.

CHAPTER 5

CONCLUSIONS

According to experiments carried out within the scope of the thesis and the characterization test results, the findings can be listed as:

1. The application of sonication with the use of solvent method for the preparation of the E/0.5EG composites resulted in better tensile and impact properties along with more homogeneous morphology with respect to other mixing methods.

2. The neat epoxy, E/EG and E/T composite mixtures were successfully prepared using the sonication with the use of solvent method. Large portions of the mixtures were cured in the silicon molds while remaining parts of the mixtures were coated on glass surfaces for each formulation, and then, cured at the same conditions.

3. The E/0.1EG composites generally exhibited the highest tensile and impact properties among all E/EG composites by increasing tensile strength, elastic modulus, elongation at break value and impact strength as 24%, 25%, 8% and 40%, respectively over that of the neat epoxy.

4. In the E/T composites, a gradual increase in all tensile and impact properties was observed with the increase in TiO_2 content, and 5 wt.% TiO_2 loading increased the tensile strength, elastic modulus, elongation at break value and impact strength as 15%, 15%, 8% and 32%, respectively over the neat epoxy.

5. A significant change in Shore D hardness value with the addition of EG or TiO_2 particles could not be observed. However, the highest hardness value, approximately 82.5, was obtained in the composites of E/0.25EG and E/5T.

6. In SEM analysis of the E/EG and E/T binary composites, it was observed that EG particles have sheet-like structure that caused formation of agglomerates after 0.1 wt.% loading whereas TiO_2 particles generally have spherical or elliptical shape and smaller size compared to EG particles. Unlike EG, TiO_2 particles could be uniformly dispersed in the epoxy matrix at high concentrations.

7. In the E/EG composites, the glass transition temperature of the neat epoxy was slightly increased up to 0.5 wt.% EG content while the increase in TiO_2 amount caused a continuous increase in the glass transition temperature.

8. In TGA analysis, it was observed that the TiO_2 addition improved the thermal stability of epoxy by increasing both the first and the second decomposition temperatures beyond 1 wt.% loading. On the other hand, the presence of EG particles in the matrix provided an increase in the first decomposition temperature while decreasing the second decomposition temperature. With the increase in EG amount, values that are closer to that of the neat epoxy were observed.

9. The sonication with the use of solvent method was modified for the preparation of the E/EG/T hybrid composites and coatings, and the successful samples were fabricated by the application of preparation process IV (PP4).

10. The E/0.05EG/0.5T composites which contained the lowest particle amount was the only hybrid formulation that showed better tensile and impact properties than those of the neat epoxy and its two binary counterparts.

11. Although a significant change in Shore D hardness value could not be observed by the hybrid formulations, the E/0.1EG/5T composites exhibited the highest hardness value of 83 among all hybrid composites, which was also higher than the maximum hardness value provided by the binary composites.

12. In SEM analysis of epoxy-based hybrid composites, it was observed that EG particles agglomerated and TiO_2 particles mostly settled in or around these agglomerates with the increase in total particle content.

13. In thermal analyses of the epoxy-based hybrid composites, it was observed that the increase in total particle content increased the glass transition temperature, the first and second decomposition temperature as well as retarding the degradation rate.

14. LOI test showed that the TiO_2 particles behaved like flame retardant materials in the epoxy matrix, and the LOI value of the neat epoxy was increased from 23 to 26 at 5 wt.% loading. On the other hand, the E/0.05EG/0.5T and the E/0.1EG/0.5T hybrid composites had a LOI value of 25 which was higher than the value obtained in their binary composite of E/0.5T. Also, further increase in particle content in hybrid formulation (E/0.1EG/5T) increased the LOI value to 26.

15. In the E/EG composites, the percolation threshold of transition in electrical conductivity was observed at 0.1 wt.% EG loading, and the resistivity of the neat epoxy was decreased from 10^{14} ohm.cm to 10^{9} ohm.cm at this concentration. The conductivity level almost remained constant beyond 0.1 wt.% EG addition. On the contrary, all hybrid formulations presented electrical resistivity of approximately 10^{10} ohm.cm.

16. The neat epoxy coated surface had WCA of 75°, which indicated its hydrophilic structure. The EG addition into epoxy matrix at all concentrations provided hydrophobicity by increasing the WCA above 90°. Among all E/EG coatings, the highest improvement in hydrophobicity was observed at 0.5 wt.% EG loading which resulted in WCA of 120°. On the other hand, the E/T coatings could barely reach the hydrophobic level at 5 wt.% TiO_2 loading. All epoxy-based hybrid coatings except for the E/0.1EG/0.5T exhibited hydrophobic property and higher WCA than their binary counterparts while the hydrophobicity was

gradually enhanced with the increase in total particle content. Among the hybrid coatings, the E/0.1EG/5T presented more hydrophobic structure by forming contact angle of 107° with water droplets.

17. Surface energy of the coatings was decreased by the incorporation of EG or TiO_2 particles. Among all E/EG coatings, the 0.5 wt.% EG added one had the lowest surface energy, which verified its highest WCA and most hydrophobic structure compared to other E/EG coatings. On the other hand, the E/5T coating, which presented higher WCA than the other E/T coatings, also had the lowest surface energy. In addition, the E/0.1EG/5T hybrid coating had the lowest surface energy among all binary and hybrid composites.

To sum up, homogeneous dispersion of the reinforcement materials which are EG and TiO_2 in the epoxy matrix plays a crucial role in the final properties of the composites and the coatings. Therefore, mixing method for the preparation of binary composites and coatings was primarily determined as sonication with the use of solvent method, and then, this method was modified as PP4 for the preparation of hybrid composites and coatings. Among all E/EG and E/T binary composites, the E/0.1EG and the E/5T exhibited better mechanical and thermal properties. On the other hand, it was found that the E/0.05EG/0.5T hybrid composite was the only formulation that presented higher mechanical and thermal properties than its binary counterparts. In addition, it was observed that EG addition at any concentration converted hydrophilic surface of epoxy to hydrophobic.

REFERENCES

[1] V. Pettarin, Injected polymer-matrix nanocomposites : Morphology-performance relationship, 2016.

[2] J. Murphy, Additives for Plastics Handbook, Elsevier Science, New York, 2001. doi:10.1016/B978-1-85617-370-4.50014-2.

[3] R.S. Bauer, Epoxy Resins, in: Appl. Polym. Sci. 21st Century, American Chemical Society Division of Polymeric Materials: Science and Engineering, 1985: pp. 931–961. doi:10.1021/bk-1985-0285.ch039.

[4] P.K. Mallick, Thermoset-matrix composites for lightweight automotive structures, Woodhead Publishing Limited, 2010. doi:10.1533/9781845697822.1.208.

[5] D.D.L. Chung, Carbon Composites: Composites with Carbon Fibers, Nanofibers, and Nanotubes, Second Edi, Elsevier Inc., 2017. doi:10.1016/B978-0-12-804459-9/00003-8.

[6] A. Liang, X. Jiang, X. Hong, Y. Jiang, Z. Shao, D. Zhu, Recent Developments Concerning the Dispersion Methods and Mechanisms of Graphene, Coatings. 8 (2018) 33. doi:10.3390/coatings8010033.

[7] S. Sun, H. Ding, X. Hou, Preparation of $CaCO_3$-TiO_2 composite particles and their pigment properties, Materials (Basel). 11 (2018). doi:10.3390/ma11071131.

[8] M. Dahl, Y. Liu, Y. Yin, Composite Titanium Dioxide Nanomaterials, Chem. Rev. 114 (2014) 9853–9889. doi:10.1021/cr400634p.

[9] P. Thori, P. Sharma, M. Bhargava, An Approach of Composite Materials in Industrial Machinery: Advantages, Disadvantages and Applications, Int. J. Res. Eng. Technol. 02 (2015) 350–355. doi:10.15623/ijret.2013.0212060.

[10] C. Zweben, Composite Materials, Mech. Eng. Handb. 46 (2000) 67. doi:10.2307/25304499.

[11] R.-M. Wang, S.-R. Zheng, Y.-P. Zheng, Introduction to polymer matrix composites, Polym. Matrix Compos. Technol. (2011) 1–548. doi:10.1533/9780857092229.1.

[12] U.S.C.O. of Technology Assessment, Advanced Materials by Design, Congress of the U.S., Office of Technology Assessment, 1988.

[13] C.A. Harper, Handbook of plastics, elastomers, and composites, (2006).

[14] M. Kutz, Applied Plastics Engineering Handbook, 2011. doi:10.1016/C2010-0-67336-6.

[15] E.R. Larson, Thermoplastic Material Selection a Practical Guide, 1st ed., Elsevier Inc, New York, 2015.

[16] F. C. Campbell, Manufacturing Processes for Advanced Composites, Elsevier Inc., 2004. doi:10.1016/B978-1-85617-415-2.50004-6.

[17] R. Van Moorleghem, Welding of thermoplastic to thermoset composites through a thermoplastic interlayer, Delft University of Technology, 2016.

[18] N. Domun, H. Hadavinia, T. Zhang, T. Sainsbury, G.H. Liaghat, S. Vahid, Improving the fracture toughness and the strength of epoxy using nanomaterials - a review of the current status, Nanoscale. 7 (2015) 10294–10329. doi:10.1039/c5nr01354b.

[19] J.-P. Pascault, R.J.J. Williams, Thermosetting Polymers, in: Handb. Polym. Synth. Charact. Process., John Wiley & Sons, Inc., Hoboken, NJ, USA, 2013: pp. 519–533. doi:10.1002/9781118480793.ch28.

[20] F. Hussain, M. Hojjati, M. Okamoto, R.E. Gorga, Review article: Polymer-matrix nanocomposites, processing, manufacturing, and application: An overview, Journal of Compos. Mater. 40 (2006) 1511–1575.

doi:10.1177/0021998306067321.

[21] P.K. Mallick, Fiber-Reinforced Composites: Materials, Manufacturing, and Design, Third Edition, CRC Press, New York, 2007.

[22] M. Motavalli, C. Czaderski, A. Schumacher, D. Gsell, Fibre reinforced polymer composite materials for building and construction, Woodhead Publishing Limited, 2010. doi:10.1533/9780845699994.1.69.

[23] E.L. Thomas, Opportunities in Protection Materials Science and Technology for Future Army Applications, 2012. doi:10.1002/9781118217498.ch13.

[24] P. Smith, J. Yeomans, Benefits of Fiber and Particulate Reinforcement, Mater. Sci. Eng. 2 (2009) 133–154.

[25] S.Y. Fu, X.Q. Feng, B. Lauke, Y.W. Mai, Effects of particle size, particle/matrix interface adhesion and particle loading on mechanical properties of particulate-polymer composites, Compos. Part B Eng. 39 (2008) 933–961. doi:10.1016/j.compositesb.2008.01.002.

[26] R. Allemang, J. De Clerck, C. Niezrecki, A. Wicks, Materials Science and Engineeing, Introduction, Conf. Proc. Soc. Exp. Mech. Ser. 45 (2014) 577–617.

[27] G. Liang, P. Ren, Z. Zhang, T. Lu, Effect of the epoxy molecular weight on the properties of a cyanate ester/epoxy resin system, J. Appl. Polym. Sci. 101 (2006) 1744–1750. doi:10.1002/app.23385.

[28] V. Parashar, Synthesis and Characterization of DGEBA Epoxy and Novolac Epoxy Blends and Studies on their Curing and Mechanical Behavior, Knowl. Res. (2015). doi:10.7598/kor2015.123.

[29] J.E. Ehlers, N.G. Rondan, L.K. Huynh, H. Pham, M. Marks, T.N. Truong, Theoretical study on mechanisms of the epoxy-amine curing reaction, Macromolecules. 40 (2007) 4370–4377. doi:10.1021/ma070423m.

[30] R. Sengupta, M. Bhattacharya, S. Bandyopadhyay, A.K. Bhowmick, A review on the mechanical and electrical properties of graphite and modified graphite reinforced polymer composites, Prog. Polym. Sci. 36 (2011) 638–670. doi:10.1016/j.progpolymsci.2010.11.003.

[31] P. Mukhopadhyay, R.K. Gupta, Graphite, graphene, and their polymer nanocomposites, 2012. doi:10.1201/b13051.

[32] M. Bhattacharya, Polymer nanocomposites - A comparison between carbon nanotubes, graphene, and clay as nanofillers, Materials (Basel). 9 (2016) 1–35. doi:10.3390/ma9040262.

[33] N. Gulnura, K. Kenes, O. Yerdos, M. Zulkhair, R. Di Capua, Preparation of Expanded Graphite Using a Thermal Method, IOP Conf. Ser. Mater. Sci. Eng. 323 (2018). doi:10.1088/1757-899X/323/1/012012.

[34] S. Gantayat, G. Prusty, D.R. Rout, S.K. Swain, Expanded graphite as a filler for epoxy matrix composites to improve their thermal, mechanical and electrical properties, Xinxing Tan Cailiao/New Carbon Mater. 30 (2015) 432–437. doi:10.1016/S1872-5805(15)60200-1.

[35] M.J. Mochane, A.S. Luyt, The effect of expanded graphite on the flammability and thermal conductivity properties of phase change material based on PP/wax blends, Polym. Bull. 72 (2015) 2263–2283. doi:10.1007/s00289-015-1401-9.

[36] T. Monetta, A. Acquesta, F. Bellucci, Graphene/Epoxy Coating as Multifunctional Material for Aircraft Structures, Aerospace. 2 (2015) 423–434. doi:10.3390/aerospace2030423.

[37] D. Reyes-Coronado, G. Rodríguez-Gattorno, M.E. Espinosa-Pesqueira, C. Cab, R. de Coss, G. Oskam, Phase-pure TiO_2 nanoparticles: anatase, brookite and rutile., Nanotechnology. 19 (2008) 145605. doi:10.1088/0957-4484/19/14/145605.

[38] D.A.H. Hanaor, C.C. Sorrell, Review of the anatase to rutile phase transformation, J. Mater. Sci. 46 (2011) 855–874. doi:10.1007/s10853-010-5113-0.

[39] D. Pinto, L. Bernardo, A. Amaro, S. Lopes, Mechanical properties of epoxy nanocomposites using titanium dioxide as reinforcement - A review, Constr. Build. Mater. 95 (2015) 506–524. doi:10.1016/j.conbuildmat.2015.07.124.

[40] S. Srivastava, R.K. Tiwari, Synthesis of epoxy-TiO_2 nanocomposites: A study on sliding wear behavior, thermal and mechanical properties, Int. J. Polym. Mater. Polym. Biomater. 61 (2012) 999–1010. doi:10.1080/00914037.2011.617326.

[41] A. Laachachi, E. Leroy, M. Cochez, M. Ferriol, J.M. Lopez Cuesta, Use of oxide nanoparticles and organoclays to improve thermal stability and fire retardancy of poly(methyl methacrylate), Polym. Degrad. Stab. 89 (2005) 344–352. doi:10.1016/j.polymdegradstab.2005.01.019.

[42] Q.F. Xu, Y. Liu, F.J. Lin, B. Mondal, A.M. Lyons, Superhydrophobic TiO_2 - polymer nanocomposite surface with UV-induced reversible wettability and self-cleaning properties, ACS Appl. Mater. Interfaces. 5 (2013) 8915–8924. doi:10.1021/am401668y.

[43] A. Yasmin, J.J. Luo, I.M. Daniel, Processing of expanded graphite reinforced polymer nanocomposites, Compos. Sci. Technol. 66 (2006) 1182–1189. doi:10.1016/j.compscitech.2005.10.014.

[44] A. Yasmin, I.M. Daniel, Mechanical and thermal properties of graphite platelet/epoxy composites, Polymer (Guildf). 45 (2004) 8211–8219. doi:10.1016/j.polymer.2004.09.054.

[45] W. Liu, S. V. Hoa, M. Pugh, Fracture toughness and water uptake of high-performance epoxy/nanoclay nanocomposites, Compos. Sci. Technol. 65 (2005) 2364–2373. doi:10.1016/j.compscitech.2005.06.007.

[46] W.S. Kang, K.Y. Rhee, S.J. Park, Thermal, impact and toughness behaviors of expanded graphite/graphite oxide-filled epoxy composites, Compos. Part B Eng. 94 (2016) 238–244. doi:10.1016/j.compositesb.2016.03.052.

[47] M.F. Abdelkarim, L.S. Nasrat, S.M. Elkhodary, A.M. Soliman, A.M. Hassan, S.H. Mansour, Volume Resistivity and Mechanical Behavior of Epoxy Nanocomposite Materials, Technol. Appl. Sci. Res. 5 (2015) 775–780. www.etasr.com.

[48] A.R. Jabur, Thermal Degradation Effect on the Fracture Toughness of Glass Fiber Reinforced Unsaturated Polyester Resin Composite, Iraqi J. Mech. Mater. Eng. 11 (2011) 709–719.

[49] L.N. Chang, M. Jaafar, W.S. Chow, Thermal behavior and flammability of epoxy/glass fiber composites containing clay and decabromodiphenyl oxide, J. Therm. Anal. Calorim. 112 (2013) 1157–1164. doi:10.1007/s10973-012-2681-z.

[50] Á. Pomázi, B. Szolnoki, A. Toldy, Flame Retardancy of Low-Viscosity Epoxy Resins and Their Carbon Fibre Reinforced Composites via a Combined Solid and Gas Phase Mechanism, Polymers (Basel). 10 (2018) 1081. doi:10.3390/polym10101081.

[51] R. Oliwa, M. Heneczkowski, M. Oleksy, H. Galina, Epoxy composites of reduced flammability, Compos. Part B Eng. 95 (2016) 1–8. doi:10.1016/j.compositesb.2016.03.074.

[52] T. Kashiwagi, F. Du, K.I. Winey, K.M. Groth, J.R. Shields, S.P. Bellayer, H. Kim, J.F. Douglas, Flammability properties of polymer nanocomposites with single-walled carbon nanotubes: Effects of nanotube dispersion and concentration, Polymer (Guildf). 46 (2005) 471–481. doi:10.1016/j.polymer.2004.10.087.

[53] J. Zhuge, Fire Retardant Polymer Nanocomposites : Materials Design And

Thermal Degradation Modeling, University of Central Florida, 2012.

[54] A.A. Hashim, W.K. Salih, N.A. Jameel, Preparation and Performance Testing of Nano Titanium Dioxide as Fire Retardant of High Density Polyethylene Composite, Int. J. Curr. Eng. Technol. 6 (2016) 1104–1109.

[55] A. Lonjon, P. Demont, E. Dantras, C. Lacabanne, Electrical conductivity improvement of aeronautical carbon fiber reinforced polyepoxy composites by insertion of carbon nanotubes, J. Non. Cryst. Solids. 358 (2012) 1859–1862. doi:10.1016/j.jnoncrysol.2012.05.038.

[56] R.B. Ladani, S. Wu, A.J. Kinloch, K. Ghorbani, J. Zhang, A.P. Mouritz, C.H. Wang, Improving the toughness and electrical conductivity of epoxy nanocomposites by using aligned carbon nanofibres, Compos. Sci. Technol. 117 (2015) 146–158. doi:10.1016/j.compscitech.2015.06.006.

[57] A. Govorov, D. Wentzel, S. Miller, A. Kanaan, I. Sevostianov, Electrical conductivity of epoxy-graphene and epoxy-carbon nanofibers composites subjected to compressive loading, Int. J. Eng. Sci. 123 (2018) 174–180. doi:10.1016/j.ijengsci.2017.11.014.

[58] S. Gantayat, G. Prusty, D.R. Rout, S.K. Swain, Expanded graphite as a filler for epoxy matrix composites to improve their thermal, mechanical and electrical Properties, Xinxing Tan Cailiao/New Carbon Mater. 30 (2015) 432–437. doi:10.1016/S1872-5805(15)60200-1.

[59] W. Zheng, S.C. Wong, Electrical conductivity and dielectric properties of PMMA/expanded graphite composites, Compos. Sci. Technol. 63 (2003) 225–235. doi:10.1016/S0266-3538(02)00201-4.

[60] V.A. Ganesh, H.K. Raut, A.S. Nair, S. Ramakrishna, A review on self-cleaning coatings, J. Mater. Chem. 21 (2011) 16304–16322. doi:10.1039/c1jm12523k.

[61] I.P. Parkin, R.G. Palgrave, Self-cleaning coatings, J. Mater. Chem. 15 (2005)

1689–1695. doi:10.1039/b412803f.

[62] S.H. Kim, Fabrication of superhydrophobic surfaces, J. Adhes. Sci. Technol. 22 (2008) 235–250. doi:10.1163/156856108X305156.

[63] X. Feng, J. Zhai, L. Jiang, The fabrication and switchable superhydrophobicity of TiO_2 nanorod films, Angew. Chemie - Int. Ed. 44 (2005) 5115–5118. doi:10.1002/anie.200501337.

[64] K. Bernland, Hydrophobic Epoxy Resin for Outdoor Electrical Insulation, Luleå University of Technology, 2005.

[65] J. Yu, X. Zhao, Q. Zhao, G. Wang, Preparation and characterization of super-hydrophilic porous TiO_2 coating films, Mater. Chem. Phys. 68 (2001) 253–259. doi:10.1016/S0254-0584(00)00364-3.

[66] Y.J. Shin, Y. Wang, H. Huang, G. Kalon, A.T.S. Wee, Z. Shen, C.S. Bhatia, H. Yang, Surface-energy engineering of graphene, Langmuir. 26 (2010) 3798–3802. doi:10.1021/la100231u.

[67] T. Monetta, A. Acquesta, F. Bellucci, Graphene/Epoxy Coating as Multifunctional Material for Aircraft structures, Aerospace. 2 (2015) 423–434. doi:10.3390/aerospace2030423.

[68] F. Hejda, P. Solar, J. Kousal, Surface Free Energy Determination by Contact Angle Measurements – A Comparison of Various Approaches, WDS'10 Proc. Contrib. Pap. 52 (2010) 1457–1461. doi:10.1002/anie.201206737.

[69] Ö. Köysüren, Preparation and Characterization of Conductive Polymer, Middle East Technical University, 2008.

[70] J. Wei, T. Vo, F. Inam, Epoxy/graphene nanocomposites - processing and properties: a review, RSC Adv. 5 (2015) 73510–73524. doi:10.1039/c5ra13897c.

[71] A. Yu, P. Ramesh, X. Sun, E. Bekyarova, M.E. Itkis, R.C. Haddon, Enhanced

Thermal Conductivity in a Hybrid Graphite Nanoplatelet – Carbon Nanotube Filler for Epoxy Composites, Adv. Mater. 20 (2008) 4740–4744. doi:10.1002/adma.200800401.

[72] R.K. Nayak, A. Dash, B.C. Ray, Effect of Epoxy Modifiers (Al_2O_3/SiO_2/TiO_2) on Mechanical Performance of epoxy/glass Fiber Hybrid Composites, Procedia Mater. Sci. 6 (2014) 1359–1364. doi:10.1016/j.mspro.2014.07.115.

[73] Polikem, Technical Data Sheet - Polires 114, İstanbul, 2012.

[74] Polikem, Technical Data Sheet - Epilox® - Hardener M 1164, İstanbul, 2007.

[75] Imerys, Technical Data Sheet - TIMREX ® C-THERM ^{TM} 001, 2018.

[76] TITAN, Technical Data Sheet - TiOx-280, Moscow, 2016.

[77] SIGMA-ALDRICH, Technical Data Sheet - Acetone, 2014.

[78] B.E.J. Mccormick, All You Need To Know About Making Silicone Molds, ArtMolds. (n.d.) 1–5.

[79] E. Topçuoğlu, Preparation And Characterization Of Polymer Composites Containing Boron Compounds, Middle East Technical University, 2016. doi:10.1111/j.1365-3156.2009.02400.x.

[80] X. Wang, J. Jin, M. Song, An investigation of the mechanism of graphene toughening epoxy, Carbon N. Y. 65 (2013) 324–333. doi:10.1016/j.carbon.2013.08.032.

[81] J. Ye, C. Chu, Z. Zhai, Y. Wang, B. Shi, Y. Qiu, The Interphase Influences on the Particle-Reinforced Composites with Periodic Particle Configuration, Appl. Sci. 7 (2017) 102. doi:10.3390/app7010102.

[82] W.M.R. Daoush, A.H.A. Elsayed, O.A.G. El Kady, M.A. Sayed, O.M. Dawood, Enhancement of Physical and Mechanical Properties of Oxide

Dispersion-Strengthened Tungsten Heavy Alloys, Metall. Mater. Trans. A Phys. Metall. Mater. Sci. 47 (2016) 2387–2395. doi:10.1007/s11661-016-3360-7.

[83] R.J. Young, M. Liu, I.A. Kinloch, S. Li, X. Zhao, C. Vallés, D.G. Papageorgiou, The mechanics of reinforcement of polymers by graphene nanoplatelets, Compos. Sci. Technol. 154 (2018) 110–116. doi:10.1016/j.compscitech.2017.11.007.

[84] V.K. Srivastava, Enhancement of Elastic Modulus of Epoxy Resin with Carbon Nanotubes, World J. Nano Sci. Eng. 01 (2011) 1–6. doi:10.4236/wjnse.2011.11001.

[85] H.A. Al-Turaif, Effect of nano TiO_2 particle size on mechanical properties of cured epoxy resin, Prog. Org. Coatings. 69 (2010) 241–246. doi:10.1016/j.porgcoat.2010.05.011.

[86] M. Altan, A. Uysal, An Experimental Study on Mechanical Behavior of Nanographene/Epoxy Nanocomposites, Adv. Polym. Technol. 37 (2018) 1061–1066. doi:10.1002/adv.21756.

[87] A.A. Wazzan, H.A. Al-Turaif, A.F. Abdelkader, Influence of submicron TiO_2 particles on the mechanical properties and fracture characteristics of cured epoxy resin, Polym. - Plast. Technol. Eng. 45 (2006) 1155–1161. doi:10.1080/03602550600887285.

[88] P.S. Shivakumar Gouda, R. Kulkarni, S.N. Kurbet, D. Jawali, Effects of multi walled carbon nanotubes and graphene on the mechanical properties of hybrid polymer composites, Adv. Mater. Lett. 4 (2013) 261–270. doi:10.5185/amlett.2012.9419.

[89] J.N. Tiwari, R.N. Tiwari, K.S. Kim, Zero-dimensional, one-dimensional, two-dimensional and three-dimensional nanostructured materials for advanced electrochemical energy devices, Prog. Mater. Sci. 57 (2012) 724–803.

doi:10.1016/j.pmatsci.2011.08.003.

[90] J. Gu, X. Yang, Z. Lv, N. Li, C. Liang, Q. Zhang, Functionalized graphite nanoplatelets/epoxy resin nanocomposites with high thermal conductivity, Int. J. Heat Mass Transf. 92 (2016) 15–22. doi:10.1016/j.ijheatmasstransfer.2015.08.081.

[91] B. Qi, S.R. Lu, X.E. Xiao, L.L. Pan, F.Z. Tan, J.H. Yu, Enhanced thermal and mechanical properties of epoxy composites by mixing thermotropic liquid crystalline epoxy grafted graphene oxide, Express Polym. Lett. 8 (2014) 467–479. doi:10.3144/expresspolymlett.2014.51.

[92] J. Asante, F. Modiba, B. Mwakikunga, Thermal Measurements on Polymeric Epoxy-Expandable Graphite Material, Int. J. Polym. Sci. 2016 (2016). doi:10.1155/2016/1792502.

[93] H.G. Brittain, G. Barbera, J. DeVincentis, A.W. Newman, Titanium Dioxide, in: Anal. Profiles Drug Subst. Excipients, 1992: pp. 659–691. doi:10.1016/S0099-5428(08)60404-9.

[94] J. Lang, V. Matejka, Graphite/Titanium Dioxide Composite, Nanotechnol. Cent. 2 (2014) 264–274. doi:10.1039/C3BM60192G.

[95] A.N. Sruti, K. Jagannadham, Electrical conductivity of graphene composites with in and In-Ga alloy, J. Electron. Mater. 39 (2010) 1268–1276. doi:10.1007/s11664-010-1208-2.

[96] Epoxy Technology, Dielectric Properties of Epoxies, Billerica, MA, n.d. Retrieved from: www.epotek.com.

[97] F. Taherian, V. Marcon, N.F.A. Van Der Vegt, What Is the Contact Angle of Water on Graphene?, Cent. Smart Interfaces, Tech. Univ. Darmstadt. 17 (2013) 251–260. doi:10.1021/la304645w.

[98] A. Syakur, Hermawan, H. Sutanto, Determination of Hydrophobic Contact

Angle of Epoxy Resin Compound Silicon Rubber and Silica, IAES Int. Conf. Electr. Eng. Comput. Sci. Informatics. 755 (2016). doi:10.1088/1742-6596/755/1/011001.

[99] Y.J. Shin, Y. Wang, H. Huang, G. Kalon, A.T.S. Wee, Z. Shen, C.S. Bhatia, H. Yang, Surface-energy engineering of Graphene, Langmuir. 26 (2010) 3798–3802.

[100] Z. Gao, X. Zhai, F. Liu, M. Zhang, D. Zang, C. Wang, Fabrication of TiO_2/EP super-hydrophobic thin film on filter paper surface, Carbohydr. Polym. 128 (2015) 24–31. doi:10.1016/j.carbpol.2015.04.014.

[101] J.H. Park, N.R. Aluru, Temperature-dependent wettability on a titanium dioxide surface, 35 (2009) 31–37. doi:10.1080/08927020802398884.

[102] S. Shamsudin, M.K. Ahmad, A.N. Aziz, R. Fakhriah, F. Mohamad, N. Ahmad, N. Nafarizal, C.F. Soon, A.S. Ameruddin, A.B. Faridah, M. Shimomura, K. Murakami, Hydrophobic rutile phase TiO_2 nanostructure and its properties for self-cleaning application, AIP Conf. Proc. 1883 (2017). doi:10.1063/1.5002048.

[103] J.F. Dai, G.J. Wang, L. Ma, C.K. Wu, Surface properties of graphene: Relationship to graphene-polymer composites, Rev. Adv. Mater. Sci. 40 (2015) 60–71.

[104] H. Perron, C. Domain, J. Roques, R. Drot, E. Simoni, H. Catalette, Optimisation of accurate rutile TiO_2 (110), (100), (101) and (001) surface models from periodic DFT calculations, Theor. Chem. Acc. 117 (2007) 565–574. doi:10.1007/s00214-006-0189-y.

APPENDICES

A. PREPARATION OF THE SILICONE MOLDS

In this study, silicone molds were preferred to fabricate epoxy-based composites since they provide much easier demolding without using any tools or releasing agent. For the preparation of silicone molds, room temperature vulcanizing (RTV) silicone and its hardener were purchased from İsbay Boya Hırdavat İthalat İhracat Ltd.Şti. Initially, they were mechanically mixed at 40 rpm for 10 minutes with a mixing ratio (silicone resin: hardener) of 100:5 by weight. At the same time, dog bone or bar shaped samples which were produced in 3D printer according to ASTM D638-10 and ISO 179 standards respectively were attached onto a bottom surface of the rectangular plastic box via silicone adhesive. Next, the mixture was poured into the box and left at room temperature for 24 hours for hardening. At the end of 24 hours, toughened silicon mold was easily taken out of the box.

B. THE CALCULATION OF CURING DEGREE FOR THE NEAT EPOXY

The DSC analysis results of uncured and cured neat epoxy are given in Figure B.1.

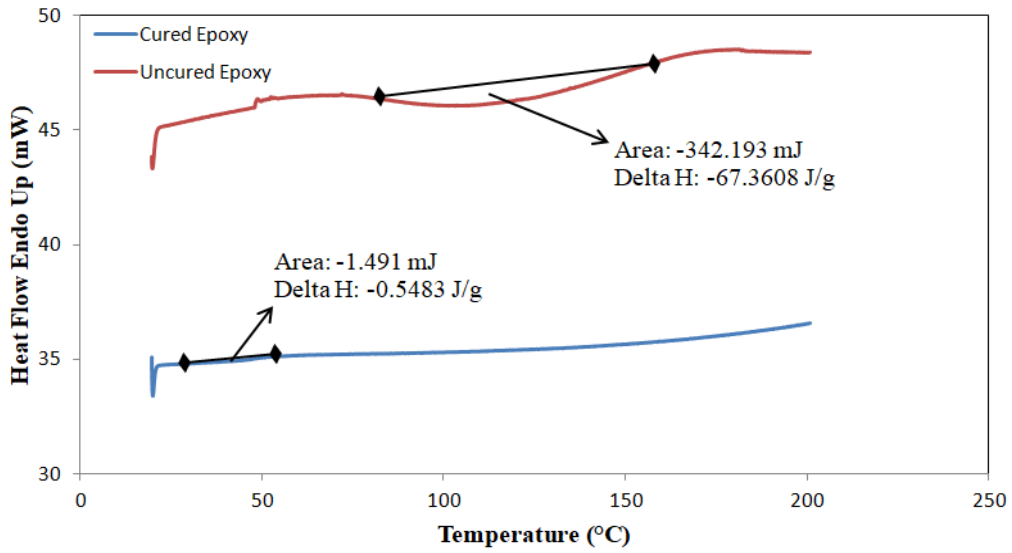

Figure B.1. DSC curve of the uncured and the cured epoxy.

The curing degree of the neat epoxy was calculated using the equation below:

$$\text{Degree of curing (\%)} = \frac{\Delta H_{\text{uncured}} - \Delta H_{\text{cured}}}{\Delta H_{\text{uncured}}} \text{x100}$$

$$\text{Degree of curing (\%)} = \frac{-67.3608 - (-0.5483)}{-67.3608} \text{x100}$$

$$\text{Degree of curing (\%)} = 99.2$$

C. CHARACTERIZATION OF THE PURE EXPANDED GRAPHITE AND THE PURE TITANIUM DIOXIDE PARTICLES

C.1. XRD Analysis Results of Pure EG and Pure TiO_2 Particles

The XRD analysis results of pure EG and pure TiO_2 particles are given in Figure C.1 and Figure C.2, respectively.

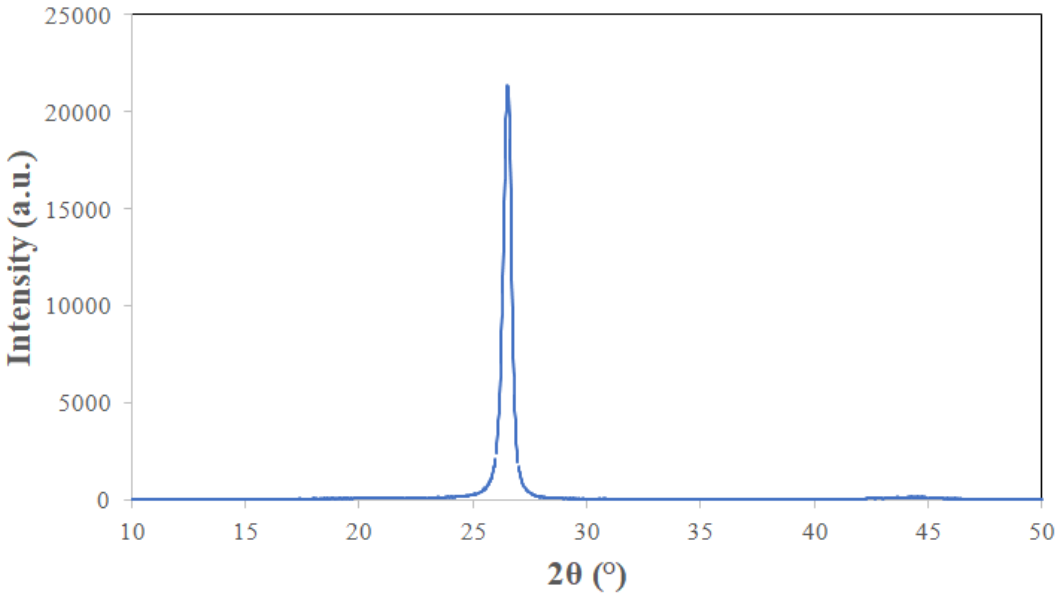

Figure C.1. XRD pattern of pure EG particles.

As seen in Figure C.1, the peaks at 2θ value of 26.53° and 44.7° indicate graphite structure with a d-spacing of 3.36 Å [43].

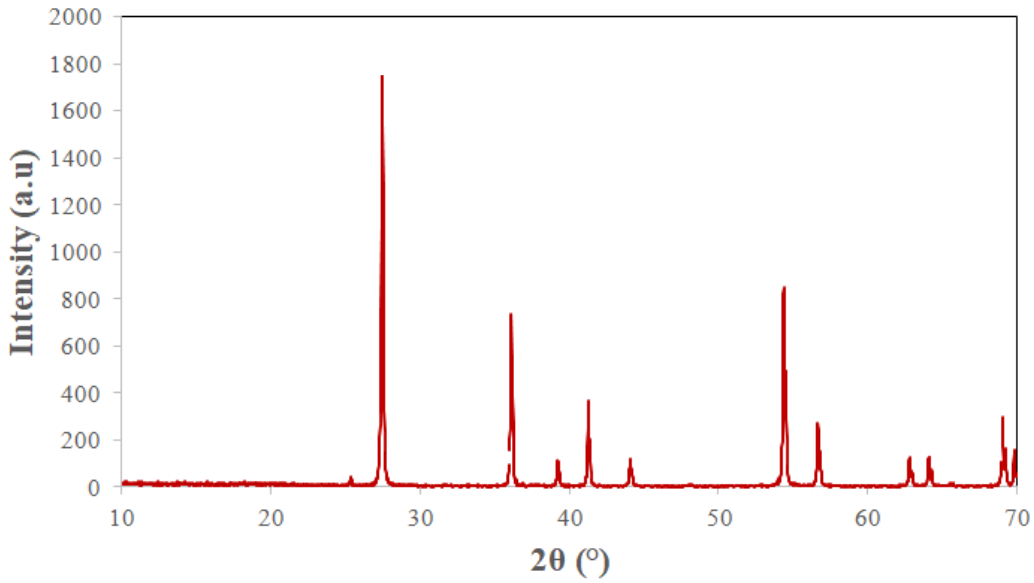

Figure C.2. XRD pattern of pure TiO_2 particles.

As seen in Figure C.2, the peaks at 2θ value of 27.50°, 36.12°, 39.26°, 41.29°, 44.10°, 54.37°, 56.68°, 62.81°, 64.09°, 69.05° and 69.84° indicates TiO_2 particles in rutile phase while the small peak at 2θ of 25.37° is the peak of anatase phase [103].

C.2. TGA Analysis Results of Pure EG and Pure TiO_2 Particles

The weight loss versus temperature curves of pure EG and pure TiO_2 particles are shown in Figure C.3.

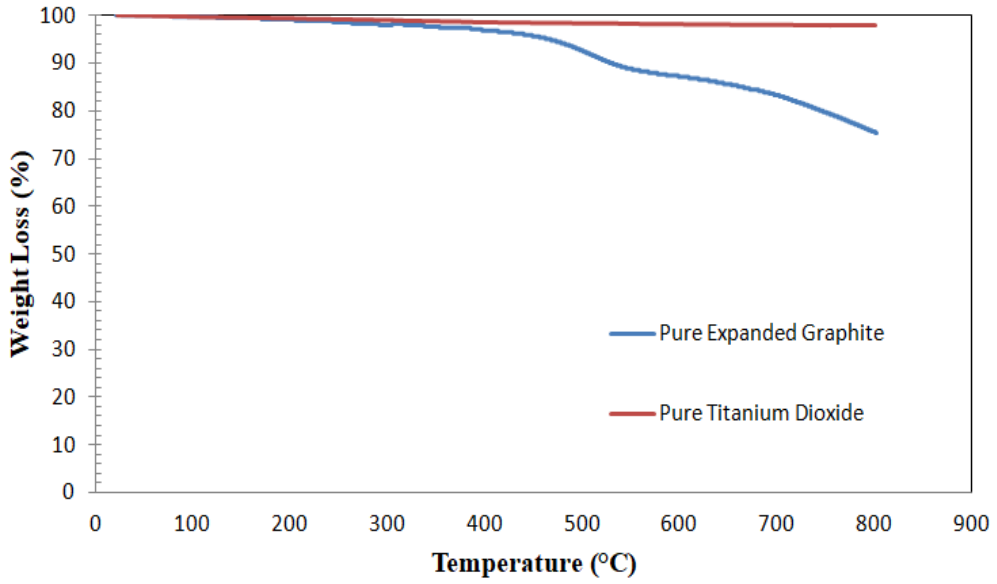

Figure C.3. TGA results of pure EG and pure TiO_2 particles.

As seen in Figure C.3, EG particles start to decompose approximately after 350°C while any significant weight loss was not observed for TiO_2 particles until 800°C.

C.3. SEM Analysis Results of Pure EG and Pure TiO_2 Particles

SEM images of pure EG and pure TiO_2 particles are given in Figure C.4.

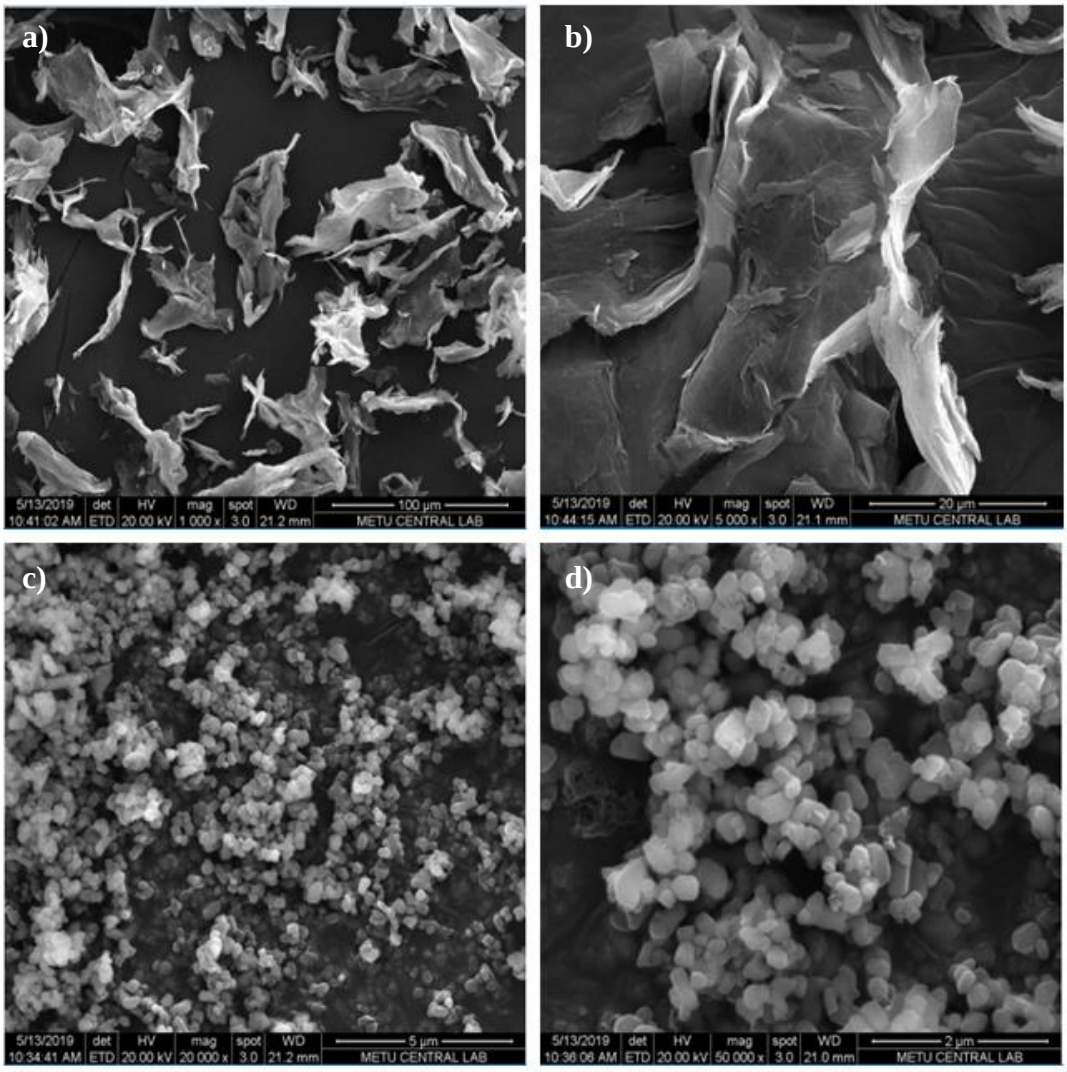

Figure C.4. SEM images of a) pure EG particles at 1000x magnification, b) pure EG particles at 5000x magnification, c) pure TiO_2 particles at 20000x magnification and d) pure TiO_2 particles at 50000x magnification.

As seen in Figure C.4a and C4b, EG particles exhibited two dimensional wrinkle-like structure with high aspect ratio whereas TiO_2 particles have spherical or elliptical shape with small diameter.

D. MECHANICAL TEST RESULTS OF THE NEAT EPOXY AND THE EPOXY-BASED COMPOSITES

D.1. Mechanical Tests Results of the E/0.5EG Composites Fabricated by Different Mixing Methods.

Table D.1. *Tensile test and impact test results of the E/0.5EG composites prepared by different mixing methods.*

Type of Mixing Method	Tensile Strength (MPa)	Elastic Modulus (MPa)	Elongation at Break (%)	Impact Strength (J/m^2)
Direct Mixing	35.7 ± 4.1	2353.8 ± 242.8	2.9 ± 0.4	7.1 ± 0.6
Solvent-free Sonication	36.9 ± 3.0	2648.5 ± 208.8	2.8 ± 0.2	8.0 ± 0.7
Sonication with the Use of Solvent	42.9 ± 3.0	2805.5 ± 212.3	3.5 ± 0.3	10.1 ± 1.2

D.2. Mechanical Tests Results of the Neat Epoxy, the Epoxy-based Binary Composites and the Epoxy-based Hybrid Composites

Table D.2. *Tensile test and impact test results of the neat epoxy, the E/EG binary composites, the E/T binary composites and the E/EG/T hybrid composites.*

Sample Code	Tensile Strength (MPa)	Elastic Modulus (MPa)	Elongation at Break (%)	Impact Strength (J/m^2)
E	43.5 ± 4.5	2435.4 ± 192.0	3.9 ± 0.4	10.4 ± 1.3
E/0.05EG	45.0 ± 2.5	2371.6 ± 237.7	4.1 ± 0.5	9.4 ± 1.4
E/0.1EG	54.0 ± 2.3	3033.9 ± 262.0	4.2 ± 0.4	14.5 ± 1.7
E/0.25EG	42.0 ± 2.8	2842.9 ± 181.2	3.5 ± 0.3	10.4 ± 1.3
E/0.5EG	42.3 ± 3.0	2805.5 ± 212.3	3.5 ± 0.3	10.1 ± 1.2
E/0.75EG	37.2 ± 2.6	2625.4 ± 325.9	2.9 ± 0.3	5.9 ± 0.5
E/1EG	47.8 ± 4.6	3186.3 ± 314.5	3.4 ± 0.1	6.3 ± 0.8
E/0.5T	46.5 ± 4.3	2494.3 ± 127.3	3.7 ± 0.3	7.5 ± 0.9
E/1T	48.4 ± 2.4	2416.9 ± 249.8	3.7 ± 0.4	9.1 ± 1.4
E/2T	48.9 ± 3.9	2528.8 ± 404.0	3.8 ± 0.3	11.5 ± 1.8

Table D.2. *(Continued) Tensile test and impact test results of the neat epoxy, the E/EG binary composites, the E/T binary composites and the E/EG/T hybrid composites.*

Sample Code	**Tensile Strength (MPa)**	**Elastic Modulus (MPa)**	**Elongation at Break (%)**	**Impact Strength (J/m^2)**
E/5T	50.1 ± 4.0	2805.2 ± 198.3	4.2 ± 0.4	13.7 ± 2.1
E/0.1EG/0.5T-PP1	39.4 ± 3.7	2247.1 ± 213.7	3.4 ± 0.6	6.8 ± 0.4
E/0.1EG/0.5T-PP2	40.2 ± 8.2	2464.0 ± 254.4	3.2 ± 0.7	7.3 ± 0.6
E/0.1EG/0.5T-PP3	49.9 ± 3.8	2660.5 ± 526.8	3.8 ± 0.4	8.0 ± 1.2
E/0.05EG/0.5T-PP4	51.8 ± 1.6	2643.9 ± 273.8	4.2 ± 0.3	11.2 ± 0.9
E/0.1EG/0.5T-PP4	51.7 ± 3.5	2674.8 ± 247.6	4.1 ± 0.8	8.3 ± 0.5
E/0.1EG/5T-PP4	43.7 ± 7.3	2238.2 ± 509.6	3.9 ± 0.4	7.1 ± 1.2

E. DSC ANALYSIS RESULTS OF THE NEAT EPOXY AND THE EPOXY-BASED COMPOSITES

Table E.1. *DSC analysis results of the neat epoxy, the E/EG binary composites, the E/T binary composites and the E/EG/T hybrid composites.*

Sample Code	T_g (°C)
E	51.9 ± 1.3
E/0.05EG	53.2 ± 0.2
E/0.1EG	55.1 ± 0.5
E/0.25EG	53.9 ± 1.0
E/0.5EG	53.6 ± 0.6
E/0.75EG	48.7 ± 0.9
E/1EG	47.2 ± 0.6
E/0.5T	49.3 ± 1.3
E/1T	52.3 ± 1.1
E/2T	51.4 ± 1.1
E/5T	57.2 ± 0.1

Table E.1. *(Continued) DSC analysis results of the neat epoxy, the E/EG binary composites, the E/T binary composites and the E/EG/T hybrid composites.*

Sample Code	**T_g (°C)**
E/0.1EG/0.5T-PP1	48.1 ± 2.4
E/0.1EG/0.5T-PP2	51.0 ± 0.8
E/0.1EG/0.5T-PP3	53.5 ± 0.3
E/0.05EG/0.5T-PP4	53.6 ± 1.4
E/0.1EG/0.5T-PP4	54.2 ± 1.7
E/0.1EG/5T-PP4	57.4 ± 5.7

F. ELECTRICAL RESISTIVITY TEST RESULTS OF THE NEAT EPOXY AND THE EPOXY-BASED BINARY AND HYBRID COMPOSITES

Table F.1. *Electrical resistivity test results of the neat epoxy, the E/EG binary composites and the E/EG/T hybrid composites.*

Sample Code	Log (Volume Resistivity), ohm.cm
E	14
E/0.05EG	10.8
E/0.1EG	9.4
E/0.25EG	9.2
E/0.5EG	9.1
E/0.75EG	9.3
E/1EG	9.3
E/0.05EG/0.5T-PP4	10.3
E/0.1EG/0.5T-PP4	10.3
E/0.1EG/5T-PP4	10.7

G. CONTACT ANGLES OF THE COATINGS WITH WATER AND DIFFERENT PROBE LIQUIDS

Table G.1. *Contact angles of the neat epoxy and the epoxy-based binary and hybrid composite mixtures coated samples with water and probe liquids.*

Sample Code	Water (°)	Diiodomethane, DIM (°)	Ethylene Glycol, EGL (°)	Formamide, FA (°)
E	74.6 ± 1.0	31.0	38.1	49.9
E/0.05EG	91.9 ± 7.6	43.5	41.2	51.0
E/0.1EG	97.6 ± 2.3	43.2	47.0	54.0
E/0.25EG	115.6 ± 6.6	44.3	46.6	52.4
E/0.5EG	120.0 ± 0.5	45.6	52.1	57.7
E/0.75EG	104.4 ± 1.2	37.9	47.3	53.9
E/1EG	106.4 ± 3.1	41.9	42.4	49.0
E/0.5T	76.6 ± 2.8	42.4	60.1	65.5
E/1T	79.7 ± 5.7	45.0	60.7	66.4
E/2T	82.0 ± 3.1	46.1	57.4	63.9

Table G.1. (*Continued) Contact angles of the neat epoxy and the epoxy-based binary and hybrid composite mixtures coated samples with water and probe liquids.*

Sample Code	**Water (°)**	**Diiodomethane, DIM (°)**	**Ethylene Glycol, EGL (°)**	**Formamide, FA (°)**
E/5T	94.6 ± 2.1	48.4	59.9	66.0
E/0.05EG/0.5T-PP4	94.7 ± 5.8	38.4	64.3	68.0
E/0.1EG/0.5T-PP4	87.0 ± 0.8	58.0	75.0	78.1
E/0.1EG/5T-PP4	107.2 ± 3.6	61.2	70.2	74.9